AD-751 513

PROBLEMS OF HEAT TRANSFER IN GAS TURBINES (COLLECTION OF ARTICLES)

Foreign Technology Division
Wright-Patterson Air Force Base, Ohio

30 August 1972

FTD-HT-23-1344-72

FOREIGN TECHNOLOGY DIVISION

PROBLEMS OF HEAT TRANSFER IN GAS TURBINES
(COLLECTION OF ARTICLES)

158

UNCLASSIFIED
Security Classification

DOCUMENT CONTROL DATA - R & D

(Security classification of title, body of abstract and indexing annotation must be entered when the overall report is classified)

1. ORIGINATING ACTIVITY (Corporate author)
Foreign Technology Division
Air Force Systems Command
U. S. Air Force

2a. REPORT SECURITY CLASSIFICATION
UNCLASSIFIED

2b. GROUP

3. REPORT TITLE

PROBLEMS OF HEAT TRANSFER IN GAS TURBINES
(COLLECTION OF ARTICLES)

4. DESCRIPTIVE NOTES (Type of report and inclusive dates)
Translation

5. AUTHOR(S) (First name, middle initial, last name)

None

6. REPORT DATE	7a. TOTAL NO. OF PAGES	7b. NO. OF REFS
1971	146	41

8a. CONTRACT OR GRANT NO.	9a. ORIGINATOR'S REPORT NUMBER(S)
b. PROJECT NO. JCN AAH9	FTD-HT-23-1344-72
c.	9b. OTHER REPORT NO(S) (Any other numbers that may be assigned this report)
d.	

10. DISTRIBUTION STATEMENT

Approved for public release; distribution unlimited.

11. SUPPLEMENTARY NOTES	12. SPONSORING MILITARY ACTIVITY
	Foreign Technology Division Wright-Patterson AFB, Ohio

13. ABSTRACT

The articles in this collection contain the results of theoretical and experimental studies of heat transfer in gas turbines, and the temperature states of turbine blades, disks, and rotors. Analysis is given of the boundary conditions formulated when stating problems of thermal conductivity relative to gas turbines. Results are given of a generalization of criterial formulas for calculating the heat-transfer coefficient in vane cascades. Certain specific problems of thermal conductivity are solved in general form and numerically for cooled hollow blades and disks. The collection is intended for specialists in gas-turbine construction. It will also be of interest to teachers and students in this discipline.

DD FORM 1 NOV 68 1473

I

UNCLASSIFIED
Security Classification

UNCLASSIFIED
Security Classification

KEY WORDS	LINK A		LINK B		LINK C	
	ROLE	WT	ROLE	WT	ROLE	WT
Turbine Blades Gas Turbine						

II

UNCLASSIFIED
Security Classification

FTD-HT-23-1344-72

EDITED TRANSLATION

FTD-HT-23-1344-72

PROBLEMS OF HEAT TRANSFER IN GAS TURBINES

English pages: 146

Source: Voprosy Teploperedachi v Gazovykh Turbinakh, No. 72, 1971, pp. 1-136.

Requester: FTD/PDTA

Translated by: John A. Miller

Approved for public release; distribution unlimited.

PREPARED BY:

TRANSLATION DIVISION
FOREIGN TECHNOLOGY DIVISION
WP-AFB, OHIO.

III

All figures, graphs, tables, equations, etc. merged into this translation were extracted from the best quality copy available.

IV

TABLE OF CONTENTS

Transliteration Table iii

Trigonometric-Function Table iv

Annotation v

Foreword vi

V. S. Petrovskiy and M. I. Tsaplin. Boundary conditions in problems of heat conduction for gas-turbine rotors . . . 1

V. S. Petrovskiy. Boundary conditions in heat-conduction problems for cooled nozzle blades 19

N. A. Petrovskaya and V. S. Petrovskiy. The question of the average heat-transfer coefficient in vane cascades. . 24

V. Z. Kitayev and V. S. Petrovskiy. Heat-transfer coefficients on the surfaces of the bladed rotor of an axial gas turbine 35

V. S. Petrovskiy. Solution of the problem of steady heat conduction for hollow cooled nozzle blades of gas turbines 48

V. S. Petrovskiy. Simultaneous solution of stationary problems of heat conduction for gas-turbine blades and disks 54

Ye. Ye. Denisov and V. S. Petrovskiy. Numerical solution of the problem of nonstationary heat conduction for a gas-turbine rotor with root-shrouded blades 65

V. S. Petrovskiy and M. I. Tsaplin. Intensifying the cooling of the leading edge of rotor blades 75

V. S. Petrovskiy and M. I. Tsaplin. Calculating the cooling of gas-turbine disks 86

A. A. Luzhin, V. S. Petrovskiy, M. I. Tsaplin, and V. I. Krichakin. Experimental study of the temperature state of the rotor of an axial gas turbine 98

M. N. Galkin and S. P. Kolesnikov. **The nonstationary heat conduction of bodies of complex configuration 122**

M. N. Galkin and S. V. Lomazov. **Heat transfer in a fluid flow with consideration of the influence of dissipation 136**

VI

U. S. BOARD ON GEOGRAPHIC NAMES TRANSLITERATION SYSTEM

Block	Italic	Transliteration	Block	Italic	Transliteration
А а	*А а*	a	Р р	*Р р*	R, r
Б б	*Б б*	b, b	С с	*С с*	S, s
В в	*В в*	V, v	Т т	*Т т*	T, t
Г г	*Г г*	G, g	У у	*У у*	U, u
Д д	*Д д*	D, d	Ф ф	*Ф ф*	F, f
Е е	*Е е*	Ye, ye; E, e*	Х х	*Х х*	Kh, kh
Ж ж	*Ж ж*	Zh, zh	Ц ц	*Ц ц*	Ts, ts
З з	*З з*	Z, z	Ч ч	*Ч ч*	Ch, ch
И и	*И и*	I, i	Ш ш	*Ш ш*	Sh, sh
Й й	*Й й*	Y, y	Щ щ	*Щ щ*	Shch, shch
К к	*К к*	K, k	Ъ ъ	*Ъ ъ*	"
Л л	*Л л*	L, l	Ы ы	*Ы ы*	Y, y
М м	*М м*	M, m	Ь ь	*Ь ь*	'
Н н	*Н н*	N, n	Э э	*Э э*	E, e
О о	*О о*	O, o	Ю ю	*Ю ю*	Yu, yu
П п	*П п*	P, p	Я я	*Я я*	Ya, ya

* ye initially, after vowels, and after ъ, ь; e elsewhere. When written as ё in Russian, transliterate as yё or ё. The use of diacritical marks is preferred, but such marks may be omitted when expediency dictates.

VII

FOLLOWING ARE THE CORRESPONDING RUSSIAN AND ENGLISH

DESIGNATIONS OF THE TRIGONOMETRIC FUNCTIONS

Russian	English
sin	sin
cos	cos
tg	tan
ctg	cot
sec	sec
cosec	csc
sh	sinh
ch	cosh
th	tanh
cth	coth
sch	sech
csch	csch
arc sin	$\sin^{-1}$
arc cos	$\cos^{-1}$
arc tg	$\tan^{-1}$
arc ctg	$\cot^{-1}$
arc sec	$\sec^{-1}$
arc cosec	$\csc^{-1}$
arc sh	$\sinh^{-1}$
arc ch	$\cosh^{-1}$
arc th	$\tanh^{-1}$
arc cth	$\coth^{-1}$
arc sch	sech^{-1}
arc csch	csch^{-1}
rot	curl
lg	log

VIII

The articles in this collection contain the results of theoretical and experimental studies of heat transfer in gas turbines, and the temperature states of turbine blades, disks, and rotors. Analysis is given of the boundary conditions formulated when stating problems of thermal conductivity relative to gas turbines. Results are given of a generalization of criterial formulas for calculating the heat-transfer coefficient in vane cascades. Certain specific problems of thermal conductivity are solved in general form and numerically for cooled hollow blades and disks.

The collection is intended for specialists in gas-turbine construction. It will also be of interest to teachers and students in this discipline.

The collection includes 4 tables, 64 illustrations, and 41 references.

X

FOREWORD

Recently, ever increasing attention has been paid to questions of heated and loaded parts of high-temperature gas turbines, since improvement of turbine cooling is one of the effective ways of improving their performance. The materials used to make turbine parts allow raising the temperature of the gas ahead of a cooled turbine to 1400-1500°K. However, imperfections of the cooling systems do not allow heating the gas to such a temperature.

Turbine cooling can be improved only after careful study of the temperature state of individual stator and rotor parts under operating conditions.

In this collection we present the results of theoretical and experimental studies of the temperature state of the most critical parts of turbine stators and rotors — the nozzle and rotor blades and disks.

The statement and solution of research problems had the aim of explaining the reasons for high heating of these parts and finding ways of improving methods for their cooling.

The first articles analyze the boundary conditions in the rotors of axial gas turbines and nozzle blades. The rules established by the authors make it possible to refine and simplify the familiar methods of heat calculations. Then, on the basis of a generalization of the criterial dependences used to determine the average heat-transfer

coefficient in vane cascades, calculation formulas are obtained for calculating this coefficient in cascades with varying reaction. As a result of an examination of steady and transient heat conduction of the rotor with the blades, disks, nozzle blades, and rotor blades and other parts, finite expressions are derived which can be used when analyzing their temperature state.

Subsequent articles study the cooling of rotor blades by blowing cooling air from inside onto the blade surface through perforated holes and show the effectiveness of this method, and also give a method for calculating disk cooling.

Of considerable interest are the results of an experimental study of the thermal state of the rotor of an axial three-stage gas turbine; these make it possible to evaluate the effectiveness of the cooling system and note ways for improving it.

The last article presents a theoretical study of the process of heat transfer in the flow of cooling liquid, considering the energy dissipation.

The results of the studies are presented in the form of mathematical dependences suitable for calculations; the most complex solutions are presented as nomograms or are reduced to numerical functions.

The authors ask that all comments on the contents of this collection be sent to the following address: Moscow, B-66, 1-y Basmannyy per., 3, Izdatel'stvo "Mashinostroyeniye."

RI

BOUNDARY CONDITIONS IN PROBLEMS OF HEAT CONDUCTION FOR GAS-TURBINE ROTORS

V. S. Petrovskiy and M. I. Tsaplin

In a theoretical study of the temperature states of gas-turbine rotors the boundary conditions are formulated on the basis of specific physical premises which depend on the structural, gas-dynamic, and operational characteristics of the turbine. In order not to complicate the solution of the initial differential equations, we usually attempt to simplify the boundary conditions within tolerable limits. In this case we will examine only one-dimensional problems.

Let us set the coordinate system as shown in Fig. 1. If the heat problem is solved separately for a rotor blade, at the base of the blade (x = 0) the boundary condition can be

$$t_{\text{ж}}(0) = t_1 \tag{1}$$

or

$$-\lambda_{\text{ж}} \frac{dt_{\text{ж}}(0)}{dx} = q_{\text{ж.в.}} \tag{2}$$

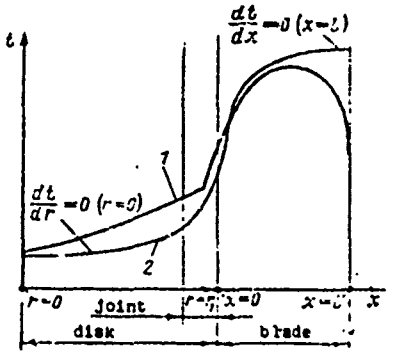

Fig. 1. Coordinate system used for stating heat problems for the cooled rotors of gas turbines: 1 – approximate experimental curve; 2 – theoretical curve.

where $\lambda_л$ is the heat conduction of the blade material.

In both cases the boundary conditions contain values which cannot be determined by calculation, and therefore a theoretical study of the temperature field is possible if we know the experimentally determined values of temperature t_1 or heat flux $q_{л.д}$.

Measurement of t_1, to say nothing of $q_{л.д}$ and $q'_{л.д}$ involves laborious experiment; however, this is justified since, first, by knowing the actual temperature on the boundary of the blade with the disk we reduce the probability of error when calculating the temperature dependence for the disk or blade, while information on heat flows $q_{л.д}$ and $q'_{л.д}$ makes it possible to predict the temperature gradient from the middle to the root of the blade or from the periphery to the center of the disk. Second, measurement of t_1, $q_{л.д}$, and $q'_{л.д}$ in conjunction with the calculation method of determining the temperature field in the blade and disk is a less laborious process than purely experimental study of the temperature state of turbine rotors.

In designing a turbine there is no need to measure temperature t_1, and therefore we assign its value in the calculations. As has been shown by experimental study of temperature distribution in gas-turbine rotor blades and disks, the value of t_1 depends to a considerable extent on the temperature of the gas at the blade root and on the cooling of its root section or footing (if such exists). If we know the calculation mean-mass temperatures of the gas at the inlet to the rotor cascade and at its outlet, we can assume that t_1 is 0.7-0.8 of the arithmetic mean of these temperatures.

We can avoid the need for measuring t_1, $q_{л.д}$, and $q'_{л.д}$ by solving the problem for a turbine rotor for the system disk/blade, i.e., by solving a system of two differential heat-conduction equations. In this case we must formulate, besides the boundary conditions for $x = l$ and $r = 0$ (or $r = r_2$), two more boundary conditions on the blade/disk joint.

In final analysis, temperature distribution in the system disk/blades is caused by the gas flow passing through the rotor cascade, and by disk and blade cooling conditions. The characteristics of the gas flow are known from previous thermal gas-dynamics calculations, while the characteristics of the cooling air are determined, for the given design, by its flow rate. The flow of air for cooling is usually 3-4% of its total flow rate through the engine. Corresponding hydraulic calculation should show the distribution of cooling air as it move through the entire cooled blading of the rotor before passing into the gas flow or to the atmosphere. Knowing the distribution of the cooling air, we can calculate its speeds of motion along the cooled surfaces, and then the values of the heat-transfer coefficient.

Thus, the characteristics which determine the temperature field in the rotor can be obtained from calculation. They can be used to determine the boundary conditions of the blade/disk system and to find the temperature field as functions of the gas-flow and cooling air parameters.

First let us examine the typical boundary conditions for turbine disks. With one-dimensional statement of the problem, the turbine disk is a symmetrical body whose temperature changes along the radius. If there is no central opening (r = 0) the heat flow in the center of the disk (because of symmetry) is zero:

$$dt_1(0)/dr=0. \tag{3}$$

For a disk with an opening in the center ($r = r_2$) the boundary condition can be given in the form of the equation

$$-\lambda_1 \frac{dt_1(r_2)}{dr} = \alpha[t_1(r_2)-t_2], \tag{4}$$

where r_2 is the radius of the opening in the disk.

Disks have variable thickness along the radius. Their profiles can be approximated by hyperbolic, linear, or parabolic functions (Fig. 2). By correcting the profile or heat-transfer conditions in

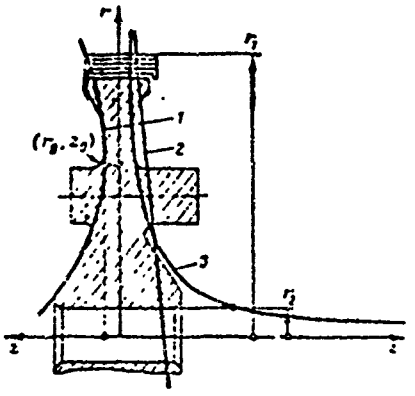

Fig. 2. Approximation of a disk profile by linear, hyperbolic, and parabolic functions:

1 - $z = z_0 + \zeta_1(r_0 - r)^n$, $n > 1$; 2 - $z = z_0 + \zeta/r$; 3 - $z = a/r$.

the central part of the disk, the boundary conditions (with $r = r_2$) can also be written in the form $[dt_д(r_2)/dr] = 0$. Here the solutions of the initial differential equations are simplified.

We can give the following example of correction. If the disk profile can be approximated by a hyperbolic function, when constructing the theoretical profile there can possibly be too strong development of its lateral surface as the center of the disk is approached. Convection heat transfer from the surface of the opening will be compensated by this increased area of heat transfer with corresponding dimensions of the disk opening. For disks of trapezoidal profile the correction can be done by increasing somewhat the heat-transfer coefficient on the lateral surface of the disk.

The boundary condition for a disk with $r = r_1$ can be written in the form

$$-\lambda_д \frac{dt_д(r_1)}{dr} = q'_{л.д} \qquad (5)$$

where $q'_{л.д}$ is the heat flow to the disk from the blades and the vane channel, with consideration of the thermal resistance in the roots.

The value of $q'_{л.д}$ in condition (5) is determined mainly by the heat from the blades to the disk. But this heat, in turn, is determined by the boundary condition with $x = 0$, which can be found from the heat-balance equation. Consequently, we can connect the temperature fields of the blade and disk at their joint using the general boundary condition; then the thermal problem for the general temperature field of the disk/blade system will be solved using only initial data from gas-dynamics and aerodynamics calculations for the gas and cooling air, respectively.

Let us see how we can associate functions $t_д(r)$ and $t_л(x)$ using the boundary conditions.

Let us assume that in the sector from $t_д(r_1)$ to $t_л(0)$ (from the disk periphery to the blade root) the temperature gradient does not change, i.e., $\Delta t/\Delta x = \text{const}$. This makes it possible to represent the temperature differential at the blade/disk boundary in the form of the difference

$$\Delta t = t_л(0) - t_д(r_1) \qquad (6)$$

and introduce the value of Δt into one of the terms of the heat-balance equations compiled for $t_л(x)$, with $x = 0$, and $t_д(r)$, with $r = r_1$, since the conduction heat flow from the blade to the disk in this case is proportional to Δt.

Thus, if we solve the differential equations for heat conduction for the blade and the disk individually, in the final expressions we get the unknown Δt which we introduced into the boundary conditions and which can be defined by supplementary equation (6). Substituting into it the values of $t_л(0)$ and $t_д(r_1)$, found from the general solutions of the heat conduction equations, we get a formula for calculating Δt in terms of known values.

As an example, let us examine the connection in terms of the temperature differential in the blade and the disk. Let the disk have blades with roots, and also an upper and lower shroud. During assembly, channels are formed for air passage during turbine operation between the surfaces of the root, the lower shroud, and the disk crown. The diagram of such a blade, mounted on a disk, is shown in Fig. 3.

For such a design it is expedient to consider the change in temperature along the blade root from $t_л(0)$ to $t_д(r_1)$ to be linear; the coordinate origin along the blade should be in a plane which coincides approximately with the middle thickness of the shroud, while the terminal coordinate of the radius coincides with r_1.

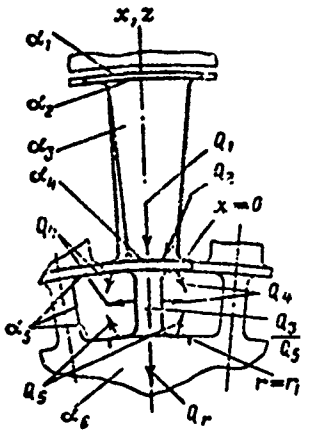

Fig. 3. Schematic drawing of a shrouded solid rotor blade with root, positioned on a turbine disk:

α – average heat-transfer coefficients of the corresponding surfaces, Q – heat removed from them.

Considering all heat-transfer surfaces when x = 0, we can compile the following heat-balance equation (see Fig. 3):

$$Q_1+Q_2=Q_3+Q_4. \qquad (7)$$

where $Q_1=\lambda_3\frac{dt_3(0)}{dx}S_3'n$ is the amount of heat fed per unit time from the working part of the blades to their lower sections S_0, which we will consider to be located in plane x = 0 (n is the number of blades); $Q_2=-\alpha_4[t_3(0)-t_r^*(0)]S_4'n$ is the heat obtained by the surfaces of the lower shrouds of the blades, turned toward the gas flow; $Q_3=\lambda_3\frac{\Delta t}{h}S_H n$ is the heat removed from boundary sections (S_0) to the blade roots (h is the height of the root, S_H is the area of its section); $Q_4=\alpha_5[t_3(0)-t_n]S_{\alpha_5}'n+\alpha_5\left[t_3(0)-\frac{\Delta t}{2}-t_n\right]S_{\alpha_5}''n$ is the heat removed by the cooling air from the convection heat-transfer surfaces S_{α_5}' and S_{α_5}'' within the channels in the lower part of the blades.

Substituting the expressions for Q_{1-4} into equation (7), after transformations we get (with x = 0)

$$\frac{d\theta_3(0)}{dx}=\varphi_1\theta_3+\varphi_2. \qquad (8)$$

Here

$$\theta_3=t_3-t_r^*,\quad \theta_3(0)=t_3(0)-t_r^*(0);$$

$$\varphi_1=\frac{\alpha_5(S_{\alpha_5}'+S_{\alpha_5}'')+\alpha_4 S_{\alpha_4}}{\lambda_3 S_0};$$

$$\varphi_2=\frac{\alpha_5(S_{\alpha_5}'+S_{\alpha_5}'')}{\lambda_3 S_0}[t_r^*(0)-t_n]+\left(\frac{S_H}{hS_0}-\frac{\alpha_4 S_{\alpha_4}}{2\lambda_3 S_0}\right)\Delta t.$$

Now let us formulate the boundary condition for the disk with $r = r_1$. The heat-balance equation

$$Q_5-Q_6=Q_r. \qquad (9)$$

where $Q_5 = \lambda_2 \frac{\Delta t}{n} S_{11} n$ is the quantity of heat fed per unit time through the root cross section from all blades to the disk crown (to an arbitrary coaxial surface of radius r = r_1); $Q_6 = \alpha_5 [t_2(r_1) - t_a] S''_{\alpha_5} n$ is the heat removed by the cooling air from the blade surfaces S''_{α_5} of convection heat transfer; $Q_7 = 2\pi r_1 H \beta \lambda_2 \frac{dt_2(r_1)}{dr}$ is the heat entering the disk through the outer surface of the crown (H is the width of the disk crown, β is a coefficient which takes into account the thermal resistance in the blade joints).

Substituting Q_{5-7} into equation (9), after transformations we get

$$\frac{d\vartheta_2(r_1)}{dr} = \varphi_3 \vartheta_2(r_1) + \varphi_4. \qquad (10)$$

Here

$$\vartheta_2(r_1) = t_2(r_1) - t_a; \qquad \varphi_3 = -\frac{\alpha_5 S''_{\alpha_5} n}{\lambda_2 2\pi r_1 H \beta};$$

$$\varphi_4 = \frac{\lambda_1 S_{11} n \Delta t}{\lambda_2 2\pi r_1 H h \beta}.$$

Boundary conditions (8) and (10), together with boundary conditions (1) and (3) or (4), make it possible to obtain particular solutions to the initial differential equations for the blade and disk, from which we can also find the formula for determining Δt. In calculations by the obtained formulas it is convenient first to find the numerical value of Δt from formula (6), and then calculate the temperature distribution in the blade and disk.

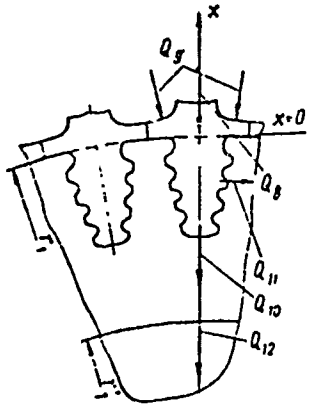

Fig. 4. Diagram for compiling heat-balance equations for lower part of solid shrouded rotor blade without root, and for a disk with r = = r'.

Let us examine the case of determination of the general boundary condition at the joint between a disk and blades without roots. The diagram for connecting the blade to the disk in this version is shown in Fig. 4. The origin of coordinate x (along the blade) is best located in the root section, and it is advisable to examine the temperature differential throughout the disk crown (coordinate r). Let us consider that plane x = 0

coincides with coordinate r_1. For blade cross section S_0 coinciding with this plane we can compile the following heat-balance equation for the amount of heat passing per unit time:

$$Q_8+Q_9=Q_{10}+Q_{11}. \qquad (11)$$

Here $Q_8=\lambda_1\frac{dt_1(0)}{dx}S_1n$ is the heat coming to the cross section from the working parts of the blades; $Q_9=\alpha_4\left[t_r^*(0)-t_1(0)\right]S_4n$ is the heat fed to the disk crown from the vane channels; $Q_{10}=\lambda_2\frac{2\pi H\Delta t}{\ln(r_1:r_1')}$ is the heat removed from the outer surface of the crown (Δt is the temperature differential throughout the crown from r_1 to r_1'); $Q_{11}\approx 2\alpha_6\left[t_1(0)-\frac{\Delta t}{2}-t_6\right]\times$ $\times\ 2\pi h_{06}\left(r_1'+\frac{h_{.6}}{2}\right)$ is the heat removed from the side surfaces of the crown by the cooling air.

Substituting Q_{8-11} into (11), after transformations we get

$$\frac{dh_1(0)}{dx}=\varphi_5\vartheta_1(0)+\varphi_6, \qquad (12)$$

where

$$\varphi_5=\frac{\alpha_1}{\lambda_1}\frac{S_{v_1}}{S_0n^2}+\frac{\alpha_2}{\lambda_2}\frac{4\pi h_{.6}\left(r_1'+h_{.6}\cdot 2\right)}{S_0n^2},$$

$$\varphi_6=\frac{\alpha_6}{\lambda_2}\frac{4\pi h_{.6}\left(r_1'+h_{.6}.2\right)}{S_0n^2}\left[t_1-t_r^*(0)\right]-$$

$$-\left[\frac{\alpha_6}{\lambda_2}\frac{2\pi h_{.6}\left(r_1'+h_{0.}\cdot 2\right)}{S_0n^2}-\frac{\lambda_2}{\lambda_2}\frac{2\pi H}{S_0n^2\ln(r_1:r_1')}\right]\Delta t.$$

For a disk with $r = r_1'$ the balance equation can be written in the form

$$Q_{12}=Q_{10}. \qquad (13)$$

Here $Q_{12}=\lambda_2 2\pi r_1' H\frac{dt_2(r_1')}{dr}$ is the heat removed per unit time from the crown to the web of the disk.

After substituting Q_{12} and Q_{10} into (13), with transformations, we get

$$\frac{d\vartheta_1(r_1')}{dr}=\varphi_7, \qquad (14)$$

where

$$\psi_1 = \frac{\Delta t}{r_1' \ln (r_1/r_1')}.$$

Obtained boundary conditions (12) and (14) include the temperature differential $\Delta t = t_л(0) - t_д(r_1')$. Just as for a disk having shrounded blades, we can first find the particular solutions for the blade and the disk, and then eliminate the unknown Δt from them.

The boundary condition at the blade tip ($x = l$) in the form

$$\frac{dt_л(l)}{dx} = 0 \qquad (15)$$

is the only item found in the literature.

Measurements show the nonagreement between the actual temperature distribution along the blade and that calculated with boundary condition (15). This is explained by the fact that the final formula for determining $t_л(x)$ does not take into account changes in gas temperature along the blade (see, e.g., [1, 2]). In addition, boundary condition (15) is physically incorrect, since there is actually a temperature gradient at the blade tip.

In [2] a solution is given for the thermal stationary problem for a blade with a profile of variable cross section, in which the change in gas temperature along the blade is taken into account; this same source recommends finding the constants in the general solution of the initial differential equation using, in particular, boundary condition (15). The function for the change in gas temperature along the blading of the rotor cascade, leading to the occurrence of a temperature gradient at the blade tip, is incommensurate when solving the heat problem with boundary condition (15). To overcome the contradiction between the proposed and the actual boundary conditions at the blade tip we can isolate, at the blade tip, a short segment of length $0.2l$, considering its temperature constant and equal to the temperature of the gas on the periphery of the blading of the rotor cascade. Such an assumption is not far wrong, since the blade tip receives a certain amount of heat from its middle part due to heat conduction, and

this to some extent compensates for heat lost to radiation in the examined segment. For rotor blades with an upper shroud we can disregard the heat fed to the shroud through the blade tip section. Then the temperature at the blade tip can be considered equal to the temperature of the shroud and defined as some steady temperature established as a result of the balance of the heat fed to the shroud by the gas flow and lost by it due to radiation. The heat lost to radiation can be defined approximately by the formula

$$Q_{\text{л}} \approx \varepsilon_{\text{б.п}} \sigma \frac{T^4_{\text{б.п}}}{100^4}, \qquad (16)$$

where $\varepsilon_{\text{б.п}}$ is the coefficient of blackness of the shroud surface; σ is the thermal-radiation constant; $T_{\text{б.п}}$ is the steady temperature of the shroud.

When compiling equation (16) we disregarded the radiation heat transfer between the gas flow, the surrounding parts, and the shroud, considering that the shroud only gives off heat. This assumption lowers $T_{\text{б.п}}$ only insignificantly.

Based on conditions of convective heating of the shroud and the heat lost to radiation, we can write the heat-flow equation in the form

$$\bar{\alpha}\left[T^*_{\text{г}}(l) - T_{\text{б.п}}\right] = \varepsilon_{\text{б.п}} \sigma \frac{T^4_{\text{б.п}}}{100^4}. \qquad (17)$$

Here $\bar{\alpha} = 0.5(\alpha_1 + \alpha_2)$ is the average heat-transfer coefficient for the upper and lower shroud surfaces; $T^*_{\text{г}}(l)$ is the gas temperature at the shroud.

Numerical solution of (17) for $T_{\text{б.п}}$ can be easily done by trial and error with subsequent approximation.

Thus, for the tip of a rotor blade of a gas turbine ($x = l$) the following boundary condition is more precise:

$$t_{\text{л}}(l) = t_{\text{б.п}} \quad \text{or} \quad \theta_{\text{л}}(l) = t'_{\text{б.п}} - t^*_{\text{г}}(l). \qquad (18)$$

where $t_{б.п}$ is the steady temperature of the blade tip, equal to the temperature of the upper shroud $\theta_{л}(\tau) = t_{л}(\tau) - t^{*}_{г}(\tau)$.

The rotor blades can be cooled from within by air, liquid, the vapors from some liquid or other, or other means. In all cases, when formulating the boundary conditions for $x = 0$, $x = l$, $r = r_1$, $r = r_2$, and $r = r'_1$, the above discussions remain valid. Certain features can appear only when compiling the equations for the heat balance at the blade/disk joint and when compiling the heat-balance equation for the determination of the equilibrium temperature of the rotor blade tip. Thus, boundary conditions (8), (10), (12), (14), and (18) can be considered as typical for gas-turbine rotor blades.

It should be noted that for rotor blades with an upper shroud, calculation of the temperature of the blade tip using boundary condition (15) is not allowed, since an erroneous rise in temperature can make it necessary to increase the area of the profile cross section due to high mechanical loads at the point where the blade touches the upper shroud. Increase cross-sectional area increases the dimensions and weight of the blade as a whole, which is very undesirable for gas turbines.

One-dimensional transient heat conduction in a gas-turbine rotor is described by the following equations:

for the disk –

$$\frac{\partial t_1(r,\tau)}{\partial \tau} = \frac{a_1}{rz(r)}\frac{\partial}{\partial r}\left[rz(r)\frac{\partial t_1(r,\tau)}{\partial r}\right] - \frac{\alpha_1(r)}{c_1\rho_1 z(r)}\left[t_1(r,\tau) - t_{\text{ж}}(r)\right], \tag{19}$$

for solid blades –

$$\frac{\partial t_1(x,\tau)}{\partial \tau} = \frac{a_1}{S(x)}\frac{\partial}{\partial x}\left[S(x)\frac{\partial t_1(x,\tau)}{\partial x}\right] - \frac{\alpha_1(x)P(x)}{c_1\rho_1 S(x)}\left[t_1(x,\tau) - t^{*}_{г}(x)\right] \tag{20}$$

and for a hollow cooled blade –

$$\frac{\partial t_1(x,\tau)}{\partial \tau} = \frac{a_1}{S(x)}\frac{\partial}{\partial x}\left[S(x)\frac{\partial t_1(x,\tau)}{\partial x}\right] - \frac{\alpha_3(x)P_{\text{г}}(x)}{c_1\rho_1 S(x)}\left[t_1(x,\tau) - t^{*}_{г}(x)\right] - \frac{\alpha_{\text{ж}}(x)P_{\text{ж}}(x)}{c_1\rho_1 S(x)}\left[t_1(x,\tau) - t_{\text{ж}}(x)\right]. \tag{21}$$

where τ is the time; $z(r)$ is half the disk thickness; $a_д$, $a_л$, $\rho_д$, $\rho_л$, $c_д$, and $c_л$ are the thermal conductivity, density, and specific heat of the disk and blade, respectively.

The equations which describe the steady heat state of the disk and blade can be obtained from equations (19)-(21), if we consider that $t_д$ or $t_л$ do not depend on τ, i.e., $\partial t_д(r,\tau)/\partial\tau$ and $\partial t_л(x,\tau)/\partial\tau$ are equal to zero.

Solution of equations (19)-(21) in general form, with consideration of the possible dependences of z, α_3, α_6, $\alpha_в$, S_1, P, $t_г^*$, and $t_в$ on x, is, as a rule, impossible due to insurmountable mathematical difficulties. In this case the simplicity of the boundary conditions allows us to compile an initial differential equation or a system of equations without significant simplifications, and thus obtain more precise final functions $t_д(r,\tau)$, $t_л(x,\tau)$, or $t_д(r)$, $t_л(x)$.

Valid simplification of the boundary conditions can be combined with the use of initial differential equations in the most general form, if we consider the features of the actual temperature distribution along the blade foil.

Experiments show that in the midsection of the blade the temperature distribution curve has a maximum. This is natural, since the shape of the dependence $t_л(x)$ of a solid or hollow cooled rotor blade is determined, to a considerable extent, by the temperature of the gas in the blading. From this it follows that in the middle of the blade foil there is no longitudinal heat flow. Therefore, if we formulate the heat problem for two independent sections of the blade $0 \leq x_1 \leq l_1$ and $0 \leq x_2 \leq l_2$ (assuming that $l_1 \approx l_2$ and $l_1 + l_2 = l$), on the boundary of sections x_1 and x_2 ($x_1 = l_1$, $x_2 = 0$) we can, with sufficient accuracy, assume that $\partial t_л(l_1,\tau)/\partial x_1 = 0$ and $\partial t_л(0,\tau)_{x_2} \div \partial x_2 = 0$.

The arbitrary division of the blade into two sections makes it possible to set up one heat problem for the disk and the root

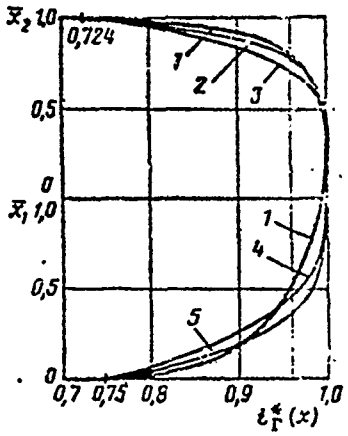

Fig. 5. Change in temperature of a stagnant gas flow along the blade cascade, in relative coordinates:

1 – graph constructed from measurement results; 2, 3 – graphs of the type $\bar{t}_r^* = 1 - \zeta_3 \bar{x}_2^n$, where n = 8 and 6; $\bar{t}_r^* \times (\bar{x}_2) = t_r^*(x_2)/t_r^*(0)_{x_2}$; 4, 5 – graphs of the type $\bar{t}_r^*(\bar{x}_1) = 1 - \zeta_3(1 - \bar{x}_1)^n$, where n = 3 and 4; $t_r^*(\bar{x}_1) = t_r^*(x_1) + t_r^*(l_1/x_1$; $\bar{t}_r^*(l_1)_{x_1} = \bar{t}_r^*(0)_{x_2} = 1.04 t_{r.cp.масс}^*$ (here $\bar{x}_1 = x_1/l_1$, $\bar{x}_2 = x_2/l_2$).

sections of the blades (segment x_1) and another independent problem for the blade tips (segment x_2).

Such a method makes it relatively simple to take into account, in initial differential equation (20), a number of functions of x, including the most important one – $t_r^*(x)$. Figure 5 shows, in relative coordinates, the most typical change in gas temperature along the blade cascade. Division of the blade into segments x_1 and x_2 makes it possible to represent function $t_r^*(x)$ in the form of two fourth-order parabolas on segment x_1 and two eighth-order parabolas on segment x_2.

When stating transient problems for gas turbines it becomes necessary, as a rule, to take into account the variable nature of the process not only along the examined direction (with one-dimensional solutions), but also on the boundaries of the corresponding coordinates. Let us examine the possible transient boundary conditions and formulate them in more general form.

In the center of a solid disk the conditions of symmetry, regardless of time, allow us to consider that $\partial t_д(r,\tau)/\partial r = 0$. This boundary condition is not always acceptable. If the central part of the disk is in contact with a shaft whose temperature is always kept lower than the disk temperature, heat will be removed from the central part of the disk. This circumstance must be considered, even though it does not change the condition $\partial t_д/\partial r = 0$.

In this case we can state the problem for the interval

$r_2 \leq r \leq r_1$, where r_2 is a certain radius; we can consider approximately that on this radius the direction of the heat flow in the disk, from the periphery to the center, coincides with the direction of reading. The value of the heat flow q_{r_2} will equal Q/S_{r_2} (Q is the total quantity of heat removed to the turbine shaft, S_{r_2} is an arbitrary coaxial surface on the disk at radius r_2). The value of q_{r_2} for particular cases can be determined from equations of the conservation of energy (heat balance).

For a disk with a central opening the inner surface of the opening can be cooled. This is taken into account by the boundary condition (with $r = r_2$)

$$\lambda_1 \frac{\partial t_1(r_2, \tau)}{\partial r} = \alpha_{r_2}[t_1(r_2) - t_n(r_2)]. \qquad (22)$$

In the absence of cooling the boundary condition will be

$$\partial t_1(r_2, \tau)/\partial r = 0.$$

At the point where the blade roots join the disk the boundary conditions consist of the heat-balance equation, just as for the case of steady problems, but with consideration of the dependence of Δt on time. In accordance with this, stationary boundary conditions (8) and (10) assume the form [3]:

when $r = r_1$

$$\frac{\partial t_1(r_1, \tau)}{\partial r} = \varphi_1' t_1(0, \tau) - \varphi_2' t_1(r_1, \tau) + \varphi_3' \qquad (23)$$

and when $x_1 = 0$

$$\frac{\partial t_1(0, \tau)}{\partial x_1} = \varphi_4' t_1(0, \tau) - \varphi_5' t_1(r_1, \tau) - \varphi_6'. \qquad (24)$$

Here

$$\varphi_1' = -\frac{\lambda_1 \frac{S_n n}{h} - \alpha_3 S_{x_3}' n}{\lambda_1 2\, r_1 H \vartheta}; \quad \varphi_2' = \frac{\alpha_1'(S_{x_1}' + S_{x_2}')\, n}{\lambda_1 2\pi r_1 H \vartheta} + \varphi_1'; \quad \varphi_3' = (\varphi_2' - \varphi_1')\, t_1(r_1); \quad \varphi_4' = \frac{\alpha_1' S_{x_1}' + \alpha_3 S_{x_3}}{\lambda_1 S_0} + \frac{S_n}{h S_0} + \frac{\alpha_1' S_{x_2}'}{2\lambda_1 S_0};$$

$$\varphi_5' = \frac{S_n}{h S_0} - \frac{\alpha_1' S_{x_2}'}{2\lambda_1 S_0}; \quad \varphi_6' = \frac{\alpha_1 S_{x_1}}{\lambda_1 S_0} t_r'(0)_{x_1} + \frac{\alpha_3 (S_{x_3}' + S_{x_4}')}{\lambda_1 S_0} t_n(r_1).$$

For blades without roots the boundary conditions have a somewhat different form. It is not advisable to use, in this case, the assumption of a logarithmic law of the change in temperature on the disk crown, as was done for the steady process, since the time dependence $t_д(r,\tau)$ is of a different nature. Let us compile a heat-balance equation with $r = r_1$ and $x_1 = 0$ (see Fig. 5):

$$Q_8' + Q_9' = Q_д, \tag{25}$$

where $Q_8' = \lambda_1 \frac{\partial t_1(0,\tau)_{x_1}}{\partial x_1} S_0 n$ is the heat from the blades to the disk in 1 second; $Q_9 = \alpha_1 \left[t_г^*(0)_{x_1} - t_1(r_1,\tau)\right] S_{к.к} n$ is the heat to the disk from the vane channels; $Q_д = \lambda_1 \frac{\partial t_1(r_1,\tau)}{\partial r} 2\pi r_1 H$ is the quantity of heat removed from a surface of radius r_1 to within the disk in 1 second.

After substituting Q_8', Q_9', and $Q_д$ into equation (25) we get

$$\frac{\partial t_1(r_1,\tau)}{\partial r} - \varphi_7' \frac{\partial t_1(0,\tau)_{x_1}}{\partial x_1} + \varphi_8' t_1(r_1,\tau) = \varphi_9', \tag{26}$$

where

$$\varphi_7' = \frac{\lambda_1 S_0 n \beta}{i\, 2\pi r_1 H}; \quad \varphi_8' = \frac{\alpha_1 S_{к.к} n}{\lambda_1 2\pi r_1 H}; \quad \varphi_9' = \varphi_8' t_г^*(0)_{x_1}.$$

Now let us determine the boundary condition for the tip of the rotor blade. With transient heating, the temperature of the blade tip changes somewhat more slowly than that of its middle section, due to temperature nonuniformity in the gas flow. First let us examine a shrouded blade. The shroud at the blade tip has a sufficiently large heat-exchange surface, and we can consider that in the general energy balance that heat which is fed from the middle, more heated, part of the blade is not definitive. Basically, the temperature of the shroud depends on convection heating by the gas, and to a lesser extent on the heat lost to radiation at a high temperature, which we can disregard. Then heating of the shroud will occur in accordance with a regular regime of the first kind, i.e., when $x_2 = l_2$

$$t_2(l_2,\tau) = t_г^*(l_2) - \left[t_г^*(l_2) - t_0\right] e^{-m\tau}, \tag{27}$$

where $t_л(l_2,\tau)$ is the temperature of the shroud (and the blade tip); t_0 is the initial temperature of the shroud; $m=\frac{\bar{\alpha}S_{б.п}}{Mc_{б.п}}$ is the rate of the regular regime ($S_{б.п}$ is the area of the surface and $M_{б.п}$ is the mass of the shroud).

According to boundary condition (27), the shroud should, in time, be heated to the temperature of the gas (as $\tau \to \infty$). This does not really happen, since as a result of the rise in temperature of the shroud, equilibrium gradually sets in between its convection heating and radiation cooling. Here we cannot use boundary condition (18) for the steady process because $t_{б.п}$ will depend, under transient conditions, on time. For precise determination of the boundary condition, considering the radiation heat losses, it would be necessary to compile a transient differential heat-balance equation using the Stefan-Boltzmann law; because of the difficulties involved in integrating this equation we can use the following method. Let us introduce into (27) a correction factor which can depend regularly on time; as $\tau \to \infty$ it becomes numerically equal to $t^*_г(l_2) - t_{б.п}$, i.e., when $x_2 = l_2$ we should have

$$t_л(l_2,\tau)=t^*_г(l_2)-[t^*_г(l_2)-t_0]e^{-m\tau}-[t^*_г(l_2)-t_{б.п}](1-e^{-m\tau}). \qquad (28)$$

For blades without a shroud we can formulate condition (27) under certain assumptions, which nevertheless lead to more precise results than does the condition $\partial t_л(l_2,\tau)/\partial x_2 = 0$ for the blade tip. In this case the blade element whose temperature changes by the law of a regular regime will be a certain section near its tip. The length of this section should be about 10% of the length of the working part of the blade. Then coordinate l_2 will pertain to the section of the blade at the boundary between the entire working part and the isolated segment. Here the assumption that $\lambda \to \infty$ for the blade tip section somewhat distorts the final temperature function. This distortion can be corrected by arbitrarily changing the trend of the temperature function $t_л(x)$ when graphically analyzing the calculation results. The corrected graph will follow along the upper boundary of the field of scatter of the results of calculating the blade temperature, and thus correspond to more rigid

conditions for operation of the upper part of the blade foil.

The examined method also makes it possible to use boundary condition (28) for a blade without a tip shroud.

This analysis of the boundary conditions for a transient process in the disk/blade system makes possible a well-founded selection of that combination of boundary conditions which is close to reality. Undoubtedly, particular cases can occur which require a certain refinement of the examined boundary conditions. These refinements obviously should be introduced into the initial heat-balance equations. Then, if refinements become necessary, the final form of the expressions for the boundary conditions when $r = r_2$, $r = r_1$, $x_1 = 0$, and $x_2 = l_2$ will hardly change in any significant manner.

The statement and solution of two independent heat problems for a disk with blade roots (x_1) and for blade tips (x_2) result in the fact that function $t_л(x,\tau)$ for the entire blade can have a discontinuity at point $x_1 = l_1$ and $x_2 = 0$. Practice has shown that the value of this discontinuity is very insignificant, and it is much less than the error of the calculation method as a whole. Therefore we can eliminate the discontinuity of the function $t_л(x,\tau)$ on the blade-section boundary x_1 and x_2, by calculating the arithmetic mean temperature $\dot{t} = \frac{t_л(l_1,\tau) + t_л(0,\tau)_{x_2}}{2}$ and using it as the only value for the coordinates $x_1 = l_1$ and $x_2 = 0$. The entire function $t_л(x,\tau)$ at this point should be corrected graphically and represented as a continuous function.

Thus, the known forms of the boundary conditions, encountered when solving the problems of heat conduction for gas-turbine rotors, do not always correspond to the actual forms. The data given in the article give grounds for considering that in certain cases we should solve the problem of heat conduction for the disk and blades simultaneously. This is advisable when the only initial data for calculating the temperature state of the rotor are data from preliminary calculation of turbine blading and hydrodynamic calculation

or rotor cooling.

The heat-balance equations compiled for the blade root and the periphery of the disk allowed us to formulate, and represent in general form, the boundary conditions with $x = 0$ and $r = r_1$ both for steady and transient processes of heat conduction. For shrouded blades the boundary condition at the blade tip can be compiled by starting from the thermal state of the upper shroud which, when the turbine operates under steady-state conditions, has a certain steady temperature which is found by solving the corresponding heat-balance equation.

REFERENCES

1. Жирицкий Г. С., Локай В. И., Максутова М. К., Струнки В. А., Газовые турбины авиационных двигателей, Оборонгиз, 1953.
2. Швец И. Т., Дыбан Е. П., Воздушные охлаждения роторов газовых турбин, изд. Киевского университета, 1959.
3. Петровский В. С., «Авиационная техника», 1969, № 1.

BOUNDARY CONDITIONS IN HEAT-CONDUCTION PROBLEMS FOR COOLED NOZZLE BLADES

V. S. Petrovskiy

Theoretical study of the temperature state of nozzle blades of a gas turbine involves solution of the boundary-value problem, which includes the boundary conditions at the blade tips. The accuracy with which the boundary conditions are given determines, to a considerable extent, the accuracy of the final result.

Let us examine one of the versions for formulating the boundary conditions at the tips of a hollow cooled nozzle blade when solving a one-dimensional steady heat problem.

At the blade tips there are shrouds, and the tips are in contact with the inner and outer shrouding strips. With steady-state operation of the gas turbine the temperature of the shrouds depends little on the design of the cooling system within the blades. If we disregard the heat which is fed to the shrouds from the working part of the blades, the shroud temperature can be found from the condition of thermal equilibrium between the heat flows from the gas to the inner surface of the shroud and from its inner surface to the cooling air. Such thermal equilibrium can be described by the corresponding equation for the balance of the heat flows.

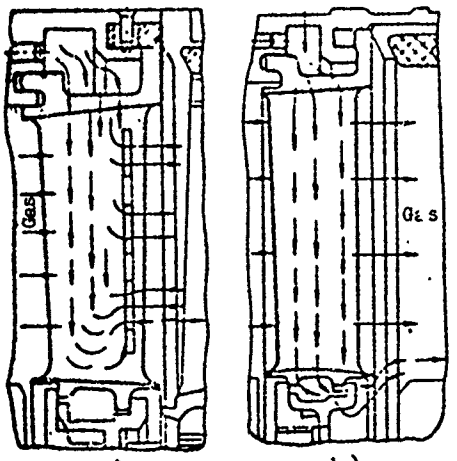

a) b)

Fig. 1. Imbedding of nozzle blades into the shrouds. The arrows show the path of the cooling air within the blades: a – emergence into the turbine blading; b – emergence to the base of the rotor blades.

Let us examine a nozzle blade to which cooling air is fed from an annular cavity in the upper shroud (Fig. 1). After cooling the blade, the air enters the blading of the turbine through openings near the rear edge on the concave part of the profile (Fig. 1a) or combines with the air flow which cools the turbine rotor, through an opening in the lower shroud (Fig. 1b). In both cases the temperature of the shroud is determined by convection and radiation heating from the gas flow and by cooling by the air flow. To compile the heat-balance equation let us schematize the design of the shroud, representing it in the form of a plane wall (Fig. 2).

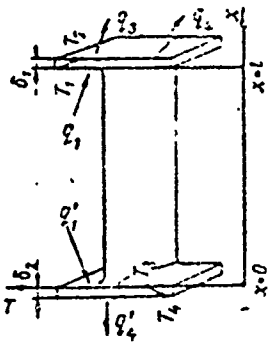

Fig. 2. Schematized nozzle blade.

Let us also give the coordinate system in which we will determine the boundary values of blade temperature and gas-flow stagnation temperature. The coordinate origin (x = 0) is made to coincide with the inner surface of the lower shroud adjacent to the inner shroud strip.

In the heat-balance equations we consider radiation heat transfer, proportional to the fourth power of the absolute temperature. This makes it necessary to express the temperature differential for convection heat flows in the form of the difference between the absolute temperatures of the medium and the wall.

Ultimately the equation for heat-flow balance for the upper shroud can be written as follows:

$$q_1 = q_2 = q_3 + q_4, \qquad (1)$$

where $q_1 = \alpha_r [T_r^*(l) - T_1]$ is the convection heat flow from the gas to the shroud (α_r is the coefficient of heat transfer of the gas); $q_2 = \frac{\lambda}{\delta_1} \cdot (T_1 - T_2)$ is the conduction heat flow through the shroud (λ is the coefficient of heat conduction of the blade, δ_1 is the shroud thickness); $q_3 = \alpha_в (T_2 - T_в)$ is the heat flow from the outer surface of the shroud to the cooling air ($\alpha_в$ is the coefficient of heat transfer from the shroud to the air); $q_4 = \varepsilon\sigma \frac{T_2^4}{100^4}$ is the heat lost to radiation from the cooled surface of the shroud (ε is the coefficient of blackness of the shroud surface, σ is the thermal radiation constant).

Equation (1) does not take into account radiation heat transfer between the inner surface of the shroud, the heated surfaces of adjacent parts, and the gas flow. We can assume that the value of this flow, determined by the Stefan-Boltzmann law, will be very small compared with the intensity of convection heat transfer, since the difference in temperatures of the inner surface of the shroud and the surfaces of the surrounding parts is not great, while the gas flow has a low radiation coefficient. In radiant heat flow q_4 no account is taken of the component of radiation of the heated surface of the shroud, since the temperature of this surface is considerably lower than temperature T_2 of the outer surfa · of the shroud.

Substituting the values of q_{1-4} into expression (1) and solving the resulting equations for T_1, we get

$$\frac{\mathrm{Bi}_r T_r^*(l) + T_2}{\mathrm{Bi}_r + 1} - T_2 = \mathrm{Bi}_в (T_2 - T_в) + \varepsilon\sigma \frac{\delta_1}{\lambda} \frac{T_2^4}{100^4}, \qquad (2)$$

where $\mathrm{Bi}_r = \frac{\alpha_r}{\lambda} \delta_1$ and $\mathrm{Bi}_в = \frac{\alpha_в}{\lambda} \delta_1$ are the Biot criteria for the inner and outer surfaces of the upper shroud.

To determine T_2 for the corresponding values of all quantities entering into equation (2), we can solve the latter by selecting that value of T_2 for which the equation becomes identical. This method allows us to find T_2 from the 3rd or 4th approximation. Using the found value of T_2, from equation (1) in the form

$$\alpha_r[T_r^*(l)-T_1]=\frac{\lambda}{\delta_1}(T_1-T_2) \qquad (3)$$

we can calculate the value of T_1.

Temperature T_1 will thus be a certain steady temperature of the blade cross section when $x = l$, which makes it possible to write the boundary conditions

$$t_3(l)=t_1. \qquad (4)$$

If the cooling air emerges into the cavity of the lower shroud, the steady temperature of the inner surface of the lower shroud is determined analogously. Using as our basis the same concepts as when compiling equation (2), we get

$$\frac{\mathrm{Bi}_r^* T_r^*(0)+T_4}{\mathrm{Bi}_r+1}-T_4=\mathrm{Bi}_3^*(T_4-T_3)+\varepsilon\frac{\delta_2}{\lambda}\frac{T_4^4}{100^4}. \qquad (5)$$

Solving equation (5) for T_4 by selecting and substituting the obtained numerical value of T_4 in equation (1) in the form

$$\alpha_r^*[T_r^*(0)-T_3]=\frac{\lambda}{\delta_2}(T_3-T_4), \qquad (6)$$

we get the formula for calculating T_3.

If the cooling air emerges into the turbine blading, the heat-balance equation has the following form:

$$q_1^*=q_2^*=q_3^*. \qquad (7)$$

where $q_1^*=\alpha_r^*[T_r^*(0)-T_3]$ is the convective heat flow from the gas to the inner surface of the lower shroud; $q_2^*=\frac{\lambda}{\delta_2}(T_3-T_4)$ is the heat flow

across the shroud; $q_4' = \varepsilon\sigma \frac{T_4^4}{100^4}$ is the heat lost to radiation by the outer surface of the shroud.

From equation (7), by substitution of the values of q_1', q_2', and q_4', we get

$$\frac{\mathrm{Bi}_r' T_r^*(0) + T_1}{\mathrm{Bi}_r' + 1} - T_4 = \varepsilon\sigma \frac{r_2}{\lambda} \frac{T_4^4}{100^4}; \tag{8}$$

$$\mathrm{Bi}_r' [T_r^*(0) - T_3] = T_3 - T_4, \tag{9}$$

from which we can calculate T_4 and then T_3.

Thus, in both cases for the lower end of a nozzle blade (x = 0) the boundary condition can be written in the form

$$t_л(0) = t_3. \tag{10}$$

Boundary conditions (4) and (10), obtained as a result of these discussions, are definitely not the only possible ones. They can change depending on the design of the fitting of the nozzle blades into the shrouds. However, for the design shown in Fig. 1 these boundary conditions give quite good coincidence between the theoretical distribution of $t_л(x)$ and the experimental distribution: the results of calculating $t_л(x)$ from the equations obtained when solving the corresponding thermal problem differed by no more than 4-5% from data on direct measurements at the nozzle blade tips.

The boundary conditions obtained can be used when setting up steady-state problems of heat conduction relative to cooled nozzle blades.

REFERENCES

1. Кутателадзе С. С., Боришанский В. М. Справочник по теплопередаче. Госэнергоиздат. 1959.

THE QUESTION OF THE AVERAGE HEAT-TRANSFER COEFFICIENT IN VANE CASCADES

N. A. Petrovskaya and V. S. Petrovskiy

The heat-transfer coefficient α in a vane cascade is one of the basic values describing the distribution of heat in gas-turbine rotors and stators. The initial differential equations for transient and steady heat conduction, compiled for solving the appropriate problems, include the coefficient of heat transfer to the blade surfaces.

The intensity of the heat transfer on blade surfaces determines, to a considerable extent, the temperature field in turbine rotor disks, since heating of the disk is caused basically by the flow of heat from the blades. The influence of the heat-transfer coefficient in a rotor vane channel on the temperature field of the blades and disk of the rotor is particularly noticeable when simultaneously solving the initial equations of heat conduction for the blades and disk. In this case, in final analysis we get temperature dependences (linear, two-dimensional, or three-dimensional) for the blades and disk which are connected, at the point where they come together, by appropriate boundary conditions. These conditions include the functions $t_л(x)$ or $dt_л(x)/dx$ when $x = 0$ (see, e.g., [5]) which also include the value of the heat-transfer intensity coefficient α on the blade surface (x is a coordinate along the blade).

For two- and three-dimensional heat-conduction problems the distribution of heat-transfer intensity along the blade profile is of interest. Such data have been obtained in certain investigations, but it is difficult to use them in calculations since it is impossible to describe the dependence $\alpha = f(x)$ by a function which would coincide with the actual distribution of α. If this can be done, however, it is extremely complex to solve the problem by introducing such a function into the initial equations. Therefore it becomes necessary to replace it by simpler dependences which only approximately correspond to the true distribution of α along the blade profile.

The distribution of heat-transfer intensity along the blade foil should have a substantial influence on the distribution of temperature along the blade.

As shown in the work by V. M. Kapinos and A. G. Knabe [1], the intensity of heat transfer in a vane cascade depends on the nature of the gas flow along the blade profile, which in turn is determined by the reaction of the cascade. Consequently, the dependence of α on x can be determined if we know how the reaction of the cascade changes along the blade.

The authors of [1] qualitatively substantiate the dependence of heat transfer on the shaping of the cascade – its reaction. Actually, as shown in the works by Ainley [2, 3] and Andrews and Bradley [4], the intensity of convection heat transfer is determined by the nature of the gas flow in the blade channel, more precisely, by the position of the point of transition of laminar into turbulent flow on the convex and concave sides of the blade.

On active profiles, on profiles with small leading-edge radius, the length of the segment with turbulent flow increases, since the point of transition of laminar into turbulent flow is displaced toward the leading edge of the profile. The probability is especially high of turbulence of the gas flow on the convex side of the profile,

where stability of the laminar flow is easily lost due to centrifugal forces. The experiments of K. Bammert [6], L. P. Lozitskiy [7], and M. N. Bodunov [8] on determining the dependence of heat transfer on the angle of attack (leak angle) are very indicative in this sense. They show that there is a leak angle for which heat transfer will be minimum. This angle, measured between the flow direction and the front of the cascade, is somewhat greater than the calculated angle of inlet of the gas flow into the cascade, since when the flow impinges against the convex side of the blade, movement along the convex surface of the profile, up to certain limits, is easier to establish than for the calculated inlet angle. The authors of [1] generalize the studies on convection heat transfer in various cascades performed by various authors. They explain the nonagreement of their obtained experimental results by the incompleteness of the similarity criteria, and to expand the range of application of the generalizing expression they introduce the value $\gamma = \sin \beta_2 / \sin \beta_1$, where β_1 and β_2 are the calculated inlet and outlet angles of the gas flow to and from the cascade. Angle β_1 is measured between the frontal line of the cascade and the tangent to the convex part of the profile at the inlet.

We cannot agree with the authors of [1] that the discrepancy of the data obtained in various studies does not depend on experiment errors. Undoubtedly, the errors arising when processing the experimental data and which depend on selection of the determining parameters do not play a major role in the spread of coefficient C and exponent n in the final criterial formulas. Analysis has shown that the ready formula in [1] is also valid only within specific limits, although it was obtained on the basis of analysis of criterial formulas reduced to the identical determining magnitudes. In our opinion, the main reason for the discrepancy in the experimental data is peculiarities in the experiments. These include differences in the shapes of the blade profiles, relative pitch, and other structural data of the cascade, and also differences in various details of the experiment methods: selection of the direction of the heat flow, ways of measuring the calculated temperatures, the amount of heat,

methods for scavenging the cascade, features in the design of the test apparatus, the forms and characteristics of the heating agents, etc. For these reasons it is quite unlikely that tests of specific cascades by various authors using, e.g., the method presented in [12], would yield identical final calculation formulas. We should note that the use of any empirical formula can give a precise result only under very specific particular conditions, although it might have the form of a criterial dependence.

The idea of generalizing criterial formulas for an entire range of change of parameter γ is of great practical significance, but it is also advisable to find criterial relationships for narrower ranges of change of the cascade characteristics. In this case we can reduce the error arising due to nonagreement of the generalizing expression with the individual particular formulas. It makes sense also to find generalizing criterial expressions with constant values of coefficient C and exponent n in a formula of the type $Nu = C\,Re^n$ for cascades of the impulse or reaction type. Such formulas are suitable for preliminary calculations of heat transfer.

In this article we have performed repeated analysis of existing criterial formulas that describe convection heat transfer in gas-turbine vane cascades. Here we considered certain of the inaccuracies admitted in [1]. As an additional similarity criterion for heat transfer in cascades, one which takes into account the geometric and hydrodynamic disparity of comparable processes, we used, unlike the authors of [1], a convergence coefficient $k = \sin \beta_1/\sin \beta_2$, where β_1 and β_2 are the calculated inlet and outlet angles of the gas flow between the front line of the cascade and the tangent to the middle line of the profile at the leading and trailing edges of the blade. This coefficient is more often used in gas-dynamic and thermal calculations and, in our opinion, is more expedient as an auxiliary criterion. The coefficients k and γ and approximately reciprocals. All initial criterial formulas are given in Table 1 and presented in order of increasing convergence coefficients of the cascades i which they were obtained. Likewise, the reaction of the cascades

Table 1

Formula No.	Author, source	Inlet and outlet angles β_1/β_2, deg	Cascade convergence $\kappa = \sin\beta_1/\sin\beta_2$	Cascade pitch-chord ratio $\bar{t}/b$	Determining temperature	Re number	Range of change of Re number	Final criterial formula of the form $Nu = C\,Re^n$	Criterial formula after reduction to C_{ax}, $W_1(\bar{c})$, $s(\bar{c},\bar{p})$, $\mu(\bar{c})$
1	Fukumoto [9]	32/32	1,00	0,75	$\lambda(t_a)$ $\varrho(t_a,\bar{p})$ $\mu(t_a)$	$\frac{\bar{w}d_{ax}\varrho}{\mu}$	(0,5—2,5) 10^5	$Nu \approx 0,137\,Re^{0,67}$	$Nu \approx 0,141\,Re^{0,67}$
2	Prosku and Shum [10]	46/46	1,00	0,525	$\lambda(\bar{t})$ $\varrho(\bar{t},\bar{p})$ $\mu(\bar{t})$	$\frac{\bar{w}d_{ax}\varrho}{\mu}$	(0,3—1,0) 10^5	$Nu \approx 0,0543\,Re^{0,78}$	$Nu \approx 0,054\,Re^{0,78}$
3	Andrews and Bradley [6]	45/45	1,00	0,62	$\lambda(t_a)$ $\varrho(t_a,\bar{p})$ $\mu(t_a)$	$\frac{\bar{w}d_{ax}\varrho}{\mu}$	(0,8—4,0) 10^5	$Nu = 0,169\,Re^{0,66}$	$Nu = 0,152\,Re^{0,66}$
4	Lokshtanov [7] (cascade No. 1)	49/45	1,065	0,803	$\lambda(t_1)$ $\varrho(t_1,p_1)$ $\mu(t_1)$	$\frac{w_1 b\varrho}{\mu}$	(0,75—3,75) 10^5	$Nu = 0,66\,Re^{0,55}$	$Nu = 0,481\,Re^{0,55}$
5	Schaffer and Richards [10]	55/19	1,085	0,715	$\lambda(\bar{t})$ $\varrho(\bar{t},\bar{p})$ $\mu(\bar{t})$	$\frac{\bar{w}d_{ax}\varrho}{\mu}$	(0,8—3,8) 10^5	$Nu \approx 0,0516\,Re^{0,78}$	$Nu \approx 0,0512\,Re^{0,78}$
6	Bedunov [8] (cascade No. 2)	10/36	1,093	0,576	$\lambda(t_1)$ $\varrho(t_1,\bar{p})$ $\mu(t_1)$	$\frac{w_1 b\varrho}{\mu}$	(1,1—6,0) 10^5	$Nu = 0,0646\,Re^{0,73}$	$Nu = 0,063\,Re^{0,73}$
7	Ainley [3]	45/33	1,123	0,687	$\lambda(t_a)$ $\varrho(t_a,\bar{p})$ $\mu(t_a)$	$\frac{w_2 b\varrho}{\mu}$	(0,9—2,15) 10^5	$Nu \approx 0,100\,Re^{0,70}$	$Nu \approx 0,099\,Re^{0,70}$
8	Shirtukly, Lokay [11] (profile No. 3)	18/41	1,13	0,70	$\lambda(\bar{t})$ $\varrho(\bar{t},\bar{p})$ $\mu(\bar{t})$	$\frac{\bar{w}d_{ax}\varrho}{\mu}$	(0,5—4,7) 10^5	$Nu = 0,140\,Re^{0,66} \times \left(\frac{T_s}{\bar{T}_r}\right)^{0,5}\left(\frac{t'}{b'}\right)^{0,112}$	$Nu \approx 0,140\,Re^{0,66}$
9	Ainley [3]	52/43	1,15	0,508	$\lambda(t_a)$ $\varrho(t_a,\bar{p})$ $\mu(t_a)$	$\frac{w_2 b\varrho}{\mu}$	(1,3—6,0) 10^5	$Nu \approx 0,0233\,Re^{0,81}$	$Nu \approx 0,023\,Re^{0,81}$
10	Shirtukly, Lokay [11] (profile No. 2)	51/31	1,39	0,70	$\lambda(\bar{t})$ $\varrho(\bar{t},\bar{p})$ $\mu(\bar{t})$	$\frac{\bar{w}d_{ax}\varrho}{\mu}$	(0,5—4,7) 10^5	$Nu = 0,135\,Re^{0,66} \times \left(\frac{T_s}{\bar{T}_r}\right)^{0,5}\left(\frac{t'}{b'}\right)^{0,112}$	$Nu \approx 0,135\,Re^{0,66}$
11	Shirtukly, Lokay [11] (profile No. 1)	56/36	1,41	0,70	$\lambda(\bar{t})$ $\varrho(\bar{t},\bar{p})$ $\mu(\bar{t})$	$\frac{\bar{w}d_{ax}\varrho}{\mu}$	(0,5—4,7) 10^5	$Nu = 0,160\,Re^{0,66} \times \left(\frac{T_s}{\bar{T}_r}\right)^{0,5}\left(\frac{t'}{b'}\right)^{0,112}$	$Nu \approx 0,160\,Re^{0,66}$
12	Bammert [6]	53/31	1,55	0,494 0,573 0,741	$\lambda(t_1)$ $\varrho(t_1,p_1)$ $\mu(t_1)$	$\frac{w_1 b\varrho}{\mu}$	(0,8—3,2) 10^5	$Nu = 0,78\,Re^{0,545}$ $Nu = 0,77\,Re^{0,545}$ $Nu = 0,76\,Re^{0,545}$	$Nu = 0,574\,Re^{0,545}$ $Nu = 0,566\,Re^{0,545}$ $Nu = 0,560\,Re^{0,545}$
13	Karpenitskiy [12]. Stage II guide vanes	66/35	1,59	0,89	$\lambda(t_1^*)$ $\varrho(t_1^*,p_1)$ $\mu(t_1^*)$	$\frac{w_1 b\varrho}{\mu}$	(0,4—5,4) 10^5	$Nu = 0,65\,Re^{0,55}$	$Nu = 0,457\,Re^{0,55}$
14	Karpenitskiy [12]. Stage I guide vanes	90/30	1,70	0,72	$\lambda(t_1^*)$ $\varrho(t_1^*,p_1)$ $\mu(t_1^*)$	$\frac{w_1 b\varrho}{\mu}$	(0,4—5,4) 10^5	$Nu = 0,65\,Re^{0,55}$	$Nu = 0,452\,Re^{0,55}$
15	Wilson and Pope [13]	60/30	1,73	0,625	$\lambda(t_a)$ $\varrho(t_a,\bar{p})$ $\mu(t_a)$	$\frac{w_2 b\varrho}{\mu}$	(1,5—7,0) 10^5	$Nu \approx 0,069\,Re^{0,71}$	$Nu \approx 0,057\,Re^{0,71}$
16	Bedunov [... as-sume Re ...]	60/28	1,84	0,721	$\lambda(t_1^*)$ $\varrho(t_1^*,\bar{p})$ $\mu(t_1^*)$	$\frac{w_1 b\varrho}{\mu}$	(1,5—7,0) 10^5	$Nu = 0,271\,Re^{0,631}$	$Nu = 0,187\,Re^{0,631}$

17	Sedyuev [8] (cascade No. 3)	59/27	1,88	0,623	$\frac{\lambda(t_1^*)}{\varphi(t_1^*, \bar{p})\,\mu(t_1^*)}$	$\frac{w_1 b \rho}{\mu}$	$(1-5)\,10^5$	$Nu = 0,0913\,Re^{0,70}$	$Nu = 0,0712\,Re^{0,70}$
18	Sedyuev [8] (cascade No. 3)	62/28	1,88	0,615	$\frac{\lambda(t_1)}{\varphi(t_1, p_1)\,\mu(t_1)}$	$\frac{w_1 b \rho}{\mu}$	$(0,71-3,75)\,10^5$	$Nu = 0,67\,Re^{0,65}$	$Nu = 0,489\,Re^{0,65}$
19	Formula obtained at the Kharkov Turbogenerator Plant [1]	75,28	2,05	0,805	$\frac{\lambda(t_л)}{\varphi(t_1, \bar{p})\,\mu(t_л)}$	$\frac{\bar{w}_1 t_{экв} \rho}{\mu}$	$(2-6)\,10^5$	$Nu = 0,394\,Re^{0,61}$	$Nu = 0,391\,Re^{0,61}$
20	Alalay [3]	90,23	2,56	0,600	$\frac{\lambda(t_л)}{\varphi(t_1, \bar{p})\,\mu(t_л)}$	$\frac{w_2 b \rho}{\mu}$	$(1,3-7,8)\,10^5$	$Nu = 0,347\,Re^{0,70}$	$Nu = 0,314\,Re^{0,53}$
21	Andrews and Bradley [6]	75,20	2,62	0,62	$\frac{\lambda(t_л)}{\varphi(t_1, \bar{p})\,\mu(t_л)}$	$\frac{w_2 b \rho}{\mu}$	$(1-9)\,10^5$	$Nu = 0,75\,Re^{0,69}$	$Nu = 0,71\,Re^{0,69}$

Designations:

λ, ρ, μ – heat conduction, density, and dynamic viscosity of the gas;

$\bar{t} = 0.5(t_1 + t_2)$; $\bar{p} = 0.5(p_1 + p_2)$;

$\bar{w} = 0.5(w_1 + w_2)$; $t = 0.5(t_л + t^*)$;

t_1, t_2 – static temperatures of the gas flow at the cascade inlet and outlet;

t^* – temperature of stagnant gas flow;

t_1^* – the same, measured at cascade inlet;

p_1, p_2 – static pressures at cascade inlet and outlet;

w_1, w_2 – relative speeds of gas flow at cascade inlet and outlet;

$t_л$ – temperature of blade surface;

t' – cascade pitch; b' – cascade width.

will increase from the beginning to the end of the table. For formulas 4, 6, 12, 16, 17, and 18, which were obtained from study of heat transfer as a function of leak angle, the values of C and n were taken for zero angle of attack. When processing the measurement results, as the determining dimension in various cases we used the profile chord b or the equivalent diameter $d_{эк}$. The determining temperature also varied. In order to be able to compare the results of the investigations, all criterial formulas were reduced to a single determining dimension and a single determining temperature. As the determining dimension we used the equivalent diameter $d_{эк} = P/\pi$, which is the one most often encountered in studies on heat transfer

in vane cascades; as the determining temperature t we used the arithmetic mean of the gas temperatures at the cascade inlet and outlet. This determining temperature is obviously more advisable that determining temperatures which include the blade temperature; usually the latter is an unknown value and therefore it must be specified for calculating heat-transfer coefficients in a theoretical study of the temperature states of a turbine stator or rotor. The use, in the calculations, of an approximate value for the determining temperature leads to an error in the value of the heat-transfer coefficient and thus reduces the accuracy of the desired temperature. The gas density led to the selected determining temperature and pressure $\bar{p}$ which is the arithmetic mean of the static pressures of the gas at the cascade inlet and outlet. As the determining velocity for the Reynolds number, in accordance with recommendations in [1], we used the arithmetic mean of the velocities of relative motion of the gas in the inlet and outlet sections of the vane cascade ($\bar{w}$).

The initial formulas are reduced to these determining parameters with consideration of the concepts presented in [1]. As the initial transfer equation we used

$$C_{пр}=C_{исх}\frac{Nu_{пр}}{Nu_{исх}}\left(\frac{Re_{исх}}{Re_{пр}}\right)^{n}. \qquad (1)$$

Basically, a change in C involves transfer to a new determining dimension and new determining speed. Therefore, dropping the ratio of determining temperatures, equation (1) can be written in the form

$$C_{пр}\approx C_{исх}\left(\frac{p_{исх}}{p_{пр}}\right)^{n}\left(\frac{l_{исх}}{d_{эк}}\right)^{n-1}\left(\frac{w_{исх}}{w_{пр}}\right)^{n}. \qquad (2)$$

The ratio $p_{исх}/p_{пр}$ in all cases was equal to, or close to, one. Hence

$$C_{пр}\approx C_{исх}\left(\frac{l_{исх}}{d_{эк}}\right)^{n-1}\left(\frac{w_{исх}}{w_{пр}}\right)^{n}. \qquad (3)$$

The flow equation for the inlet and outlet sections of the cascade allows us to represent expression (3) in the following form:

$$C_{пр}\approx C_{исх}\left(\frac{l_{исх}}{d_{эк}}\right)^{n-1}\left[\frac{2\varepsilon_{исх}}{\varepsilon_{\cdot}\left(\frac{V_0 l_1}{V_1 l_2}k+1\right)}\right]. \qquad (4)$$

Here k is the convergence coefficient, V_1 and V_2 are the specific volumes of the gas, and l_1 and l_2 are the blade heights at the cascade inlet and outlet.

To obtain criterial expressions which generalize all formulas, reduced to parameters $d_{эк}$, $\bar{t}$, $\bar{p}$, and $\bar{w}$ from Table 1, we first found the dependence n(k) (Fig. 1). Then, from those values of n for each formula in Table 1 which gave the dependence n(k), and from the corresponding average values of criteria Nu and Re, we found the thus corrected values of constants C. The obtained constants C were used to find the dependence C(k) (Fig. 2). As a result, for convection heat transfer in any type of cascade we obtained the following criterial formula:

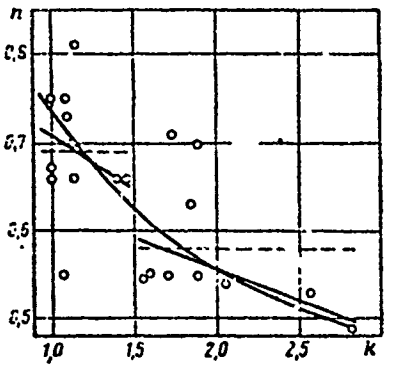

Fig. 1. Form of the generalizing dependences n(k). The points show the values of n from individual experiments.

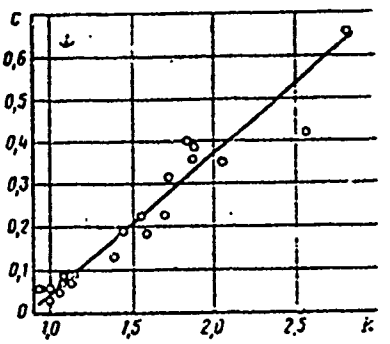

Fig. 2. The dependence C(k) for 0.9 < < k < 2.8.

$$Nu = C(k)Re^{n(k)}, \qquad (5)$$

where C = 0.328k - 0.282, and $n = 0.736k^{-0.4}$. As the calculations showed, the difference in the values of the heat-transfer coefficients calculated from formula (5) and from the appropriate formulas in Table 1 depends on Re. For the interval $Re = 7 \cdot 10^4$ to $3 \cdot 10^5$ it does not exceed 3-8%, and only in four cases does it reach 15%. For Re = = 10^4 to $7 \cdot 10^4$ and $3 \cdot 10^5$ to 10^6 the discrepancy increases to 10-15%, and to 20-30% in individual cases. The obtained formula can be used to calculate the average coefficient of heat transfer along the blade profile and along the vane cascade. For this, if k depends on the cascade height, it is necessary to find its average value along the entire blade and then, from this value of k, determine n and C in

calculation formula (5) using graphs (Figs. 1 and 2). As the average value we can use the half-sum of the convergence coefficient at the blade root and tip, since the dependence of k on the coordinate along the blade is close to linear.

When compiling the boundary condition for the blade surface with hermetic twisting, i.e., with variable reaction along the blade, we must take into consideration the change in heat transfer along the blade foil. For this we should know the dependence k(x), which we then substitute into equation (5), from which we can obtain the dependence $\alpha(x)$. To simplify the equation for the boundary conditions we can recommend the following method. For specific values of k corresponding to the coordinates x = 0 (blade root), x = l (blade tip), and certain intermediate values of x, we calculate the heat transfer coefficients α from formula (5). From the found values of α we can construct the dependence $\alpha(x)$ and describe it by the most suitable and simple equation.

Equation (5), written for the entire range of change of k, leads to considerable spread of the results at the end of this interval, i.e., in those regions where cascades of a specific type are grouped. To refine equation (5), if there is no need for using it over a broad range of change of k, we can propose linear dependences of the change in C and n for impulse and reaction blades, respectively. As such dependences (Figs. 1 and 3) we will have, for impulse cascades (0.9 < k < 1.5)

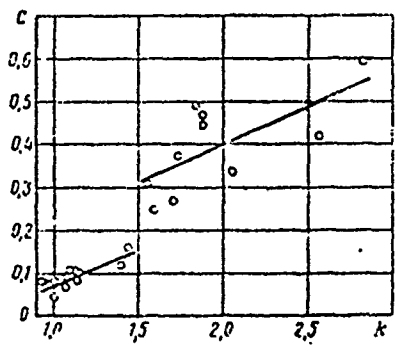

Fig. 3. Dependence C(n) for 0.9 < k < 1.5 (impulse cascade) and for 1.5 < k < 2.8 (reaction cascade).

$$C=0{,}165k-0{,}104;\quad n=0{,}835-0{,}125k \qquad (6)$$

and for reaction cascades (1.5 < k < 2.8)

$$C=0{,}177k+0{,}012;\quad n=0{,}632-0{,}0475k. \qquad (7)$$

Both the initial as well as the generalizing criterial formulas allow us to calculate the heat-transfer coefficient only with an error whose magnitude

depends not only on the accuracy of the calculation formula. It is determined, in addition, by the degree of agreement of the gas-dynamic parameters used as the initial ones for calculating α from the appropriate formulas, their true value, the incomplete similarity of the actual process of heat transfer in the cascade to that described by the calculation formula, and a number of other factors mentioned above. In this connection it is advisable to examine how the inaccuracy of the value of α for a vane cascade influences the error of the calculated value of the blade or disk temperature.

As calculations have shown, the decisive factors for the accuracy with which the temperature field in blades or a disk can be determined are the correctness of the formula for the boundary conditions and consideration, in the initial differential equations, of the change in gas temperature along the vane cascade. In addition, the coefficient α often enters to the 0.5 power in the calculation equations used for theoretical determination of the temperature of gas-turbine rotors or disk. This reduces the value of the relative error, introduced by an inaccurate value of the heat-transfer coefficient into the final result, by one-half.

From this it follows that, in addition to generalizing formula (5), it makes sense to find approximate criterial relationships which would allow us, with acceptable accuracy, to calculate relatively simply the average heat-transfer coefficient on the blade surface for cascades with impulse or reaction profiles. As can be seen from Fig. 1, the finding of such relationships is simplified by the fact that in the entire field of scatter of points n(k) we observe an expressed tendency toward grouping around two average values: with $k < 1.5$ and with $k > 1.5$. This can be explained by the fact that the nature of the gas flow in the vane channel of a cascade with a value of k of about 1.5 is such that the position of the point of transition of laminar into turbulent flow is unstable. Therefore, the relationshop between the extent of the sections of laminar and turbulent flow continually changes and, consequently, the value of the exponent n for Re will also be unstable.

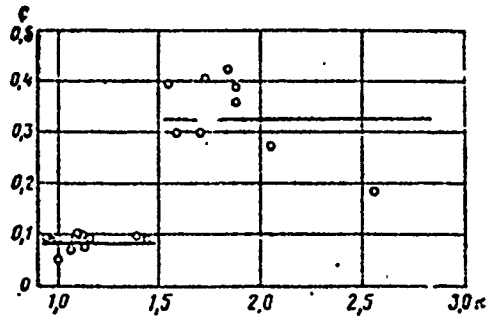

Fig. 4. Constant values of C for impulse and reaction cascades.

As the criterial formulas with constant values of C and n we can propose the following (Figs. 1 and 4): for impulse cascades ($k < 1.5$)

$$Nu = 0{,}085\,Re^{0.69}; \qquad (8)$$

for reaction cascades ($k > 1.5$)

$$Nu = 0{,}326\,Re^{0.58}. \qquad (9)$$

In conclusion we should note that in this article we have generalized the results of studies of convection heat transfer in nonmoving cascades. In a moving cascade the heat-transfer coefficient coefficient increases 1.3-1.4-fold compared with a nonmoving one.

REFERENCES

1. Каппос В. М., Кнабе А. Г., Известия вузов СССР, «Энергетика», 1967, № 6.
2. Ainley D. G., Journal of The Royal Aeronautical Society, No 549, 1955.
3. Ainley D. G., Waldren N. E., Hughes K., Ministry of Supply aeronautical research Council, Reports and Memoranda, No 2975, 1957.
4. Andrews S. J., Bradley P. C., Ministry of Supply Aeronautical reserch Council current papers, No 294, 1957.
5. Петровский В. С., Известия вузов СССР, «Авиационная техника», 1969, № 1.
6. Баммерт К., «Вопросы ракетной техники», 1953, № 6.
7. Лозицкий Л. П., Известия Киевского политехнического института т 30, 1960.
8. Бодунов М. Н., Труды Казанского авиационного института, вып. 63, 1961; Известия вузов СССР, «Авиационная техника», 1961, № 2.
9. Pohlmann E., „Forschungsbericht", Nr. 1879, 1943.
10. Ellerbrock H., Proceedings of General Discussion on Heat Transfer., London, 1951, p. 410.
11. Жирицкий Г. С., Локай В. И., Труды Казанского авиационного института, вып. 23, 1949.
12. Карпожицкий В. Н., «Энергетика и электротехническая промышленность», 1963, № 3.
13. Wilson D. G., Pope J. A., Proceedings of the Institution of Mechanical Engineers, No 36, v. 168, 1954.

HEAT-TRANSFER COEFFICIENTS ON THE SURFACES OF THE BLADED ROTOR OF AN AXIAL GAS TURBINE

V. Z. Kitayev and V. S. Petrovskiy

The diversity of conditions for convection heat transfer in gas turbines and, in particular, on rotor surfaces, and the complexity of a clear determination of the hydrodynamics of this process make the finding of the heat-transfer coefficient values an independent, specific, important problem. Existing recommendations for calculating heat-transfer coefficients are based both on ıe use of generally-known criterial formulas, obtained for certain comparatively simple cases of convection heat transfer, as well as on the results of individual experimental studies under conditions close to those of heat transfer in real operating turbine constructions. Up to the present, convection heat transfer in vane cascades has been studied most completely.

As a rule, the calculation formulas are obtained from study of an immobile object consisting of several blades. For an operating gas turbine, however, these formulas are applicable only after careful analysis of the similarity of the specific case of heat transfer to that for which the criterial equation employed was obtained.

The need for conducting the operations discussed below arose in connection with solution of the problem of heat conduction for a

system turbine disk/rotor blade. Unlike problems solved individually for a disk, blade, or other part of a gas turbine, it was necessary to introduce, into the boundary conditions, the heat-transfer coefficient α on various surfaces of a bladed rotor. Naturally, the accuracy of the calculation results was determined, to a considerable extent, by the sum of the errors which can be introduced into the problem by coefficients α. This necessitated a more accurate validation of selection of the criterial formulas, explanation of the general picture of convection heat transfer over the entire gas-turbine rotor, and determination of the dependence of the heat-transfer coefficients on the turbine operating conditions and, what is particularly important, on the ambient conditions characterized by specific t_H and p_H.

Errors in the values of the heat-transfer coefficients can occur due to discrepancies in the real conditions of heat transfer from those conditions under which the calculation formula was obtained, and due to errors in the values of the initial determining parameters (the temperature of the flow medium, its pressure, flow rate, and determining dimensions).

With combined study of convection heat transfer in the entire rotor it was possible, by comparing various coefficients α, to explain how correctly the values of the initial determining parameters were chosen.

Figure 3 of the first article in this collection (see p. 6) shows a diagram of a shrouded rotor blade with base attached to a disk, and gives values for the average heat-transfer coefficients entering into the initial equations of heat conduction and into the boundary conditions when solving the appropriate problem for a specific three-stage axial turbine.

Let us examine, in sequence, each heat-transfer surface of interest to us, and validate the selection of some criterial expression for calculating the average value of α.

The upper blade shrouds, closing, create two heat-transfer surfaces: an external cylindrical surface and an internal vane surface on the side toward the gas flow. When stating the problem of heat conduction the boundary condition at the blade tip is as follows (when $x = l$):

$$t_л(l, \tau) = t_{в.п}(\tau) \tag{1}$$

for a transient process, and

$$t_л(l) = t_{в.п}. \tag{2}$$

for a steady process.

The value of $t_{в.п}$ is determined from the heat-balance equation for the upper shroud

$$\bar{\alpha}\left[T_г^*(l) - T_{в.п}\right] = \varepsilon_л c_0 T_{в.п}^4 \varphi_л \tag{3}$$

where $\bar{\alpha} = 0.5(\alpha_1 + \alpha_2)$, and $T_г^*$ and $T_{в.п}$ are in °K.

The coefficient $\bar{\alpha}$ also appears in the expression for $t_{в.п}(\tau)$. Convection heat transfer on the outer and inner surfaces of the upper shroud occurs under varying conditions. We can assume that the determining temperature and pressure will be identical on the outer and inner surfaces of the shroud. Heat transfer on the outer cylindrical surface moving relative to the stator surface can be examined as convection in a slot channel or as heat transfer in a plane of length πd. The high degree of turbulization of the gas in the gap between the outer shroud surface and the stator surface does not allow us to assume laminar flow in the gap. Even if we consider that flow of the gas in the axial direction creates relatively low washing speeds, the high peripheral speeds of the rotor result in high Reynolds numbers in the gap and, consequently, high gas turbulence. Such conditions of convection do not allow us to use the criterial formulas recommended for slot gaps and labyrinth seals: this would lead to a lowering of the heat-transfer coefficient. In this case it is advisable to use a formula that describes convection heat transfer in a plane with turbulent motion of the washing medium:

$$Nu = 0{,}032\,Re^{0{,}80}. \qquad (4)$$

Theoretical gas-dynamics calculation shows that at the upper shrouds the temperature of the gas is somewhat higher than at the level of the middle section of the blade. This was not actually observed. The temperature of the gas in the turbine blading is sharply reduced in the lower and upper parts of the vane cascades. Consequently, as the determining temperature we must use not the gas temperature obtained from gas-dynamics calculation but a somewhat lower value.

In the absence of experimental data on gas-temperature distribution along the vane cascade we can, based on numerous measurements, consider it equal to 0.85-0.90 of the gas temperature in the middle section of the blade. Then the determining temperature in (4) is

$$\bar{t}_1 = 0{,}9\,\frac{t_{1II} + t_{2II}}{2}. \qquad (5)$$

Here t_{1II} and t_{2II} are the temperatures in the middle section of the blade at the inlet to and outlet from the rotor cascade for the appropriate stage, taken from gas-dynamics calculation.

The determining pressure and the relative speed will be

$$\bar{p} = 0{,}5(p_{1II} + p_{2II}) \text{ and } w = \pi dn. \qquad (6)$$

(Subscripts 1 and 2 pertain to the cascade inlet and outlet, respectively; the values of p_I and p_{II} are taken from gas-dynamics calculation; n is the number of turbine rotor revolutions per unit time; d is the diameter of the upper shroud of the rotor cascade.)

The determining dimension in formula (4) should be plate length l. In this case it is advisable to use the length of the generatrix of the cylindrical surface πd as the determining dimension.

The coefficient of heat transfer on the inner surface of the upper shrouds (in the vane channel) can be determined, based on the following concepts. The bottom of the vane channel can be represented

as a flat surface whose length is equal to the length of the cascade blading, as part of a short channel of variable section, and, finally, as one of the surfaces of the vane cascade for which the value of α_2 is determined from known criterial expressions. There are no equations for convection heat transfer for short channels of variable cross section. The use of the criterial relationships recommended for a vane cascade is also unacceptable here. The flow of gas along the blade profile, to which the formulas for convection heat transfer in vane cascades, obtained in various studies, obtain, is of a different nature than flow along the inner surface of the upper shroud. Correspondingly, there is no hydrodynamic similarity of the processes, i.e., the criterial formulas for convection heat transfer should be different. We see, in the given case, just as for the outer shroud surface, that the most suitable formula for calculating α will be formula (4) in which the determining temperature and pressure remain the same, while the determining velocity is equal to the arithmetic mean of the gas velocities at the cascade inlet and outlet in the upper section of the blade (subscripts I, II, and II in Fig. 1, p. 56):

$$\bar{w}=0{,}5(w_{1II}+w_{2II}). \tag{7}$$

The determining dimension will be the length of the vane channel l_I along its middle line.

The next heat-transfer coefficient is α_3, which describes heat transfer in the vane cascade itself. To determine this coefficient we have many criterial relationships of the form

$$Nu=C\,Re^n, \tag{8}$$

differing in the values of C and n. These relationships were obtained in experiments with various cascades, with various gas-flow leak angles, for a broad range of change of temperatures and other parameters describing heat transfer. At present attempts are being made to find a more or less universal criterial relationship for calculating coefficient α. The first results obtained require additional verification and comparisons. Therefore, it is most advisable to use a formula which takes into account a sufficient number

of similarity criteria for processes of heat transfer in vane cascades. Such a formula

$$Nu = C\,Re^{0.66} K_T^{0.5} K_p^{0.12} \qquad (9)$$

has been obtained at the Kazan' Aviation Institute [1]. Here $K_T = T_л/T_г$ is a temperature factor; $K_p = y/b$ is the cascade pitch-chord ratio.

The value of C in (9) depends on the radius of the leading edge of the blade. The determining temperature and pressure are found as the arithmetic mean for the cascade inlet and outlet:

$$\bar{t}_л = 0{,}5(t_{1л} + t_{2л}) \quad \text{and} \quad \bar{p}_л = 0{,}5(p_{1л} + p_{2л}).$$

As the determining dimension we use the equivalent diameter $d_{эк} = P_л/\pi$. The determining velocity is found from formula (7), except that the gas velocities are taken at the level of the middle section (subscript II). Formula (9) was obtained for a static cascade. According to existing recommendations, the coefficient α for the rotor cascade of a working turbine should be increased by a factor of 1.25-1.30.

The heat-transfer coefficient on the inner (turned toward the gas flow) surface of the lower shroud is determined based on the same concepts as for the inner surface of the upper shroud. Here the determining temperature will be the same as for α_2 (i.e., $\bar{t}_{III} = \bar{t}_I$). The determining pressure and velocity are calculated from formulas (6) and (7), but the initial values of p and w are taken for the lower blade section (subscript III).

Stages I and II of a turbine have unique heat chokes in the form of cooling channels in the blade roots between the lower shroud and the disk crown. The influence of the passage of air through these channels on the total temperature field of the blade and disk, as appropriate calculations have shown, is extremely great. In this connection the coefficient α_5, which characterizes heat transfer in the cooling channels, is of particular importance.

An error in calculating coefficient α_5 occurs mainly not due to the selected criterial relationship's not corresponding to the examined heat-transfer conditions, but due to the low accuracy in determining the rate of flow of cooling air through the channels. The air speed here can be determined by using the continuity equation, but the initial values of the flows through each channel are not reliable. It should be noted that for any turbine, in the absence of well-organized air flow, its flow rate for cooling the individual rotor elements can only be determined with high error.

At the same time, gas-dynamics calculation for the blading gives, with sufficient accuracy, values of the gas pressure at the vane cascade inlet and outlet at the base. If we consider that the pressure differential from the cavity ahead of the cooling chanel to the turbine blading is approximately equal to the differential behind the cooling channel, the pressure differential of the cooling air in the channel of a turbine of the given design is approximately equal to $\Delta p = p_{1III} - p_{2III}$. Using this value for the differential we can obtain an expression for determining the velocity through an individual channel in the form of the Bernoulli equation for arbitrary sections ahead of the inlet to the channel and at its outlet:

$$p_1 + \frac{\rho_1 w_u^2}{2} = p_2 + \frac{\rho_2 w_2^2}{2}. \qquad (10)$$

Here $w_u = u \sin \varphi$ is the speed of the cooling air, occurring due to the compressor effect during peripheral movement of the blade row positioned at angle φ to the flow axis, u is the peripheral speed of the cooling channels, p and ρ are air pressure and density. Subscripts 1 and 2 pertain to sections at the channel inlet and outlet.

If we assume that $p_1 - p_2 \approx p_{1III} - p_{2III}$, then Δp is known. Speed w_2 is taken as the determining one when calculating α_5. We get the calculation formula for w_2 from equation (10):

$$w_2 = \sqrt{\frac{1}{\rho_2}(2\Delta p + \rho_1 w_u^2)}. \qquad (11)$$

The resistance coefficient ζ must be determined considering the recommendations presented in [2]. It depends on the speed of rotation of the disk and is found from the formula

$$\zeta = \frac{1}{\xi^2}, \tag{12}$$

where $\xi = \frac{\xi_1}{1 + 0{,}5K - 0{,}09K^2}$ is the flow factor; $\xi_1 = (1 + \zeta')^{-1}$ is the flow factor for a static disk; ζ' is the hydraulic resistance of a short channel with different inlet and outlet cross sections; $K = u/w_2$ is a parameter which defines the dependence of ξ on the peripheral speed for known w_2.

From the formulas derived we see that before finding the value of w_2 we must know the coefficient ζ which, in turn, depends on w_2. Here we can proceed as follows. First, from the flow equations find the approximate value of w_2. Then from formula (11) find the more accurate value for the speed in the cooling channel and repeat the calculation using the corrected value of ζ. In determining w_2 using the continuity equation we used the results of a preliminary tentative hydraulic calculation. An initial approximate value of w_2 is required both for parameter K as well as for determining coefficient ζ'. This coefficient depends on the ratio of the areas of the channel inlet and outlet (S_1/S_2), and on the Reynolds number, which is calculated from the initial value of w_2 [3]. The refined speed of the cooling air in the channels is then used to calculate the Reynolds number; as the determining dimension we used the equivalent channel diameter $d_{эк} = 4S/P$, where S is the channel section and P is its perimeter.

As calculations have shown, the Reynolds number for cooling channels of stage I of a rotor does not exceed 10^4, while for stage II it does not exceed 10^3. Consequently, the airflow here can be considered laminar, or at least transitional, but not turbulent. Then the formula for determining α_5 will have the form

$$Nu = 0{,}17\,Re^{0{,}33}\varepsilon_l; \tag{13}$$

here $K_0 = NuPr^{-0.43}$ is a complex that depends on the Reynolds number; ε_l is a coefficient which takes into account the dependence of heat transfer on the ratio $l/d_{эк}$ for short channels.

The values of K_0 for the appropriate Reynolds number can be found from graphs given in [4]. The coefficient ε_l is defined in this same work. The determining temperature and pressure when using formula (13) will be the ambient temperature and pressure.

The next heat-transfer coefficient of interest to us is α_6, which describes convection heat transfer on the side surface of the disk. To calculate α_6 it is expedient to use the formula

$$Nu = 0{,}0348\,Re^{0.77}, \qquad (14)$$

obtained at the Kazan' Aviation Institute. As parameters we use here the air temperature and pressure and the diameter of the disk bed. The Reynolds number is calculated from the relative air speed. The air flows for disk cooling are relatively slow, and therefore the relative speed found from the continuity equation can be determining only for the central part of the disk. For the peripheral region, however, it is advisable to consider the relative air speed equal to the peripheral speed of the rotating disk.

The examined heat-transfer coefficients were calculated for two turbine operating modes – idle and nominal (rated) – at ambient air temperature t_H = -50, -30, +15, and +50°C. The data obtained are represented in the form of graphic dependences in Figs. 1-5. Operation of a turbine in the nominal regime is characterized by the dependences of coefficient α_{1-4} on t_H, shown in Fig. 1. The same order of magnitude of these coefficients is observed for most gas turbines. Convection heat transfer is most intense in the vane cascade. This has the result that with low heat-transfer intensity to the disk, the temperature of solid blades is almost the same as that of the gas throughout the length of the rotor section, except for a small area near the root.

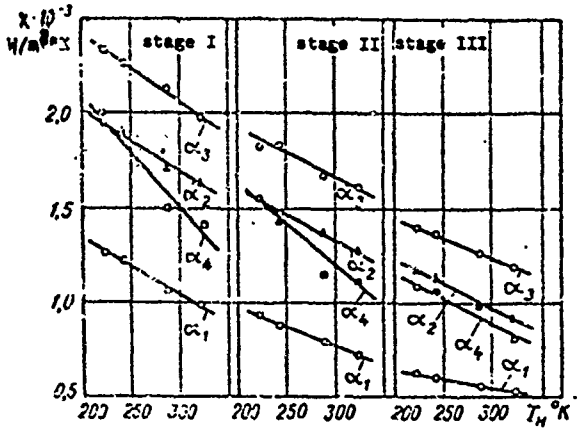

Fig. 1. Dependences of coefficients α_{1-4} on T_H with rated turbine operation.

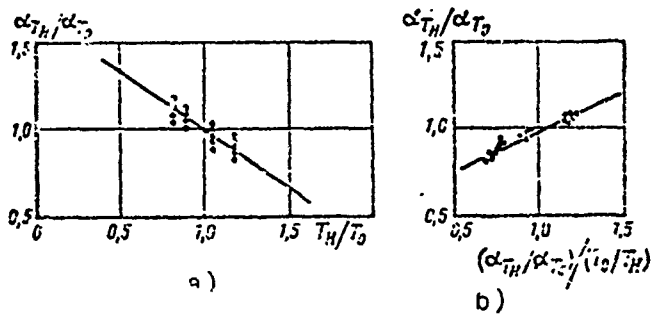

Fig. 2. Fu.. ions $\alpha_{T_H}/\alpha_{T_0}(T_H/T_0)$ and $\alpha_{T_H}/\alpha_{T_0}\left(\frac{\alpha_{T_H}T_0}{\alpha_{T_0}T_H}\right)$ [sic] for coefficients α_{1-4} for all modes and all turbine stages.

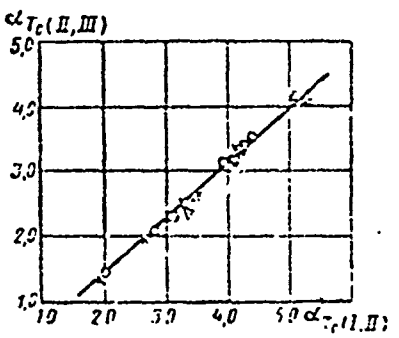

Fig. 3. Connection between heat-transfer coefficients α_{1-4} of turbine stages I, II, and III.

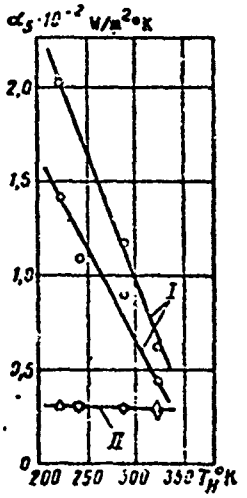

Fig. 4. Dependence of heat-transfer coefficients α_5 on T_H in cooled channels of stages I and II. The upper graph of stage I pertains to the idle mode [in stage II $\alpha_5(T_H)$ changes identically in the idle and nominal modes].

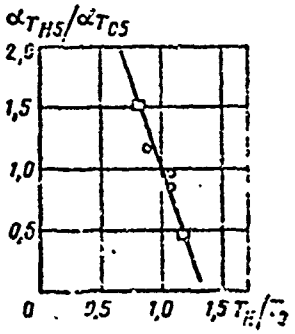

Fig. 5. Function $\alpha_{T_H}/\alpha_{T_0}(T_H/T_0)$ for α_5 of stage I in idle and rated regimes.

The decrease in the heat-transfer coefficients with an increase in t_H is explained by the associated decrease in air density and, correspondingly, the gas density. The pressure of the gas, and its temperature, decrease from stage to stage. The combined influence of these factors also results in decreased gas density. Therefore the heat-transfer coefficients become less in each successive stage. The change in speed of the gas flow has a lesser influence on the reduction in coefficients α from stage to stage.

Figures 2a and 2b show the generalized results of calculating the coefficients α_{1-4} for all rotor stages and both turbine operating modes in the form of the dependences

$$\frac{\alpha_{T_H}}{\alpha_{T_0}}\left(\frac{T_H}{T_0}\right) \text{ and } \frac{\alpha_{T_H}}{\alpha_{T_0}}\left(\frac{\alpha_{T_H}T_0}{\alpha_{T_0}T_H}\right)$$

respectively, where $T_0 = 273°K$ (or 0°C). When constructing these graphs the values of α_{T_0} were found from Fig. 1, as well as by calculation. All calculated points lie quite well on the line

$$\alpha_{T_H} = \alpha_{T_0}(1{,}62 - 0{,}0023T_H) \tag{15}$$

(Fig. 2a) and

$$\alpha_{T_H} = 1{,}16\alpha_{T_0}\left(2{,}17 - \frac{T_0}{T_H}\right)^{-1} \tag{16}$$

(Fig. 2b). Dependence (16) is more accurate, since the field of scatter of the calculation data is narrower.

Formulas (15) and (16) can be used to determine the heat-transfer coefficients for various T_H, but we must first know the coefficient α_{T_0} of each stage, which complicates the calculation. It is considerably simpler to use the dependence of the heat-transfer coefficients of each successive turbine stage on the heat-transfer coefficients of stage I (Fig. 3).

In constructing the graph, along the horizontal we plotted the values of α_{T_0} for stage I, and along the vertical – the corresponding

values of α_{T_0} for stage II. Then along the horizontal we plotted α_{T_0} for stage II, and along the vertical – the values for stage III. The connection between the heat-transfer coefficients with T_0 = = 273°K for various stages, based on this graph, can be represented by the formula

$$\alpha_{T,n}=\frac{\alpha_{T,1}}{1,34^{n-1}}, \tag{17}$$

where n is the sequence number of the turbine stage.

Substituting this expression into (16) in place of α_{T_0}, we obtain the following dependence, which is more convenient for practical use:

$$\alpha_{T_H}=1,16\alpha_{T,1}\left(2,17-\frac{T_2}{T_H}\right)^{n-1}1.34^{1-n}. \tag{18}$$

The change in coefficient α_5 in the cooling channels of stages I and III of a turbine rotor is shown in Fig. 4. From the absolute values of α_5 we see that this coefficient is approximately one order of magnitude smaller than α_1, α_2, α_3, and α_4. Because of the extremely weak air flow through the cooling channels of stage II, the value of α_5 here is practically independent of T_H. For stage I this coefficient is very sensitive to a change in temperature of the ambient air, and decreases abruptly when the latter is increased. As was noted above, coefficient α_5 has a very slight influence on the nature of temperature dependence $t_л(x)$ and $t_д(r)$; consequently, its sharp decrease with an increase in T_H will, to a considerable extent, determine the nature of the temperature field in the blades and disk of turbine stage I.

Figure 5 gives the generalized dependence $\frac{\alpha_{T_H}}{\alpha_{T_0}}\left(\frac{T_H}{T_0}\right)$ for α_5. It is described by the equation

$$\alpha_{T_{H5}}=\alpha_{T_{05}}(3,9-0,011T_H). \tag{19}$$

The value of $\alpha_{T_{05}}$ in formula (19) is determined from the graphs given in Fig. 4.

Thus, in this article, using the criterial formulas which are most expedient for calculating convection, we have obtained calculation dependences of α on t_H for the examined axial turbine. From them it follows that the intensity of convection in the turbine is reduced with a rise in t_H and the coefficients of heat transfer on the surfaces of the vane cascades are reduced from stage I to III. The value of t_H has an especially great influence on reducing the heat-transfer coefficient in the cooling channels.

From the results of calculation of heat-transfer coefficients for the given turbine we have found formulas by which we can, relatively easily, calculate the value of the heat-transfer coefficient for any turbine operation mode and for any temperature t_H.

The method used to process the results of this theoretical study of convection heat transfer in a gas turbine can be useful in heat calculations of other types of turbines.

REFERENCES

1. Жирицкий Г. С., Локай В. И., Максутова М. К., Струнков В. А., Газовые турбины авиационных двигателей, Оборонгиз, 1963.
2. Швец И. Т., Дыбан Е. П., Воздушное охлаждение роторов газовых турбин, Изд. Киевского университета, 1959.
3. Идельчик И. А., Гидравлические сопротивления, Госэнергоиздат 1954.
4. Михеев М. А., Основы теплопередачи, Госэнергоиздат, 1956.

SOLUTION OF THE PROBLEM OF STEADY HEAT CONDUCTION FOR HOLLOW COOLED NOZZLE BLADES OF GAS TURBINES

V. S. Petrovskiy

Let us examine the dy heat problem for a cooled nozzle blade having construction as shown in Fig. 1. Cooling air enters the annular cavity of the upper shroud and then the inner blade channels. To increase the cooling effect, a deflector can be installed in the inner cavity of the blade. After cooling the blade the air goes to the rotor cavity and then to the turbine flow channel.

The influence of the deflector on blade cooling can be taken into account by a certain coefficient k. Then $\alpha_в = k\alpha'_в$, where $\alpha'_в$ is the heat-transfer coefficient, calculated by known [1, 2] criterial relationships. We can set k = 1 for cooling without a deflector, k = 1.3-1.8 for cooling with a deflector, and k = 2.1-2.6 for jet cooling using a deflector.

To facilitate solution of the problem and obtain finite expressions in a form convenient for practical use, let us divide the blade lengthwise into two approximately equal parts x_1 and x_2 (Fig. 2). We will seek the solution for each part individually.

The initial equations for section x_1, considering the change in

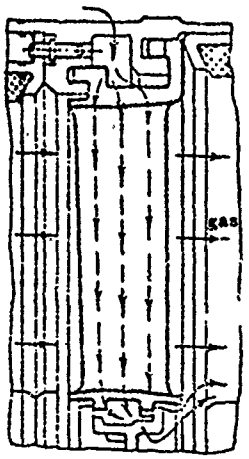

Fig. 1. Diagram of hollow cooled nozzle blade mounted between the upper and lower shrouds. The arrows show the path of the cooling air.

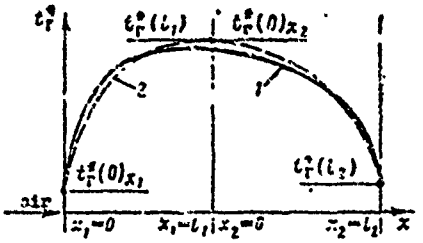

Fig. 2. Arrangement of the coordinate system when stating the thermal problem, and the approximate behavior of the dependences $t_г^*(x_1)$ and $t_г^*(x_2)$ from equations (3) and (23): 1 – experimental curve; 2 – exponents [$t_г^*(0)_{x_1}$ = (0.80-0.86)$t_г^*(l_1)$; $t_г^*(l_1)$ = 1.05 × × $t_{гс}^*$ ($t_{гс}^*$ – mean-mass temperature of the gas)].

temperature of the gas along the blade, can be written as follows:

$$\frac{d^2t_л(x_1)}{dx_1} - k_1 t_л(x_1) + k_2 t_п(x_1) = -k_3 t_г^*(x_1); \qquad (1)$$

$$\frac{dt_п(x_1)}{dx_1} - k_4 t_л(x_1) + k_5 t_п(x_1) = 0. \qquad (2)$$

Here

$$k_1 = \frac{\alpha_в P_в + \alpha_г P_г}{\lambda S}; \quad k_2 = \frac{\alpha_в P_в}{\lambda S}; \quad k_3 = \frac{\alpha_г P_г}{\lambda S}; \quad k_4 = \frac{\alpha_в P_в}{G c_p}$$

($P_в$ and $P_г$ are the perimeters of the blade profile, washed by the air and gas; S is the blade section; G is air flow). For section x_1

$$t_г^*(x_1) = k_5 \left[1 - e^{-\xi_1(x+r_0)}\right]. \qquad (3)$$

Solution of system of equations (1) and (2) for $t_л(x_1)$ gives a linear nonhomogeneous third-order differential equation:

$$\frac{d^3t_л(x_1)}{dx_1^3} + k_4 \frac{d^2t_л(x_1)}{dx_1^2} - k_1 \frac{dt_л(x_1)}{dx_1} - k_2 k_4 t_л(x_1) = -(A_1 + B_1 e^{-\xi_1 r_1}), \qquad (4)$$

where $A_1 = k_3 k_4 k_5$; $B_1 = (\xi_1 - k_4) k_3 k_5$.

Setting

$$k_3 k_4 t_л(x_1) + A_1 = y, \qquad (5)$$

we get

$$\frac{d^3y}{dx_1^3}+k_4\frac{d^2y}{dx_1^2}-k_1\frac{dy}{dx_1}-k_3k_4y=-k_3k_4B_1e^{-\xi_1x_1}. \tag{6}$$

We will seek the solution of equation (6) as the sum of the solutions of the homogeneous and nonhomogeneous parts of the equation, i.e.,

$$y=\bar{y}+y_0. \tag{7}$$

For $\bar{y}$ we can write the characteristic equation

$$r^3+k_4r^2-k_1r-k_3k_4=0. \tag{8}$$

For the interval of change of coefficients k_1, k_3, and k_4 which is possible under the examined conditions, the discriminant of equation (8) is less than zero. Consequently, it has three real roots. On this basis the solution of the homogeneous part of the equation can be represented in the form

$$\bar{y}=C_1e^{r_1x_1}+C_2e^{r_2x_1}+C_3e^{r_3x_1}. \tag{9}$$

Here

$$r_1=-\left(2v\cos\frac{\varphi}{3}-\frac{k_4}{3}\right);\quad r_2=2v\cos\left(60^\circ-\frac{\varphi}{3}\right)-\frac{k_4}{3};$$

$$r_3=2v\cos\left(60^\circ+\frac{\varphi}{3}\right)-\frac{k_4}{3};$$

$$v=-\sqrt{|p|};\quad \varphi=\arccos\frac{q}{\sqrt{v^3}};$$

$$p=-\left(\frac{k_4}{3}+\frac{k_4^2}{9}\right);\qquad q=\frac{k_4^3}{27}+\frac{k_1k_4}{6}-\frac{k_3k_4}{2}.$$

The solution of the nonhomogeneous part can be obtained from the equation

$$y_0=D_1e^{-\xi_1x_1}. \tag{10}$$

Successively differentiating it, and substituting the obtained expressions into equation (6), we find

$$D_1=\frac{k_3k_4B_1}{\xi_1^3-k_4\xi_1^2-k_1\xi_1+k_3k_4}. \tag{11}$$

Substituting (9) and (10) into (7), and considering (5), we get

$$t_3(x)=(C_1e^{r_1x_1}+C_2e^{r_2x_1}+C_3e^{r_3x_1})\frac{1}{k_3k_3}+\frac{D_1e^{-c_1x_1}}{k_3k_4}+\frac{A_1}{k_3k_4}. \quad (12)$$

Constants C_1, C_2, and C_3 are defined by the following boundary conditions:

when $x_1 = 0$ $$t_3(0)_{x_1}=t_{в.п}; \quad (13)$$

when $x_1 = l_1$ $$dt_3(l_1)/dx_1=0. \quad (14)$$

In addition, from equation (1) it follows that when $x_1 = 0$

$$\frac{d^2t_3(0)_{x_1}}{dx_1^2}=k_1t_{в.п}-k_2t_3(0)_{x_1}-k_3t_г(0)_{x_1}. \quad (15)$$

In boundary condition (13) $t_{в.п}$ is the steady equilibrium temperature of the surface of the upper shroud turned toward the gas flow. Temperature $t_{в.п}$ can be determined from the heat-balance equation for the condition of steady heat conduction through the shroud from the cavity with the cocling air to the flow channel of the turbine vane cascade. This equation for a shroud represented in the form of a flat wall will be as follows:

$$q_1=q_2=q_3+q_4, \quad (16)$$

where q_1 is the convective heat flow from the gas to the shroud ($t_{в.п}$ enters into the expression for q_1), q_2 is the conduction heat flow across the shroud, q_3 is the convective heat flow from the cooled surface of the shroud into the air flow, and q_4 is heat lost to radiation from the air-cooled shroud surface.

Simultaneous solution of equations (13)-(15) gives

$$C_1=\frac{D_{C_1}}{D_{123}}; \quad C_2=\frac{D_{C_2}}{D_{123}}; \quad C_3=\frac{D_{C_3}}{D_{123}}, \quad (17)$$

where

$$D_{C_1}=(r_3e^{r_3l_1}-r_2e^{r_2l_1})r_2r_3K_1+(r_2^2-r_3^2)K_2+(r_2e^{r_2l_1}-r_2e^{r_3l_1})K_3; \quad (18)$$

$$D_{C_2}=(r_1e^{r_3l_1}-r_3e^{r_1l_1})K_1+(r_3^2-r_1^2)K_2+(r_1e^{r_1l_1}-r_3e^{r_3l_1})K_3; \quad (19)$$

$$D_{C_3}=(r_2e^{r_1l_1}-r_1e^{r_2l_1})r_1r_2K_1+(r_1^2-r_2^2)K_2+(r_2e^{r_2l_1}r_1e^{r_1l_1})K_3; \quad (20)$$

$$D_{123}=(r_2^2-r_3^2)r_1e^{r_1l_1}+(r_3^2-r_1^2)r_2e^{r_2l_1}+(r_1^2-r_2^2)r_3e^{r_3l_1}. \quad (21)$$

In expressions (18)-(21)

$$\left.\begin{aligned} K_1 &= k_3 k_4 t_{\text{н.п}} - D_1 - A_1; \quad K_2 = \zeta_1 D_1 e^{-\zeta_1 l_1}; \\ K_3 &= \left[k_1 t_{\text{н.п}} - k_2 t_{\text{в}}(0)_{x_1} - k_3 t_{\text{г}}^{*}(0)_{x_1}\right] k_3 k_4 - \zeta_1^2 D_1. \end{aligned}\right\} \tag{22}$$

The initial differential equations for section x_2 of the blade will be the same as for x_1. The function is described by the expression

$$t_{\text{г}}^{*}(x_2) = t_{\text{г}}^{*}(0)_{x_2} - \left[t_{\text{г}}^{*}(0)_{x_2} - t_{\text{г}}^{*}(l_2)\right] \frac{1 - e^{\zeta_2 x_2}}{1 - e^{\zeta_2 l_2}}. \tag{23}$$

Repeating the series of discussions for section x_2 we get

$$t_{\text{л}}(x_2) = (C_4 e^{r_1 x_2} + C_5 e^{r_2 x_2} + C_6 e^{r_3 x_2}) \frac{1}{k_3 k_4} + \frac{D_2 e^{\zeta_2 x_2}}{k_3 k_4} - \frac{A_2}{k_3 k_4}. \tag{24}$$

Here

$$D_2 = \frac{k_3 k_4 B_2}{\zeta_2^3 + k_1 \zeta_2^2 - k_1 \zeta_2 - k_3 k_4};$$

$$A_2 = \left[\frac{t_{\text{г}}^{*}(0)_{x_2} - t_{\text{г}}^{*}(l_2)}{1 - e^{\zeta_2 l_2}} - t_{\text{г}}^{*}(0)_{x_2}\right] k_3 k_4;$$

$$B_2 = (\zeta_2^2 + k_4) k_3 \left[\frac{t_{\text{г}}^{*}(0)_{x_2} - t_{\text{г}}^{*}(l_2)}{1 - e^{\zeta_2 l_2}}\right].$$

Constants C_4, C_5, and C_6 can be found from the following boundary conditions:

when $x_2 = 0$ $$dt_{\text{л}}(0)_{x_2}/dx_2 = 0; \tag{25}$$

when $x_2 = l_2$ $$t_{\text{л}}(l_2) = t_{\text{н.п}}; \tag{26}$$

when $x_2 = 0$ $$t_{\text{л}}(0)_{x_2} = t_{\text{л}}(l_1)_{x_1}. \tag{27}$$

Here $t_{\text{н.п}}$ is the steady equilibrium temperature of the surface of the lower shroud turned toward the gas flow. It is found in the same way as $t_{\text{в.п}}$. Temperature $t_{\text{л}}(l_1)$ is calculated using (24).

From conditions (25)-(27) we find

$$C_4 = \frac{D_{C_4}}{D_{4\times6}}; \quad C_5 = \frac{D_{C_5}}{D_{4\times6}}; \quad C_6 = \frac{D_{C_6}}{D_{4\times6}}, \tag{28}$$

where

$$L_{C_4}=(e^{r_3 l_3}-e^{r_2 l_2})K_4+(r_3-r_2)K_5+(r_3e^{r_3 l_3}-r_2e^{r_2 l_2})K_6; \quad (29)$$

$$D_{C_5}=(e^{r_3 l_3}-e^{r_2 l_2})K_4+(r_1-r_2)K_5+(r_3e^{r_3 l_3}-r_1e^{r_2 l_2})K_6; \quad (30)$$

$$D_{C_6}=(e^{r_3 l_3}-e^{r_2 l_2})K_4+(r_2-r_1)K_5+(r_1e^{r_3 l_3}-r_2e^{r_2 l_2})K_6; \quad (31)$$

$$D_{4-6}=(r_3-r_2)e^{r_3 l_3}+(r_1-r_2)e^{r_2 l_2}+(r_2-r_1)e^{r_1 l_1}, \quad (32)$$

$$K_4=-\xi_2 D_2; \quad K_5=k_3 k_4 I_{n.n}-D_3 e^{r_3 l_3}+A_3; \quad (33)$$

$$K_6=k_3 k_4 I_n(l_1)-D_3+A_3.$$

Thus we obtain all the required calculation expressions for calculating the temperature along the blade.

The proposed calculation method makes it possible to take into account relatively easily the changes in gas temperature along a vane cascade. This method can be used to calculate the steady temperature state of cooled nozzle blades.

REFERENCES

1. Швец И. Т., Дыбан Е. П., Воздушное охлаждение роторов газовых турбин. Изд. Киевского университета. 1959.

2. Жаворонков Г. С., Локай В. И., Максутова М. К., Струнков В. А., Газовые турбины авиационных двигателей. Оборонгиз. 1963.

SIMULTANEOUS SOLUTION OF STATIONARY PROBLEMS OF HEAT CONDUCTION FOR GAS-TURBINE BLADES AND DISKS

V. S. Petrovskiy

In this paper we examine stationary heat problems for the shrouded rotor blades and the disk of a gas turbine with a central opening, where the profile of the disk can be approximated by a hyperbolic function.

Solution of stationary heat problems for gas-turbine blades and disks has been examined in [1-3]. In this article we aim to show how we can associate the independent solutions of heat problems for the blades and disks into a single temperature function. In addition, we show how to formulate the boundary conditions for shrouded blades with a root and for a disk containing such blades. The examined method for associating the distributions of temperature in the blade $t_л(x)$ and in the disk $t_д(r)$ in terms of the linear temperature differential in the root showed that it yields a comparatively simple finite system of expressions for calculating the temperature of the disk and blade in the form of a continuous function. The need is also eliminated for giving the temperature at any point of the disk or blade a priori, in order that further calculation be done based on this temperature. The only initial data which we use in calculations by the proposed formulas are the results of pre-thermal gas-dynamics calculation.

First let us examine the thermal problem for the blade. In general form it can be described by the equation

$$\frac{d}{dx}\left[\lambda_л(t_л) S(x) \frac{dt_л}{dx}\right] = \alpha_в(x)[t_л - t_г^*(x)] P(x). \quad (1)$$

In equation (1) the values of heat conduction of the blade material ($\lambda_л$), the area of its section (S), and the perimeter (P), and also the average heat-transfer coefficient ($\alpha_в$) and the stagnant gas-flow temperature ($t_г^*$), depend on coordinate x along the blade. Considerable difficulties are involved in solving equation (1) with substitution of functions $\lambda_л(t_л)$, S(x), $\alpha_в(x)$, $t_г^*(x)$, and P(x). It was obtained, using certain assumptions, in [1] and [2].

Let us examine the case when $\lambda_л$, $\alpha_в$, and $t_г^*$ do not depend on x. The area of the blade cross section will be considered to change by the law $S = S_0 e^{-k\alpha/L}$, where k is a constant which defines the steepness of curve S(x), and L is the blade length.

The function P(x) can also be represented by an exponent, but a more sloping one, since the perimeter of the blade changes more slowly than the area or its section. Calculations have shown that this makes it possible, when $P(L)/P(0) \geq 0.8$, to introduce into (1), in place of function P(x), the value of the average perimeter $\bar{P}$, which does not depend on x and is equal to the arithmetic mean perimeter of the base and tip of the blade.

Here equation (1) assumes the form

$$\frac{d^2\theta_л}{dx_2} - \frac{k}{L}\frac{d\theta_л}{dx} - \frac{\alpha_в \bar{P}}{\lambda_л S_0} e^{kx/l}\theta_л = 0; \quad (\theta_л = t_л - t_{гII}^*), \quad (2)$$

where $t_{гII}^*$ is the temperature of the gas at the level of the average blade cross section (Fig. 1). Equation (2) is solved by substituting $e(k/z)x = z$:

$$\theta_л = e^{kx/L}\left[A_1 I_2(2m_1 e^{kx/2L}) + B_1 K_2(2m_1 e^{kx/2L})\right], \quad (3)$$

where $m_1 = \sqrt{\frac{\alpha_в \bar{P} L^2}{\lambda_л S_0 k^2}}$, $I_2()$ and $K_2()$ are modified Bessel functions.

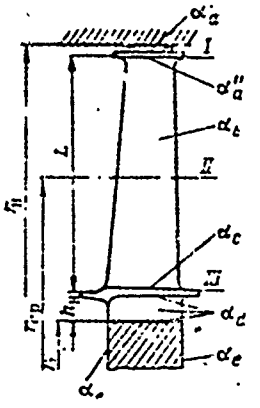

Fig. 1. Diagram of a shrouded blade on a root (α designates the mean heat-transfer coefficients).

Constants A_1 and B_1 are found from the boundary conditions at the blade base and tip.

Let us superpose the reference origin x and the plane of the blade base section. Let us assume that the temperature along the root changes linearly, while it remains constant throughout the lower shroud, equal to the temperature of the blade base. Then the boundary condition with x = 0 can be obtained from the heat-balance equation (Fig. 2)

$$Q_\lambda + Q_{\alpha_c} = Q_l + Q'_{\alpha_d}, \qquad (4)$$

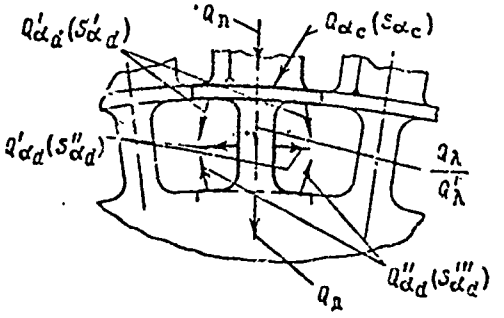

Fig. 2. Diagram for compiling heat-balance equations with x = 0 and r = r_1.

where $Q_\lambda = \lambda_\lambda \frac{dt_1}{dx} S_0$ is the heat entering section S_0 per unit time from the working part of the blade; $Q_{\alpha_c} = -\alpha_c (t_\lambda + t^*_{rII} - t^*_{rIII}) S_{\alpha_c}$ is the heat obtained by the surface of the lower shroud, turned toward the gas flow; $Q_l = \lambda_\lambda \frac{\Delta t}{h} S_{II}$ is the heat removed from section S_0 across the blade root to the turbine disk (here $\Delta t = t_\lambda(0) - t_\lambda(r_1)$. $t_\lambda(r_1)$ is the temperature of the disk when r = r_1); $Q'_{\alpha_d} = \alpha_d (t_\lambda + t^*_{rII} - t_\lambda) S_{\alpha_d} + \alpha_d \left(t_\lambda - \frac{\Delta t}{2} - t^*_{rIII} - t_\lambda\right) S_{\alpha_d}$ is the heat removed from surfaces S'_{α_d} and S''_{α_d} by the cooling air.

As can be seen from the last expression, the intensity of convection heat transfer depends not on α_d but on the gas temperature at the butt section (t^*_{rIII}). The difference in the values of t^*_{rII} and t^*_{rIII} takes into account the drop in gas temperature at the blade boundary (when x = 0). The gas-temperature distribution section thus given, with consideration of its lowering at the blade , is of rectangular shape (Fig. 3). Actually, the change in temperature will be smoother. Above it was noted that t^*_r along the blade foil is assumed to be constant, to facilitate solution of

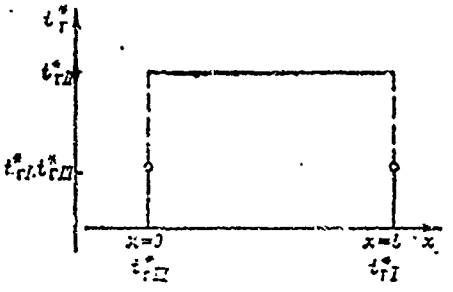

Fig. 3. Distribution of t_r^* along the blade, used to state the problem.

equation (1). Thus, assuming the gas-temperature distribution function to be rectangular we can reduce, to the best of our ability, the unfavorable role of the approximation made when stating the problem.

We must also explain why the second term appears in the equation for Q'_{α_d}. Although the area of cooling S''_{α_d} does not correspond to coordinate x = 0, nonetheless convection cooling of the side surfaces of the root occurs and it can be taken into account by this te . In final analysis it also influences the value of $t_л(0)$. Thus the boundary condition for x = 0 will be refined.

Substituting $Q_л$, Q_{σ_c}, Q_λ, and Q'_{α_d} into equation (4) we get

$$\frac{d^2t_л}{dx^2} - \varphi_1 t_л + \varphi_2 \qquad (5)$$

where

$$\varphi_1 = \frac{\alpha_d (S'_{\alpha_d} + S^*_{\alpha_d}) + \alpha_c S_{\alpha_c}}{\lambda_л S_0};$$

$$\varphi_2 = \frac{\alpha_c (t^*_{r\,II} - t^*_{r\,III}) S_{\alpha_c}}{\lambda_л S_0} + \frac{\alpha_d (S'_{\alpha_d} + S^*_{\alpha_d})}{\lambda_л S_0} (t^*_{r\,II} - t_л) + \left(\frac{S_H}{nS_0} - \frac{\alpha_d S^*_{\alpha_d}}{2\lambda_л S_0}\right) \Delta t.$$

Unlike the boundary condition $dt_л/dx = C$, where x = L, used by many authors, we can assume that the temperature of the upper shroud and, consequently, the blade tip, is constant. Actually the upper shroud, having a developed surface, easily reacts to a change in the dynamic equilibrium thermal state, and its temperature is determined by the heat-balance equation, in which the convective influx of heat from the gas to the shroud is equal to the heat lost to radiation, i.e.,

$$Q_{\alpha_c} = Q_\varepsilon. \qquad (6)$$

It is also essential that the boundary condition $dt_л/dx = 0$, when $x = L$, is completely unconfirmed by experimental data. These data indicate that the temperature has a maximum value in the middle of the blade and drops off toward the base and the tip.

It is not possible to precisely express the components Q_{α_a} and Q_ε, since the first of these is determined by the heat-transfer coefficient and the gas temperature, which will differ at various points on the shroud surface. The value of Q_ε depends on the temperature of the parts surrounding the shroud and the mutual irradiation surface, which will change as the rotor rotates.

To calculate the equilibrium temperature of the blade in this case we can use the equation of the values of the convective and radiant fluxes which are average for the entire shroud surface:

$$\bar{q}_{\alpha_a} = q_\varepsilon, \tag{7}$$

where

$$\bar{q}_{\alpha_a} = \bar{\alpha}_a (T_{г1}^* - T_{л0}^*); \quad q_\varepsilon = \varepsilon \sigma \frac{T_{л0}^4 - T_{дет}^4}{100^4}, \quad \bar{\alpha}_a = \frac{\alpha_a^* + \alpha_a^*}{2}.$$

By temperature $T_{дет}$ we mean the tentative average temperature of the surfaces of all parts surrounding the upper shroud. It will be approximately 150-200° lower than $T_{л0}$. For practical calculations we can disregard $T_{дет}^4$ and then, substituting $\bar{q}_{\alpha_a}$ and q_ε into equation (7), we get

$$\bar{\alpha}_a (T_{г1}^* - T_{л0}^*) = \varepsilon \sigma \frac{T_{л0}^4}{100^4}. \tag{8}$$

The boundary condition assumed when $x = L$ is written in the form

$$\vartheta_л = t_{л0}^* - t_{г1}^*. \tag{9}$$

Using boundary conditions (5) and (9), let us find the particular solution of equation (2):

$$\vartheta_л = [C_1 I_2(2m_1 e^{kx/2L}) + C_2 K_2(2m_1 e^{kx/2L})] \frac{e^{kx/L}}{C_5} + \\ + [C_1 I_2(2m_1 e^{kx/2L}) - C_2 K_2(2m_1 e^{kx/2L})] \frac{C_3 e^{kx/L}}{C_5}. \tag{10}$$

Here

$$C_1=(t_{ж2}-t_{г1}^*)[K_1(2m_1)+\varphi_1K_2(2m_1)];$$
$$C_2=(t_{ж2}-t_{г1}^*)[I_1(2m_1)-\varphi_1I_2(2m_1)];$$
$$C_3=e^kK_2(2m_1e^{k\cdot2});\quad C_4=e^kI_2(2m_1e^{k\cdot2})$$

and

$$C_5=e^kK_2(2m_1e^{k\cdot2})[I_1(2m_1)-\varphi_1I_2(2m_1)]+$$
$$+e^kI_2(2m_1e^{k\cdot2})[K_1(2m_1)+\varphi_1K_2(2m_1)].$$

Thus we have solved the first part of the general thermal problem, for the turbine rotor.

Now let us find the particular solution for the differential equation of stationary heat conduction for the turbine disk. The equation for an elemental annular section of the disk will be (Fig. 4)

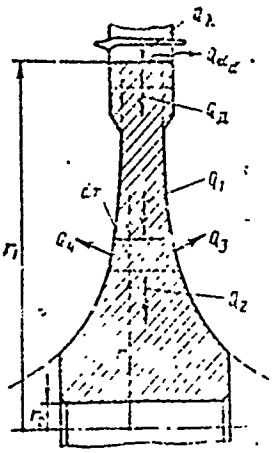

Fig. 4. Diagram for formulation of initial differential equation for stationary heat conduction for a gas-turbine disk.

$$Q_1 - Q_2 = Q_3 + Q_4, \qquad (11)$$

where $Q_1-Q_2=\frac{d}{dr}\left[\lambda_2 2\pi r 2y(r)\frac{dt_1}{dr}\right]dr$ is the quantity of heat propagating along the radius of the disk in 1 second by means of heat conduction; $Q_3+Q_4=$ $=\{\alpha_{e3}(r)[t_{ж}-t_{в3}(r)]+\alpha_{e4}(r)[t_{ж}-t_{в4}(r)]\}2\pi r dr$ is the quantity of heat given off by the lateral surfaces of the annular section of the disk ($2\pi r$ is the length of an elemental ring of width dr; y(r) is half the thickness of the disk as a function of r; $\alpha_{e3}(r)$ and $\alpha_{e4}(r)$ are heat-transfer coefficients on the lateral surfaces of the disk, $t_{в3}(r)$ and $t_{в4}(r)$ are the temperatures of the air which cools the lateral surfaces of the disk).

In further discussions we will set

$$\alpha_{e3}(r)=\alpha_{e4}(r)=\alpha_e(r) \text{ and } t_{в3}(r)=t_{в4}(r)=t_в(r).$$

As shown by comparison of the results of calculation with experimental data, we can consider approximately that α_e and $t_в$ do not depend on r.

Substitution of $Q_1 - Q_2$ and $Q_3 + Q_4$ into equation (11) with consideration of the approximations made gives

$$\frac{d}{dr}\left(4\pi\lambda_д y \frac{dt_д}{dr}\right) dr = 2\alpha_e (t_д - t_в) 2\pi r dr. \qquad (12)$$

By α_e we can also mean the arithmetic mean of the heat-transfer coefficient between $\alpha_{в3}$ and $\alpha_{в4}$.

After differentiation of equation (12) we get

$$y\frac{d^2\theta_д}{dr^2} + \frac{y}{r}\frac{d\theta_д}{dr} + \frac{dy}{dr}\frac{d\theta_д}{dr} - \frac{\alpha_e}{\lambda_д}\theta_д = 0, \qquad (13)$$

where $\theta_д = t_д - t_в$.

As an example, let us examine a disk having a hyperbolic profile with a central opening ($y = a/r$, where a is a constant). Usually, the crown of the disk is thicker than its bed, but for solving the heat problem we can replace the stepped transition from the crown to the bed by an approximate monotonic hyperbolic function, correcting it with a profile coefficient such that the change in the average value of the thermal resistance of a real disk is the same as that of the present hyperbolic-profile disk.

For a disk with the selected profile, equation (13) has the form

$$\frac{d^2\theta_д}{dr^2} - \frac{\alpha_e}{a\lambda_д} r\theta_д = 0. \qquad (14)$$

It can be represented as

$$\frac{\left[\left(\frac{2}{3}m_2\right)^{2/3} r\right]^2}{\left[\left(\frac{2}{3}m_2\right)^{2/3}\right]^2}\cdot\frac{d^2\theta_д}{dr^2} - \frac{9}{4}\left[\left(\frac{2}{3}m_2\right)^{2/3} r\right]\theta_д = 0;\quad m_2 = \sqrt{\frac{\alpha_e}{a\lambda_д}}. \qquad (15)$$

Setting $\left(\frac{2}{3}m_2\right)^{2/3} r = z$ we get

$$z^2\frac{d^2\theta_д}{dz^2} - \frac{9}{4}z^2\theta_д = 0. \qquad (16)$$

Equation (16) is one of the particular cases of the generalized Bessel equations, and its general solution will be

$$\theta_2 = \sqrt{z}\left[A_2 I_{1/3}(z^{3/2}) + B_2 I_{-1/3}(z^{3/2})\right]. \quad (17)$$

Returning to the initial independent variable we have

$$\theta_2 = \left(\frac{2}{3} m_2 r^{3/2}\right)^{1/3}\left[A_2 I_{1/3}\left(\frac{2}{3} m_2 r^{3/2}\right) + B_2 I_{-1/3}\left(\frac{2}{3} m_2 r^{3/2}\right)\right]. \quad (18)$$

Constants A_2 and B_2 are found from the boundary conditions when r = r_2 and r = r_1 (see Fig. 4). For coordinate r = r_1 we can compile the following heat-balance equation:

$$Q'_\lambda - Q''_{\alpha_д} = Q_\lambda. \quad (19)$$

Here $Q_\lambda = \lambda_2 \frac{d\theta_2}{dr} 2\pi r_1 H\beta$ is the amount of heat fed within the disk per 1 second from the arbitrary cylindrical generating surface of a disk with radius r_1 and width H (it is assumed that the isothermal surfaces in the body of the disk are positioned coaxially); β is a coefficient which takes into account the thermal resistance of the blade roots; $Q'_\lambda = \lambda_1 \frac{\Delta t}{h} S_н h$ is the heat which enters the disk through the above-mentioned arbitrary cylindrical generating surface ($S_н$ is the cross section of the blade root); n is the number of blades; $Q''_{\alpha_д} = \alpha_2 \theta_1 S''_{\alpha_д} n$ is the heat removed by the cooling air from the sections of the surface of the disk crown included between the grooves of the blade roots (see Fig. 4).

Substituting the values of $Q_д$, Q'_λ, and $Q''_{\alpha_д}$ into (19) we get, when r = r_1,

$$\frac{d\theta_2}{dr} = \varphi_3 \theta_2 + \varphi_4, \quad (20)$$

where

$$\varphi_3 = -\frac{\alpha_2 S''_{\alpha_д} n}{\lambda_2 2\pi r_1 H\beta}; \quad \varphi_4 = \frac{\lambda_1 S_н n \Delta t}{\lambda_2 2\pi r_1 H\beta}. \quad (20')$$

The boundary conditions when r = r_2 are compiled based on the following concepts. Since we are using a hyperbolic disk profile, the theoretical profile of its stepped part will be too strongly developed in the axial direction. This greatly increases the area of the central part of the disk, air-cooled with heat-transfer

coefficient α_e. To compensate for the artificially elevated heat removal in the stepped section we can stipulate that there is no heat transfer along the inner surface of the opening, and then the boundary condition when $r = r_2$ will be

$$d\theta_д/dr=0. \tag{21}$$

Boundary conditions (20) and (21) determine the values of constants A_2 and B_2 in equation (18), whose particular form in this case will be as follows:

$$\theta_д=\frac{\varphi_4}{C_6}\sqrt{\frac{r}{r_1}}\Big[I_{-2/3}\left(\frac{2}{3}m_2r_2^{3/2}\right)I_{-1/3}\left(\frac{2}{3}m_2r^{3/2}\right)-$$
$$-I_{2/3}\left(\frac{2}{3}m_2r_2^{3/2}\right)I_{1/3}\left(\frac{2}{3}m_2r_2^{3/2}\right)\Big], \tag{22}$$

where

$$C_6=I_{-2/3}\left(\frac{2}{3}m_2r_2^{3/2}\right)\left[m_2r_1^{1/2}I_{2/3}\left(\frac{2}{3}m_2r_1^{3/2}\right)-\varphi_3I_{-1/3}\left(\frac{2}{3}m_2r_1^{3/2}\right)\right]-$$
$$-I_{2/3}\left(\frac{2}{3}m_2r_2^{3/2}\right)\left[m_2r_1^{1/2}I_{-2/3}\left(\frac{2}{3}m_2r_1^{3/2}\right)-\varphi_3I_{1/3}\left(\frac{2}{3}m_2r_1^{3/2}\right)\right].$$

In equations (10) and (22) the constants φ_2 and φ_4 include the temperature differential along the root $\Delta t = t_л(0) - t_д(r_1)$.

First let us find $\theta_л(0)$ and $\theta_д(r_1)$:

$$\theta_л(0)=\frac{\varphi_2}{C_5}[C_1I_2(2m_1)+C_2K_2(2m_1)]C_5^{-1}+[C_3I_2(2m_1)-C_4K_2(2m_1)]; \tag{23}$$

$$\theta_д(r_1)=\frac{\varphi_4}{C_6}\Big[I_{2/3}\left(\frac{2}{3}m_2r_2^{3/2}\right)I_{-1/3}\left(\frac{2}{3}m_2r_1^{3/2}\right)-$$
$$-I_{2/3}\left(\frac{2}{3}m_2r_2^{3/2}\right)I_{1/3}\left(\frac{2}{3}m_2r_1^{-3/2}\right)\Big]. \tag{24}$$

Let us introduce the designations

$$C_7=\frac{\alpha_c(t^*_{г11}-t^*_{111})S_ч}{\lambda_1S_0}+\frac{\alpha_д(S'_{зд}-S'_{зд})}{\lambda_1S_0}(t^*_{г11}-t_н);$$

$$C_8=\frac{S_н}{hS_0}-\frac{\alpha_дS'_{зд}}{2\lambda_1S_0};\quad C_9=\frac{\lambda_з\frac{S_рn}{h}-\alpha_дS'_{зд}n}{\lambda_12\pi r_1H\beta};$$

$$C_{10}=I_{-2/3}\left(\frac{2}{3}m_2r_2^{3/2}\right)I_{-1/3}\left(\frac{2}{3}m_2r_1^{3/2}\right)-$$
$$I_{2/3}\left(\frac{2}{3}m_2r_2^{3/2}\right)I_{1/3}\left(\frac{2}{3}m_2r_1^{3/2}\right).$$

Then, considering the values of φ_2 and φ_4 from formulas (5) and (20), equations (23) and (24) can be rewritten in the form

$$t_л - t^*_{д11} = -\{C_1 I_2(2m_1) + C_2 K_2(2m_1)\} C_5^{-1} + \\ + \{C_1 I_2(2m_1) - C_2 K_2(2m_1)\} C_5^{-1}(C_7 + C_6 \Delta t); \quad (25)$$

$$t_л - t_п = -C_6^{-1} C_9 C_{10} \Delta t. \quad (26)$$

Subtracting (26) from (25) we get

$$\Delta t = \frac{t^*_{д11} - t_п + \{C_1 I_2(2m_1) + C_2 K_2(2m_1)\} C_5^{-1} + \{C_1 I_2(2m_1) - C_2 K_2(2m_1)\} C_5^{-1} C_7}{1 - \{C_1 I_2(2m_1) - C_2 K_2(2m_1)\} C_5^{-1} C_6 - C_6^{-1} C_9 C_{10}}. \quad (27)$$

The right side of (27) does not depend on x or r, and therefore the value of $\Delta t = t_л - t_д$ can be determined on the basis of initial data of gas-dynamics calculations before determining functions $t_л(x)$ and $t_д(r)$. This does not contradict physical sense, since Δt in final analysis depends on blade temperature when $x = 0$ and disk temperature when $r = r_1$. In other words, the values of $t_л(0)$ and $t_д(r_1)$ are interconnected unambiguously by conditions of heat transfer and heat conduction, which also determine the nature of functions $t_л(x)$ and $t_д(r)$ themselves. Thus, substituting (27) into (10) and (22) we get interrelated dependences $t_л(x)$ and $t_д(r)$ in final form. In practice it is advisable to substitute the numerical value of Δt directly into (10) and (22).

Theoretical calculation of blade and disk temperature using these calculation functions begins with determination of the heat-transfer coefficients. For this we must have data from gas-dynamics calculation and data on air used to cool the turbine. The next step in calculating the temperature state will be solution of the intermediate equations in numerical form: first to find the value of Δt and then to calculate the constants C_1/C_5, C_2/C_5, $C_3\varphi_2/C_5$, $C_4\varphi_2/C_5$ $\frac{z_1}{C_6}\frac{I_{-2/3}\left(\frac{2}{3}m_1 r_2^{3/2}\right)}{\sqrt{r_1}}$ and $\frac{z_1}{C_6}\frac{I_{2/3}\left(\frac{2}{3}m_1 r_2^{3/2}\right)}{\sqrt{r_1}}$ in equations (10) and (22), reduced to comparatively simple form, changing coordinate x within limits from 0 to L, and r within limits from r_2 to r_1, we can find the radial distribution of temperature in a gas-turbine rotor disk and blade.

Thus, solution of the simultaneous problem of heat conduction for a turbine disk and blades allows us to calculate the temperature field of a turbine rotor, using only initial data from gas-dynamics calculations for the blading and hydrodynamic calculations for cooling.

The use of the temperature different[illegible]t the root makes it possible to compile boundary conditions for the blade base and the disk periphery such that after colution of individual initial equations for the disk and blade we get a single temperature function for the rotor disk and blades.

REFERENCES

1. Тирский Г. А., О распределении температуры в неоднородном стержне переменного сечения, обтекаемом газом. Известия АН СССР, ОТН, 1957, № 1.

2. Швец И. Т., Дыбан Е. П. Определение температуры в охлаждаемых турбинных лопатках с учетом переменности площади сечения по высоте лопатки. Труды института теплоэнергетики АН УССР, 1955, № 12.

3. Костюк А. Г., Температурное поле турбинного диска. Известия АН СССР, ОТН, 1954, № 6.

NUMERICAL SOLUTION OF THE PROBLEM OF NONSTATIONARY HEAT CONDUCTION FOR A GAS-TURBINE ROTOR WITH ROOT-SHROUDED BLADES

Ye. Ye. Denisov and V. S. Petrovskiy

The one-dimensional nonstationary process of heat conduction for a gas-turbine rotor with blades will be described by the following system of equations:

for the disk

$$\frac{\partial t_1(r,\tau)}{\partial \tau} = \frac{a_1}{rz(r)} \frac{\partial}{\partial r}\left[rz(r)\frac{\partial t_1(r,\tau)}{\partial r}\right] - \frac{\alpha_1(r)}{c_1\gamma_1 z(r)}[t_1(r,\tau) - t_{\text{ж}}(r)]; \qquad (1)$$

for a solid blade

$$\frac{\partial t_2(x,\tau)}{\partial \tau} = \frac{a_2}{S(x)} \frac{\partial}{\partial x}\left[S(x)\frac{\partial t_2(x,\tau)}{\partial x}\right] - \frac{\alpha_2(x)P(x)}{c_2\gamma_2 S(x)}[t_2(x,\tau) - t_{\text{ж}}(x)]. \qquad (2)$$

We will examine a disk with a central opening. The designation of the heat-transfer coefficients on the appropriate surfaces, the direction of the heat flow, the quantities of heat passing across specific heat-transfer surfaces in 1 second and used in the heat-balance equations when formulating the boundary conditions are given in Fig. 3 on p. 6.

To obtain equations convenient for numerical analysis, let us use the feature of the actual distribution of temperature in the blade and formulate, for the system disk/blades, two heat problems

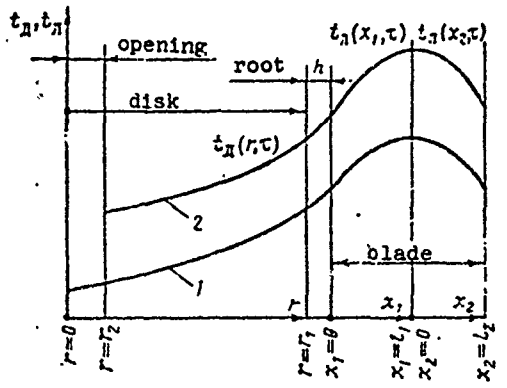

Fig. 1. Position of coordinates and approximate form of the temperature dependence for the system disk/blades: 1 – disk without opening; 2 – disk with opening.

(Fig. 1): the first for the disk ($r_2 \leq r \leq r_1$) and the root sections of the blades ($0 \leq x_1 \leq l_1$), and the second for the blade tip sections ($0 \leq x_2 \leq l_2$). Here the total length of the blade $l = l_1 + l_2$ and $l_1 \approx l_2$. With such individual statement of the heat problem we can formulate relatively simple boundary conditions for the entire system and obtain the function $\tau_\Gamma^*(x)$ which is of decisive significance for the distribution of temperature in the blade in the following form:

for section $0 \leq x_1 \leq l_1$

$$t_r^*(x_1) = t_r^*(l_1) - \zeta_1(l_1 - x_1)^4; \tag{3}$$

for section $0 \leq x_2 \leq l_2$

$$t_r^*(x_2) = t_r^*(0) - \zeta_1' x_2^2. \tag{4}$$

We will solve the problem relative to a gas turbine, for which functions γ in initial equations (1) and (2) can be written thusly:

$$z(r) = z_0 + \zeta_2(r - r_0)^2, \qquad (r_2 \leqslant r \leqslant r_1), \tag{5}$$

$$a_0(r) = a_0(r_2)\, e^{\ldots r}, \qquad (r_2 \leqslant r \leqslant r_1), \tag{6}$$

$$\left.\begin{aligned} P(x) &= P(0)\, e^{\ldots x}, \\ S(x) &= S(0)\cdot e^{\ldots x}, \end{aligned}\right\} \quad (0 \leqslant x_1 \leqslant l_1); \tag{7}$$

$$(0 \leqslant x_2 \leqslant l_2). \tag{8}$$

The temperature of the cooling air $t_в$ and the average heat-transfer coefficient in the vane cascade α_3 will be considered to be constants.

Let us formulate boundary conditions for the first heat problem. We will consider the surface of the central opening to be adiabatic. Then

$$\frac{\partial t_1(r_2\tau)}{\partial r} = 0 \tag{9}$$

when $r = r_2$. From the heat-balance equation, compiled for coordinate $r = r_1$ [3]

$$Q_1 + Q_2 = Q_3 \tag{10}$$

we can obtain the following boundary conditions:

$$\frac{\partial t_1(r_1, \tau)}{\partial r} = \varphi_1 t_1(0, \tau)_{x_1} - \varphi_2 t_1(r_1, \tau) + \varphi_3. \tag{11}$$

From the heat-balance equation compiled for coordinate $x_1 = 0$,

$$Q_4 + Q_5 = Q_6 + Q_7 \tag{12}$$

we get

$$\frac{\partial t_2(0, \tau)_{x_1}}{\partial x_1} = \varphi_4 t_1(0, \tau)_{x_1} - \varphi_5 t_1(r_1, \tau) - \varphi_6. \tag{13}$$

And, finally, for $x_1 = l_1$ we can set

$$\frac{\partial t_2(l_1, \tau)}{\partial x_1} = 0. \tag{14}$$

In boundary conditions (11) and (13)

$$\varphi_1 = \frac{\lambda_1 S_{y_2} n}{\lambda_1 2\pi r_1 H h_2}; \quad \varphi_2 = \frac{\alpha_2 S_{y_2}^{*} n}{\lambda_1 2\pi r_1 H \beta} + \varphi_1;$$

$$\varphi_3 = (\varphi_2 - \varphi_1) t_0;$$

$$\varphi_4 = \frac{\alpha_3 S_{x_2}' + \alpha_4 S_{x_3}}{\lambda_2 S_2(0)} + \frac{S_H}{h S_1(0)} + \frac{\alpha_3 S_{x_2}'}{2\lambda_2 S_2(0)};$$

$$\varphi_5 = \frac{S_H}{h S_1(0)} - \frac{\alpha_3 S_{x_2}}{2\lambda_2 S_2(0)};$$

$$\varphi_6 = \frac{\alpha_3 S_{x_2}}{\lambda_2 S_2(0)} t_2^{*}(0) + \frac{\alpha_3 \left(S_{x_2}' + S_{x_3}^{*}\right)}{\lambda_2 S_2(0)} t_0.$$

Let us write equations (1) and (2) as follows:

$$\frac{\partial t_1(r, \tau)}{\partial \tau} - a_1 \frac{\partial^2 t_1(r, \tau)}{\partial r^2} - b_1(r) \frac{\partial t_1(r, \tau)}{\partial r} - c_1(r) t_1(r, \tau) = f_1(r); \tag{15}$$

$$\frac{\partial t_2(x_1, \tau)}{\partial \tau} - a_2 \frac{\partial^2 t_2(x_1, \tau)}{\partial x_1^2} - b_2(x_1) \frac{\partial t_2(x_1, \tau)}{\partial x_1} - c_2(x_1) t_2(x_1, \tau) = f_2(x_1). \tag{16}$$

Here

$$b_1(r) = \frac{a_1}{z(r)} \frac{dz(r)}{dr} + \frac{a_1}{r}; \quad c_1(r) = -\frac{\alpha_m(r)}{c_1 \varrho_1 z(r)}; \quad f_1(r) = -c_1(r) t_0(r);$$

$$b_2(x_1) = \frac{a_2}{S(x_1)} \frac{dS(x_1)}{dx_1}; \quad c_2(x_1) = -\frac{\alpha_2(x_1) P(x_1)}{c_2 \varrho_2 S(x_1)}; \quad f_2(x_1) = -c_2(x_1) t_0^{*}(x_1).$$

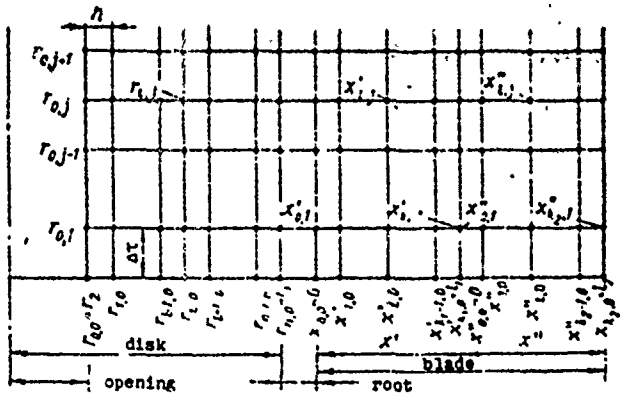

Fig. 2. Calculation diagram using the grid method.

The time variable varies within the limits $0 < \tau < \infty$.

As the initial condition let us assume (when $\tau = 0$)

$$t_д(r, 0) = t_л(x_1, 0) = t_0. \qquad (17)$$

We will seek the solution in the rectangles $r_2 \leq r \leq r_1$, $0 \leq \tau \leq T$, and $0 \leq x_1 \leq l_1$, $0 \leq \tau \leq T$ (Fig. 2) which are associated with the appropriate boundary conditions.

Let us examine a node grid formed by the points of intersection of two families of parallel straight lines. The first family

$$\left[r^{[i]} = ih + r_2,\ (i = 0, 1, 2, \ldots, n),\ n = \frac{r_1 - r_2}{h};\right.$$
$$\left.x_1^{[i]} = ih,\ (i = 0, 1, 2, \ldots, k_1),\ k_1 = l_1/h\right];$$

the second family $[\tau = j\Delta\tau,\ (j = 0, 1, 2, \ldots)]$.

Step h along axes x and r_1 and time step $\Delta\tau$ along axis τ are taken the same for the disk and the blade.

The nodes lying on the lines $r = r_2$, $r = r_1$, $x_1 = 0$, and $x_1 = l_1$ will be boundary nodes for the examined problem; all others are internal nodes.

If some node in the rectangle for the disk/blade pertains to function $t_д(r,\tau)$ or $t_л(x_1,\tau)$, respectively, for it we can write the difference which approximates the real values of the derivatives at this point. For

$$\partial t_д(r, \tau)/\partial r \text{ and } \partial t_л(x_1, \tau)/\partial x_1$$

this is

$$\frac{\theta^{[i+1,j]} - \theta^{[i-1,j]}}{2h}, \qquad (18)$$

while for

$$\partial^2 t_3(r, \tau)/\partial r^2 \quad \text{and} \quad \partial^2 t_3(x_1, \tau)/\partial x_1$$

this is

$$\frac{\theta^{[i+1,j]} - 2\theta^{[i,j]} + \theta^{[i-1,j]}}{h^2}. \tag{19}$$

The derivative $\partial t/\partial \tau$ in node [i,j] can be represented in three forms:

$$\frac{\theta^{[i,j+1]} - \theta^{[i,j]}}{\Delta\tau}; \tag{20}$$

$$\frac{\theta^{[i,j]} - \theta^{[i,j-1]}}{\Delta\tau}; \tag{21}$$

$$\frac{\theta^{[i,j-1]} - \theta^{[i,j-1]}}{2\Delta\tau}. \tag{22}$$

In accordance with (20)-(22) we can use three schemes for approximating initial equations (1) and (2). To solve the posed problem on a computer with limited storage, the first difference scheme is more convenient, since the initial condition gives the value of the approximating functions $\theta_д$ and $\theta_л$ for all nodes of the first series ($\tau = 0$). Using these data we can calculate the values corresponding to the second-series nodes ($\tau_{i,0} + \Delta\tau$).

The values in the nodes located on the boundaries of the rectangles can be obtained using boundary conditions (9), (11), (13), and (14). Then all calculation operations are repeated for the next series of nodes $\tau_{i,1} + \Delta\tau$, etc.

The use of a difference scheme involving equation (21) makes it necessary to solve a system of $[(n + 1) + (k_1 + 1)]$ equations with the same number of unknowns, which is too much of a load on the computer memory.

The difference scheme using equation (22) is unstable. The calculation errors in this case accumulate extremely rapidly, and after only several time steps in many nodes they become commensurate with the value of the approximating function.

Using the first scheme for approximating initial differential

equations (1) and (2), we get the following system of difference equations:

$$\theta_1^{l,j+1} = \left(a_1 \frac{\theta_1^{l+1,j} - 2\theta_1^{l,j} + \theta_1^{l-1,j}}{h^2} + \right.$$

$$\left. + b_1 \frac{\theta_2^{l+1,j} - \theta_1^{l-1,j}}{2h} + c_1^{l} \theta_2^{l,j} + f_1^{l}\right) \Delta\tau + \theta_2^{l,j}, \qquad (23)$$

where

$$b_1^{l} = \frac{a_1}{z_l} \frac{z_{l+1} - z_{l-1}}{2h} + \frac{a_1}{r_l}; \quad c_1^{l} = -\frac{\alpha_0^{l}}{c_{10}\rho_1 z_l};$$

$$f_1^{l} = -c_1^{l} t_n^{l}, \ (l = 1, 2, \ldots, n-1 \text{ и } j = 0, 1, 2, \ldots);$$

and

$$\theta_2^{l,j+1} = \left(a_2 \frac{\theta_2^{l+1,j} - 2\theta_2^{l,j} + \theta_2^{l-1,j}}{h^2} + \right.$$

$$\left. + b_2^{l} \frac{\theta_2^{l+1,j} - \theta_2^{l-1,j}}{2h} + c_2^{l} \theta_2^{l,j} + f_2^{l}\right) \Delta\tau + \theta_2^{l,j}, \qquad (24)$$

where

$$b_2^{l} = \frac{a_2}{S_l} \frac{S_{l+1} - S_l}{2h}; \quad c_2^{l} = -\frac{\alpha_2 P_l}{c_{20}\rho_2 S_l}; \quad f_2^{l} = -c_2^{l} t_{r_1}^{c}.$$

The boundary conditions must also be represented in difference form. For the line $r = r_2$

$$\frac{\theta_2^{l,j} - \theta_2^{0,j}}{h} = 0, \text{ or } \theta_2^{0,j} = \theta_2^{1,j}; \qquad (25)$$

for lines $r = r_1$ and $x_1 = 0$

$$\frac{\theta_2^{n,j+1} - \theta_2^{n-1,j+1}}{h} = \varphi_1 \theta_2^{0,j+1} - \varphi_2 \theta_2^{n,j+1} + \varphi_3; \qquad (26)$$

$$\frac{\theta_2^{1,j+1} - \theta_2^{0,j+1}}{h} = \varphi_4 \theta_2^{0,j+1} - \varphi_5 \theta_2^{n,j+1} - \varphi_6; \qquad (27)$$

for the line $x_1 = l_1$

$$\frac{\theta_2^{k_1,j} - \theta_2^{k_1-1,j}}{h} = 0, \text{ or } \theta_2^{k_1,j} = \theta_2^{k_1-1,j}. \qquad (28)$$

The initial conditions for the examined problem can be written as follows:

$$\theta_2^{l,0} = t_0, \ l = 0, 1, 2, \ldots, n;$$
$$\theta_2^{l,0} = t_0, \ l = 0, 1, 2, \ldots, k_1. \qquad (29)$$

The problem is formulated such that the rectangular grid for a disk on line $r = r_1$ has no independent boundary condition. The

values of approximating function $\theta_д$ in nodes belonging to line r = = r_1 are determined from the associated boundary conditions for lines r = r_1 and x_1 = 0. In turn, each of the values of the numerical solution in the nodes on these lines is defined, on the one hand, by $\theta_д^{[n-1,j]}$ and $\theta_л^{[0,j]}$ according to (26), and on the other hand, by $\theta_л^{[1,j]}$ and $\theta_д^{[n,j]}$ according to (27).

Consequently, to associate equations (23) and (24) by means of such difference relationships, in which there would be successive transition from known values in the nodes on the lines $r^{[n-1]}$ and $x_1^{[n]}$ to unknown values of the approximating functions in nodes on the lines r = r_1 and x_1 = 0, we must solve equations (26) and (27) for $\theta_д^{[n,j]}$ and $\theta_л^{[0,j]}$; we get

$$\theta_д^{[n,j]} = \frac{\Delta_1}{\Delta}; \quad \theta_л^{[0,j]} = \frac{\Delta_2}{\Delta}, \tag{30}$$

where

$$\Delta = h^2(\bar{\tau}_3\bar{\tau}_1 - \bar{\tau}_4\bar{\tau}_2) - h(\bar{\tau}_4 - \bar{\tau}_2) - 1;$$

$$\Delta_1 = h^2(\bar{\tau}_4\bar{\tau}_5 - \bar{\tau}_6\bar{\tau}_1) + h(\bar{\tau}_1 - \bar{\tau}_4\theta_д^{[n-1,j]} - \bar{\tau}_1\theta_л^{[j,j]}) - \theta_д^{[n-1,j]};$$

$$\Delta_2 = h^2(\bar{\tau}_3\bar{\tau}_5 - \bar{\tau}_6\bar{\tau}_2) - h(\bar{\tau}_6 - \bar{\tau}_2\theta_л^{[1,j]} - \bar{\tau}_3\theta_д^{[n-1,j]}) - \theta_л^{[1,j]}.$$

The set of initial difference equations (23) and (24) and boundary conditions (25)-(28), where (26) and (27) are presented in the form of (30), allow us to determine, on a computer, the approximate numerical solution of the thermal problem for the disk and the lower part of the blades.

Let us formulate the problem for the blade tips ($0 \le x_2 \le l_2$). The node grid for the approximate solutions is also shown in Fig. 3. It is adjacent to the node grid for the lower part of the blades ($0 \le x_1 \le l_1$), and is formed by the intersection of the families of parallel lines $x_2^{[i]}$ = ih (i = 0, 1, 2, ..., k_2) and τ_j = $j\Delta\tau$.

The process of heat conduction in this case is described by equation (2), which in difference form will look like (24), except

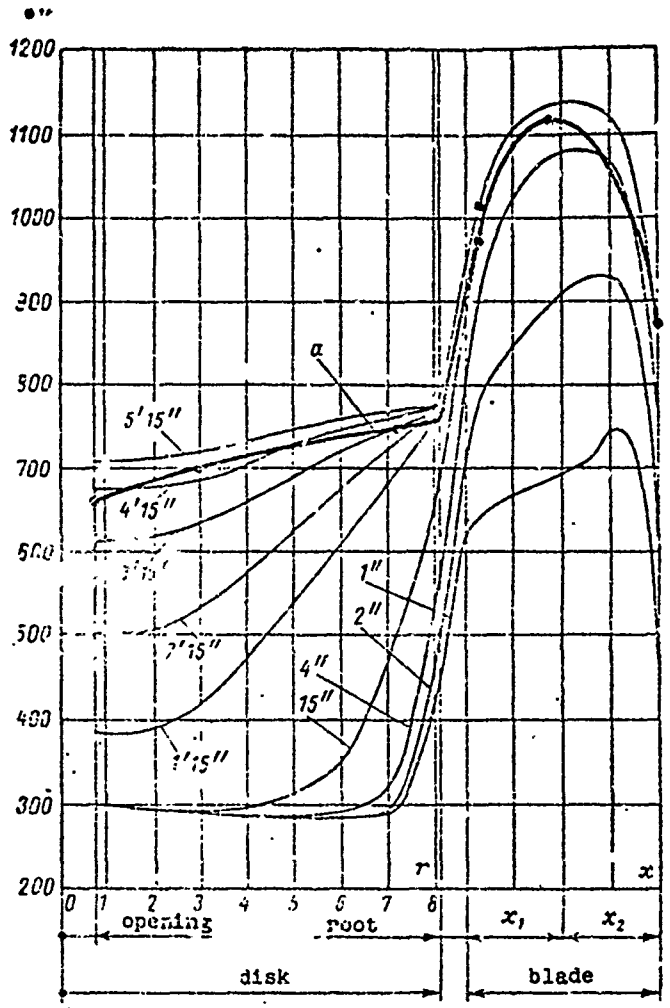

Fig. 3. Results of numerical solution for stage I of a gas turbine: a – experimental curve for the steady process.

that i changes from 1 to $k_2 - 1$. Functions α_3, P, and S_n have the same form as for the blade root section (x_1), but the numerical values of P(0), $S_n(0)$, ζ_4, and ζ_5 will differ Function t_r^* is represented by parabolic equation (4).

As the boundary conditions we have: when $x_2 = 0$

$$\frac{\partial t_1(0, \tau) x_2}{\partial x_2} = 0; \qquad (31)$$

when $x_2 = l_2$

$$t_2(l_2, \tau) = t_r^*(l_2) - \\ - [t_r^*(l_2) - t_0] e^{-m\tau} - \\ - [t_r^*(l_2) - t_{0.n}] (1 - e^{-m\tau}). \qquad (32)$$

The last equation is based on the ideas that the temperature of the blade tip is equal to that of the upper shroud, whose heating is determined mainly by convection and radiation heat transfer with the ambient medium and occurs by a law similar to those for regular heat regimes.

In difference form, conditions (31) and (32) are written as follows:

for line $x_2 = 0$

$$t_3^{[0,j]} = t_3^{[1,j]}, \qquad (33)$$

for line $x_2 = l_2$

$$\theta_2^{[k_2,j]} = t_r^*(l_2) - \left[t_r^*(l_2) - \theta_2^{[k_1,0]}\right] e^{-m[j\Delta\tau]} - \\ - \left[t_r^*(l_2) - t_{0,n}\right]\left[1 - e^{-m[j\Delta\tau]}\right]. \quad (34)$$

The boundary conditions for $x_1 = l_1$ and $x_2 = 0$ do not provide for equality of the temperature functions on the left and right; therefore it is possible that the approximate numerical solutions for sections x_1 and x_2, obtained for the same moment of time $j\Delta\tau$, will differ somewhat from one another. This difference does not exceed the error of the calculation method as a whole, and therefore we can use as the final result one of the two temperature values obtained for the boundary of blade sections x_1 and x_2. Obviously, to increase reserve blade strength it is best to take the higher of the two adjacent temperature distributions.

Figure shows the results of numerical integration by the proposed method, and gives data on direct measurement of temperature for stage I of a turbine rotor. We see the good agreement between the theoretical and experimental results. The theoretical dependence for a prolonged time (approaching the stationary mode) is somewhat above the experimental dependence because the calculation was done for the mean-mass temperature in the vane cascade of stage I, $t_r^* =$ = 1176°K, while the experimental data were obtained at 1133°K.

With numerical integration by the grid method of the heat-conduction problem examined in this article, we used an explicit scheme. In this case it is possible, since under stable conditions

$$\Delta\tau \leq \frac{h^2}{2\max S(x)} \quad \text{and} \quad \Delta\tau \leq \frac{h^2}{2\max P(r)} \quad (35)$$

functions $S(x)$ and $P(r) = rz(r)$ do not change rapidly.

The integration steps were selected as follows. We first gave the step $h \approx 0.15r_1$. The selected step, identical for the disk and for the blade (the problem was posed for a disk of small diameter), allowed us to reduce the time step $\Delta\tau$ to 0.5 seconds. Trial calculations with three values of $\Delta\tau$, from maximum to minimum, showed the good convergence of the solution.

The proposed calculation method allows us to divide the general heat-conduction problem into two simpler ones: one for the disk and root sections, the other for the upper peripheral parts of the blades. This method can be recommended for theoretical study of the temperature state of the rotor of any gas turbine.

Use of the grid method for solving the examined problem using a computer with limited storage is more feasible and economical.

REFERENCES

1. Лыков А. В., Теория теплопроводности, изд-во «Высшая школа», 1967.
2. Березин И. С., Жидков Н. П., Методы вычислений, т. 2, Физматгиз, 1959.
3. Петровский В. С., «Авиационная техника» 1969, № 1.

INTENSIFYING THE COOLING OF THE LEADING EDGE OF ROTOR BLADES

V. S. Petrovskiy and M. I. Tsaplin

With internal cooling of gas-turbine rotor blades it is not always possible to guarantee a lowering of the temperature of the hottest parts of the blade. We know that one of the hardest-to-cool parts is the leading edge which receives about 25% of the heat fed to the blade.

At present, great interest has arisen in so-called penetration cooling. However, the development of such a cooling method has been hampered by the lack of porous materials having the requisite strength and hydraulic characteristics. Therefore, a number of organizations have studied cooling methods similar to penetration cooling - perforation of a finished blade by electroerosion, laser, or electron beam. The figure shows a blade in which cooling of the leading and trailing edges is intensified by this method.

Naturally, the operating conditions of a wall perforated with a specific spacing and a wall made of a porous material are different, particularly relative to the protective action. When air is blown in in the form of individual jets, the decrease in heat flow at the point of intake is of a clearly expressed local nature which leads, on the whole, to a lowering of the effectiveness of the pro-

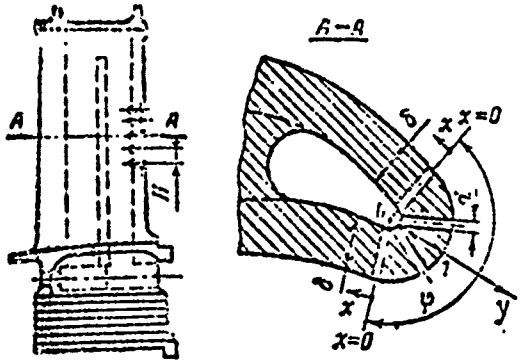

Blade with perforated leading edge.

tective effect. However, with exhausting of the air there develops a noticeable aftereffect, protecting certain parts of the blade in the direction of gas flow. Thus we can consider that cooling by blade perforation is midway between purely penetration cooling and film cooling. In this regard it is advisable to examine the possibility of cooling the leading edge of a blade which combines the high effect of internal cooling, characteristic of a permeable wall, with the protective aftereffect at the point of inlet. The diagram of such leading-edge cooling is shown in the figure, which also shows the location of the coordinate system with an indication of the reference origin and the heat-flow scheme.

Let us examine the distribution of temperature on the leading edge of a blade. Let us isolate a sector on the inlet edge which is bounded by radius of curvature r_0 and lines connecting the coordinate origin with the points of discharge of air onto the blade surface. A heat flow with known value α_r acts on a cylindrical surface of radius r_0. The influence of the discarded walls on the temperature of the leading edge is replaced by a heat flow of intensity q, uniformly distributed along the boundary lines, considering that this value is known.

Under such conditions the heat-balance equation for an elemental volume will have the form

$$\frac{d}{dr}\left[\lambda F(r)\frac{dt}{dr}\right]-\alpha_r u_r(t-\theta)=2qh, \qquad (1)$$

where t is the current value of the temperature of the leading edge along the radius; θ is the temperature of the cooling medium; r is the current radius; $F(r) = \varphi rh$ is the area of a cylindrical section of an element of the leading edge; h is the thickness of the isolated

element, equal to the distance between the channels along the blade; d is the channel diameter; $\alpha_в$ is the heat-transfer coefficient inside the channel to the cooling air; $\xi = l/r_0$ is the proportionality factor, which takes into account the difference between channel length and radius r_0.

Let us introduce the dimensionless parameter $m = \frac{\pi d \alpha \xi r_0}{\lambda \varphi h}$ and the relative coordinate $y = r/r_0$.

Let us rewrite the initial equation in the form

$$y \frac{d^2t}{dy^2} + \frac{dt}{dy} - m(t-\theta) = 2q \frac{r}{\varphi\lambda}. \qquad (2)$$

We take into account the heating of the cooling medium.

For the given cooling scheme we can assume that heat transfer on the inner radius of curvature of the inlet edge is practically equal to zero. Then the current value of the temperature θ of the cooling medium can be associated with the initial value θ_0 by the relationship

$$\theta = \theta_0 + \frac{\lambda \varphi h}{G c_p} y \frac{dt}{dy}, \qquad (3)$$

where G is the air flow arriving per element of length of the blade.

Substituting the value of θ into equation (2) we get

$$y \frac{d^2t}{dy^2} + (1 + sy) \frac{dt}{dy} - m(t - \theta_0) = \frac{2qr_0}{\varphi\lambda}, \qquad (4)$$

where $s = \frac{\pi d \alpha_в \xi r_0}{G c_p}$ is a dimensionless parameter. Let us introduce the new variable z = sy and set

$$\vartheta = t - \theta_0 + \frac{2qr_0}{\varphi\lambda m}. \qquad (5)$$

Then equation (4) can be rewritten in the form

$$z \frac{d^2\vartheta}{dz^2} + (1 + z) \frac{d\vartheta}{dz} - n\vartheta = 0, \qquad (6)$$

where $n = \frac{G c_p}{\lambda \varphi h}$ is a dimensionless parameter.

For integral values of n, the general solution can be found using exponential series.

The general solution for the second-order equation will be

$$\vartheta = C_1\vartheta_{n,1}(z) + C_2\vartheta_{n,2}(z),$$

while the first particular solution [1]

$$\vartheta_{n,1}(z) = \sum_{k=0}^{n} \frac{n!}{(k!)^2(n-k)!} z^k. \tag{7}$$

Since for boundary conditions of the form

$$\left.\begin{aligned} d\vartheta/dz &= \mathrm{Bi}_r(t_W^* - t) \quad \text{when } z = s; \\ \frac{d\vartheta}{dz} &= 0 \qquad\qquad\quad \text{when } z = 0 \end{aligned}\right\} \tag{8}$$

the integration constant C_2 should be zero, it is not necessary to seek a second particular solution.

Determining integration constant C_1 from conditions (8) and converting to the initial variables, we can obtain a calculation expression for determining the temperature across the in edge

$$t = t_{\text{экв}} + \frac{t_1 - t_{\text{экв}}}{\vartheta_n(1)} \vartheta_n(y). \tag{9}$$

Here

$$t_{\text{экв}} = t_c - \frac{2q_r}{\pi d\alpha_{\text{к}}} \tag{10}$$

is the equivalent temperature of the cooling medium;

$$\vartheta_n(y) = \sum_{k=0}^{n} \frac{n!}{(k!)^2(n-k)!} (sy)^k;$$

$\vartheta_n(1)$ is the value of function $\vartheta_n(y)$ when y = 1; t_1 is the temperature on the surface of the edge, i.e., when y = 1,

$$t_1 = \frac{\mathrm{Bi}_r t_W^* + t_{\text{экв}} \frac{1}{\vartheta_n(1)} \frac{d\vartheta_n(1)}{dy}}{\mathrm{Bi}_r + \frac{1}{\vartheta_n(1)} \frac{d\vartheta_n(1)}{dy}}, \tag{11}$$

where $\mathrm{Bi}_r = \alpha_{r.\text{к}} r_0/\lambda$ is the Biot criterion for the leading edge. Thus we have obtained an expression for calculating the temperature

of the inlet edge which contains, in addition to the known values, the value of q which is still unknown. Let us find the value of q from the condition that on the blade wall there is a protective film of air which passes through the opening on the leading edge.

Under the assumption of a one-dimensional scheme for heat flows, the initial heat-conduction equation will be

$$\frac{d}{dl}\left(\lambda f \frac{dt}{dl}\right) + \alpha_г H (t_{ад} - t) - \alpha_в H (t - t_0) = 0, \qquad (12)$$

where δ and $f = H\delta$ are the wall thickness and area; H is the distance between the channels emerging on one side of the blade; l is the distance from the point of air exhaust.

Introducing the concept of the average temperature of the washing medium

$$T = \frac{\alpha_г t_{ад} + \alpha_в t_0}{\alpha_г + \alpha_в}, \qquad (13)$$

where $t_{ад}$ is the adiabatic wall temperature, and designating the relative coordinate as $x = l/\delta$, we get initial equation (12) in the form

$$\frac{d^2t}{dx^2} - k^2(t - T) = 0, \qquad (14)$$

where $k^2 = \frac{2\alpha_{ср}\delta}{\lambda}$ is a dimensionless parameter; $\alpha_{ср} = \frac{\alpha_г + \alpha_в}{2}$ is the average heat-transfer coefficient.

The adiabatic temperature $t_{ад}$ is equal to the temperature of the gas at the heat-insulated wall. It depends on the flow and temperature of the coolant, the temperature of the gas flow, and the distance from the point of injection. Usually, the adiabatic temperature is determined experimentally and is the basic factor which takes into account the aftereffect of injection. The experimentally determined adiabatic gas temperature at the wall approximated quite well by the formula

$$t_{ад} = t_1 + (t_w^* - t_1) e^{-k_в P_{охл} l}. \qquad (15)$$

Here $p_{вых}=\frac{10^3 G_{охл}}{2H(\gamma w)_r}$, where $(\gamma w)_r$ is the mass velocity of the gas flow at the point of injection; $G_{охл}/2$ is the flow of coolant to one side of the blade profile; θ_1 is the air temperature at the outlet from the cooling channels; $k_в$ is a coefficient which takes into account the direction of injection: for tangential injection $k_в = 0.337$, for normal inkection $k_в = 0.186$.

Since T is a complex function of x, to simplify the calculations dependence (13) can be approximated by the expression

$$T=T_0+(T_\infty-T_0)(1-e^{-\beta x}), \tag{16}$$

where T_0 is the initial temperature of the washing medium when x = 0; T_∞ is the temperature of the washing medium as $y \to \infty$; β is an approximation coefficient.

Setting $\Delta T = T - t$ and bearing in mind that

$$\frac{d^2T}{dx^2}=-\beta^2(T_\infty-T_0)e^{-\beta x}, \tag{17}$$

we get

$$\frac{d^2(\Delta T)}{dx^2}-k^2(\Delta T)=-\beta^2(T_\infty-T_0)e^{-\beta x}. \tag{18}$$

The general solution of the given equation is obtained as the sum of the general solution of the corresponding homogeneous equation

$$(\Delta T)_1=C_1e^{kx}+C_2e^{-kx}$$

and the particular solution

$$(\Delta T)_{частн}=De^{-\beta x}.$$

Substituting the numerical solution into the initial equation and solving it for D, we get

$$(\Delta T)_{частн}=-\frac{\beta^2}{\beta^2-k^2}(T_\infty-T_0)e^{-\beta x}.$$

Then the general solution will have the form

$$(\Delta T)=C_1e^{kx}+C_2e^{-kx}-\frac{\beta^2}{\beta^2-k^2}(T_\infty-T_0)e^{-\beta x}. \tag{19}$$

The integration constant is determined from the following boundary conditions:

$$\left.\begin{aligned} t &= t_{1,0} \text{ when } x = 0, \\ t &= t_{\infty} \text{ when } x = \infty \end{aligned}\right\}. \tag{20}$$

where $t_{1,0}$ is the average temperature of the inlet edge,

$$t_{1,0} = \int_0^1 t\,dy. \tag{21}$$

Thus, the distribution of temperature along the blade profile near the inlet edge can be defined by the formula

$$t = -\left[T_0 - t_{1,0} + \frac{k^2}{\beta^2 - k^2}(T_{\infty} - T_0)\right] e^{-kx} + \frac{\beta^2}{\beta^2 - k^2}(T_{\infty} - T_0)\, e^{-\beta x}. \tag{22}$$

Let us find the heat flow from the shaped part of the blade when x = 0:

$$\begin{aligned} Q &= -\lambda \delta H \left(\frac{dt}{dl}\right)_{l=0} = -\lambda H \left(\frac{dt}{dx}\right)_{x=0} = \\ &= -\lambda H k (T_{\infty} - T_0)\left(\frac{\beta}{\beta + k} - \bar{t}_{1,0}\right), \end{aligned} \tag{23}$$

where $\bar{t}_{1,0} = \frac{t_{1,0} - T_0}{T_{\infty} - T_0}$ is the average relative temperature of the leading edge.

Consequently, the unknown intensity of the heat flow $q = Q/2r_0h$.

Solving equations (9), (10), (11), (21), and (23) simultaneously we can define $\theta_{0,эк}$, t_1, and Q, corresponding to the given cooling conditions. Setting $t_{1,0} = \int_0^1 t\,dy \approx \frac{t_1 + t_0}{2}$, where t_0 is the temperature of the leading edge of the blade at radius y = 0, we can write the expression for the average temperature of the inlet edge

$$t_{1,0} \approx \frac{t_1[1 + \vartheta_n(1)] - t_{0,эк}[1 - \vartheta_n(1)]}{2\vartheta_n(1)}. \tag{24}$$

Setting $\frac{2\pi Hk}{\pi d\alpha_{эк} z r_0} = \Phi$, we get

$$\theta_{0,\text{эк}} = \frac{2\left[\mathrm{Bi}_r \vartheta_n(1) + \frac{d\vartheta_n(1)}{dy}\right]\left[\frac{3\Phi}{3+k}(T_\infty - T_0) + T_0\Phi + t_0\right] - \Phi\,\mathrm{Bi}_r t_w^*[1 + \vartheta_n(1)]}{2\frac{d\vartheta_n(1)}{dy}(\Phi+1) + \mathrm{Bi}_r \vartheta_n(1)(\Phi+2) - \mathrm{Bi}_r\Phi} \qquad (25)$$

and

$$t_1 = \frac{\mathrm{Bi}_r t_w^* + \theta_{0,\text{эк}}\frac{1}{\vartheta_n(1)}\frac{d\vartheta_n(1)}{dy}}{\mathrm{Bi}_r + \frac{1}{\vartheta_n(1)}\frac{d\vartheta_n(1)}{dy}}. \qquad (26)$$

The air temperature at the channel outlet

$$\vartheta_1 = \vartheta_0 + \frac{Q_\Sigma}{Gc_p}, \qquad (27)$$

where Q_Σ is the total heat fed to the leading edge;

$$Q_\Sigma = \lambda h \frac{t_1 - t_{0,\text{эк}}}{\vartheta_n(1)}\frac{d\vartheta_n(1)}{dy} = 2\lambda H k (T_\infty - T_0)\left(\frac{3}{3+k} - \bar{t}_{1,0}\right). \qquad (28)$$

It should be noted that the second term in expression (28) can be both positive and negative, i.e., there can be additional heat removal to the wall adjacent to the leading edge or there can be heat feed.

The direction of the heat flow is determined by the sign of the complex $\left(\frac{3}{3+k} - \bar{t}_{1,0}\right)$.

When $\beta/(\beta + k) > \bar{t}_{1,0}$ there will be heat feed, while when $\beta \div (\beta + k) < \bar{t}_{1,0}$ there will be heat removal. Thus, with an increase in the value of β the ratio $\beta/(\beta + k)$ will increase, and this means that the temperature of the washing medium as a function of the distance from the point of injection will change very rapidly. Therefore, to decrease the heat fed from the wall, in all cases it is necessary to strive to increase the coefficient $k = \sqrt{2\mathrm{Bi}}$, where $\mathrm{Bi} = (\alpha_{cp}/\lambda)\delta$.

Below, by way of illustration, we give an example of calculation of cooling the leading edge of a rotor blade for the following initial data:

$T_w^* = 1243°$ K; $\theta_0 = 738°$ K; $\alpha_{r\,н} = 4060$ W/m²°K;
$r_0 = 2{,}25 \cdot 10^{-3}$ m; $\lambda = 21$ W/m°K; $\alpha_r = 2100$ W/m²°K;
$d = 0{,}3 \cdot 10^{-3}$ m; $\alpha_n = 267$ W/m²°K; $\delta = 1{,}5 \cdot 10^{-3}$ m;
$H = h = 10^{-3}$ m; $\beta = 0{,}55$; $\xi = 0{,}94$; $\varphi = 1.2$ rad;
$G = 6{,}5 \cdot 10^{-5}$ kg/s (air flow through one channel on the leading edge).

On the basis of these initial data we calculate the following complexes which appear in the calculation expression:

$$\mathrm{Bi}_r = \frac{\alpha_{r,н} r_0}{\lambda} = 0{,}437; \quad n = \frac{Gc_p}{\lambda \xi h} = 2{,}76;$$

$$s = \frac{\pi d \alpha_n \xi r_0}{Gc_p} = 0{,}0855; \quad \alpha_{ср} = \frac{\alpha_r + \alpha_n}{2} = 1220 \text{ W/m}^2\text{°K};$$

$$k = \sqrt{\frac{2\alpha_{ср}\beta}{\lambda}} = 0{,}418; \quad \Phi = \frac{2\beta H k}{\pi d \alpha_n \xi r_0} = 5{,}91.$$

Since we obtained n = 2.76, to calculate the values of the functions $\$_n(1)$ and $d\$_n(1)/dy$ we must round n off to the nearest whole number. When the calculation must be precise, we must calculate the initial values (i.e., t_1, $\theta_{0,эн}$, $t_{1,0}$) for a number of values of n including the interval of interest to us, and by interpolation calculate the true values of t_1, $\theta_{0,эн}$, and $t_{1,0}$, corresponding to the fractional value of n. Let us take n = 3; then

$$\$_n(y) = \$_3(y) = 1 - 3sy + \frac{3}{2}(sy)^2 + \frac{(sy)^3}{6} = 1{,}257;$$

$$\frac{d\$_3(y)}{dy} = 3s + 3s^2 y + \frac{s^3}{2} y^2 = 0{,}255;$$

$$T_0 = \frac{\alpha_r \theta_1 + \alpha_n \theta_0}{\alpha_r + \alpha_n} = 764°\text{K};$$

$$T_w = \frac{\alpha_r T_w^* + \alpha_n \theta_0}{\alpha_r + \alpha_n} = 1171°\text{K}.$$

Here we assume that in first approximation $\theta_1 \approx \theta_0 + 30$, since heating of the air in the channels is still unknown.

Setting n = 3, we can calculate, from formula (25), $\theta = 654°$K, from formula (26) $T_1 = 1054°$K, and from formula (24) $T_{1,0} = 908°$K.

Then let us find $\bar{t}_{1,0} = \frac{t_{1,0} - T_0}{T_w - T_0} = 0{,}6$ and $\frac{s}{s+k} - \bar{t}_{1,0} = 0{,}569 - 0{,}6 < 0$, i.e., we obtained the case of heat removal to the wall adjacent to the

leading edge.

Then, using formulas (28) and (27) we get

$$Q_{\Sigma}=2{,}02\cdot10^{-3}\ \text{W} \quad \text{and} \quad \theta_1=771^{\circ}\text{K}.$$

This result corresponds to the case when the protective aftereffect of the air discharged from the openings on the leading edge was estimated from the dependences for normal injection (at right angles to the incoming flow). If we consider that at an injection angle of less than 90° (in practice it can be about 60°) the protective aftereffect is intensified and will be somewhere between the aftereffect with tangential and normal injection (at injection angles from 0° to 30° the protective aftereffect will be identical), with injection at an angle of 60° the protective effect can be estimated by the coefficient $k_в$, which is approximately equal to the arithmetic mean of the values for normal and tangential injections.

Considering the influence of the injection angle and taking coefficient $\beta = 0.376$, we get $\theta_{0,эк} = 583^{\circ}\text{K}$, $T_1 = 1031^{\circ}\text{K}$, and $T_{1,0} = 985^{\circ}\text{K}$, i.e., the maximum temperature of the leading edge is reduced from 1054 to 1031°K.

The relative depth of cooling $\bar{\eta}=\frac{t_{\text{г}}^{*}-t_1}{t_{\text{г}}^{*}-t_{\text{к}}}=0.331$, where $t_к$ is the temperature of the air behind the compressor.

Thus, the depth of cooling is very great.

The method of cooling the leading edge of a rotor blade, examined in this article, is very expedient since with the appropriate materials it allows us to reduce the blade temperature and raise the temperature of the gas in a turbine.

The given calculation example shows that as a result of the simultaneous action of internal (in the channels) and external air cooling (by creating a low-temperature protective film on the blade

surface), the temperature of the leading edge is noticeably reduced compared with that of an uncooled blade.

REFERENCE

1. Камке Э. Справочник по обыкновенным дифференциальным уравнениям. изд-во «Наука», 1965.

CALCULATING THE COOLING OF GAS-TURBINE DISKS

V. S. Petrovskiy and M. I. Tsaplin

The reliability and longevity of gas-turbine installations depend, to a considerable extent, on the efficiency of one of the most important parts – the turbine disks. The efficiency of the disks is greatly influenced by the level of permitted temperatures, which is guaranteed by using cooling.

When calculating air cooling we must solve the heat-balance equation for the turbine rotor as a whole, using dependences which associate the heat flow with the temperatures of individual characteristic points of the rotor. In particular, to perform such calculations we must establish the dependence of heat transfer to the disk on the temperature of the crown for the given geometric dimensions, the thermophysical properties selected, and the boundary conditions.

The question of calculating the temperature in cooled disks has already been examined in the technical literature. For example, [1] contains a survey of methods for solving the heat-conduction equation compiled on the assumption of a one-dimensional heat-flow scheme:

$$\frac{d}{dx}\left[\lambda F(x)\frac{dt}{dx}\right]-2\alpha\pi r_{cyl}(t-t_f)=0, \qquad (1)$$

where F(x) is the area of a cylindrical disk section; λ and α are

coefficients of the heat conduction of the disk material and heat transfer from its lateral surface; t and θ are the temperatures of the disk and the coolant; r and $x = r/r_{об}$ are current and dimensionless radii; $r_{об}$ is the radius of the disk crown.

On the basis of the survey the conclusion is drawn that simultaneous consideration of variability, along the radius, of the area of the cylindrical section, the temperature of the coolant, and the heat-transfer coefficients leads to a substantial complication of the calculation expressions, which hinders their practical application. This same work poses the problem of developing sufficiently accurate and simple engineering calculation methods. In particular, a number of simplifying assumptions are proposed which reduce the problem to one of solving the heat-conduction equation for a disk of constant thickness when the temperature of the coolant and the heat-transfer and heat-conduction coefficients are constant along the radius.

Under these assumptions, the expressions for calculating the temperature distribution along the radius and heat transfer from the disk with boundary conditions

$$\left.\begin{aligned} t &= t_{об} \text{ when } x = 1, \\ dt/dx &= 0 \text{ when } x = 0 \end{aligned}\right\} \qquad (2)$$

assume the form

$$t = \theta + \frac{t_{об} - \theta}{I_0(n)} I_0(nx); \qquad (3)$$

$$Q = 2\pi H_{об} \lambda n (t_{об} - \theta) \frac{I_1(n)}{I_0(n)}, \qquad (4)$$

where $I_0(n)$, $I_0(nx)$, and $I_1(n)$ are Bessel functions of the first kind of an imaginary argument; $n = \sqrt{\frac{2\alpha r_{об}^2}{\lambda H_{об}}}$ is a dimensionless parameter; $t_{об}$ and $H_{об}$ are the temperature and width of the disk crown.

The error in the method of calculating temperatures with such assumptions is too great, and therefore the proposed simplifications raise a number of objections.

First, the disks of modern gas-turbine installations, particularly transport installations, are of complex shape due to attempts to achieve uniform-strength designs. Here the width of the disk crown near the root joints is considerably greater than that of the shank $b_ш$ with which the crown is attached with smooth fillets (Fig. 1). Obviously, approximation of such a disk by a profile of constant thickness leads to a substantial increase in heat transfer.

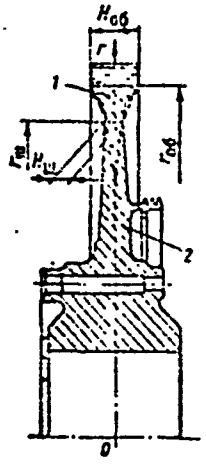

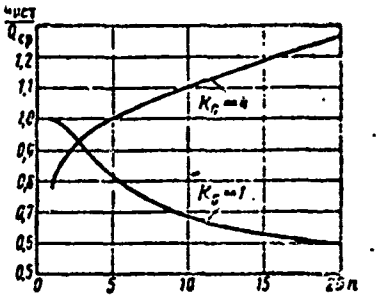

Fig. 2. Change in relative heat transfer from a disk of constant thickness as a function of parameter n, when the temperature of the cooling medium is replaced by the arithmetic mean for various values of $K_0 = Gc_p/4\pi H_{об}\lambda$.

Fig. 1. Disk profile.

Second, when organizing the cooling, the relative flow of air to one stage is usually 0.3-0.5%. With such low flows the heating of the air becomes noticeable. Introduction into the calculation of the average temperature of the coolant does not allow proper correction of the heat-transfer value. By way of illustration, Fig. 2 shows curves of the change in relative heat transfer from a disk of constant thickness when the coolant temperature is replaced by the arithmetic mean temperature. As we can see, with a decrease in flow the error can reach 40%, and increases heat transfer.

Third, when $n \geq 10$ the peripheral parts of the disk have the greatest influence on heat transfer. In this case, use in the calculations of heat-transfer coefficient values which are average over the entire disk surface will also yield an error, since the local heat-transfer coefficients in the region of the crown will be greater than the average coefficients.

Thus, the problem posed in [1] of developing a simple and sufficiently accurate method for calculating disk temperature cannot be considered as having been satisfactorily solved.

Let us examine the problem of distribution of temperature in the disk shown in Fig. 1. Let us divide a disk of complex shape into two parts: peripheral part 1 adjacent to the crown, characterized by an abrupt contraction in profile, and central part 2, having a slight taper.

For the contour which approximates the contracting part of the disk, the change in area of the cylindrical section

$$F(x) = F_{об} x^p, \tag{5}$$

where $F_{об} = 2\pi r_{об} H_{об}$ is the area of the cylindrical section of the crown, and p is a certain constant.

Equation (1) can be solved in quadratures only for the case p = 3 and constant temperature of the coolant. This solution, for boundary conditions (2), has the form

$$t = \theta + (t_{об} - \theta) x^m, \tag{6}$$

where $m = -1 + \sqrt{1 + n^2}$ is a dimensionless parameter.

For real turbine disks the contracting peripheral part cannot always be reproduced by the contour p = 3 and, in addition, the temperature of the cooling air is not constant along the radius.

Let us assume that the temperature difference t - θ will change along the radius by an exponential law

$$t - \theta = \Delta t x^s, \tag{7}$$

where s is a certain constant.

Then the solution of equation (1) with boundary conditions (2) will be

$$t = \theta_{вх} + (t_{об} - \theta_{вх}) x^k, \tag{8}$$

where k is a dimensionless parameter, $\theta_{вх}$ is the initial temperature of the cooling air, and Δθ is air heating due to heat transfer with the disk.

The parameter

$$k = -\frac{p-1}{2} + \sqrt{\left(\frac{p-1}{2}\right)^2 + n^2 \frac{t_{c.k} - \theta_{ux} - \Delta\theta}{t_{o6} - \theta_{ux}}}. \quad (9)$$

From (8) and (9) it follows that $\Delta t = t_{o6} - (\theta_{ux} + \Delta\theta)$ and s = k + p - 3. In this case, heat transfer from the disk

$$Q = 2\pi H_{oc} \lambda k (t_{o6} - \theta_{ux}). \quad (10)$$

Let us express heating of the cooling air as a result of heat transfer with the disk as fcllows:

$$\Delta\theta = \frac{Q}{Gc_p} = qk(t_{o6} - \theta_{ux}), \quad (11)$$

where $q = \frac{2\pi H_{oc}\lambda}{Gc_p}$ is a dimensionless parameter and G is the flow of cooling air on both sides of the disk, and substitute it into expression (9). After certain transformations we finally get

$$k = -\frac{p-1+qn^2}{2} + \sqrt{\left(\frac{p-1+qn^2}{2}\right)^2 + n^2}. \quad (12)$$

Assumption (7) is valid when the temperature in the center of the disk equals that of the cooling air. Such a condition can be strictly satisfied only for disks which are constricted toward the center. The thickness of the disk can also be expressed as H = $= H_0 x^{p-1}$, which means that

$$p > 2. \quad (13)$$

It is interesting to note that for disks of constant thickness, for which the parameter n is rather high, the temperature in the center approaches that of the cooling air. When n = 5 the temperature difference is several degrees, while when n > 10 there is practically no difference. Consequently, under such conditions formulas (6) and (8) can be used to calculate temperatures and heat flow in disks of constant thickness as well.

To illustrate this, Fig. 3 shows a curve of the change in $\bar{Q}$ for p = 1 and q = 0, the ratio of the values of heat transfer in a flat disk, calculated from formulas (4) and (10). When $n \geq 10$ the error in determining the heat flow from (12) is less than 5%.

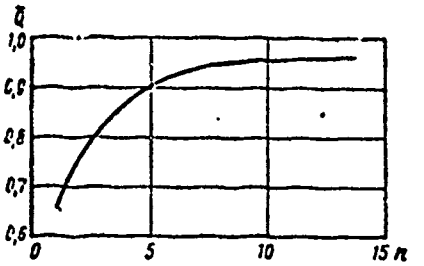

Fig. 3. Change in relative error when determining heat transfer from a disk of constant thickness, using simplified formulas, as a function of values of parameters n and q.

This same result can be obtained by expanding the functions $I_0(n)$ and $I(n)$. Then

$$\bar{Q} = \frac{1 - \frac{3}{8n} + \frac{15}{128n^2} - \dots}{1 + \frac{1}{8n} + \frac{1}{128n^2} + \dots}. \qquad (14)$$

As can be easily seen, this relationship tends toward one for large values of n.

As already noted, the central parts of gas-turbine disks have a slight taper. For fixed and portable gas-turbine plants with such disks, $n \gg 5$ as a rule. For these cases the additional heat transfer along the turbine shaft, and also the central opening in the disk (where there is no heat transfer), have no noticeable effect on the distribution of temperature along the radius or on the intensity of heat transfer from the disk. Consequently, for these conditions, according to [2], we can use the familiar dependences for a disk of constant thickness derived relative to boundary conditions (2).

Let us write the distribution of temperature along the disk radius relative to boundary conditions (2) in the form

$$t = t_{\infty} + \frac{t_{n.6} - t_{\infty}}{\chi(1)} \chi(x), \qquad (15)$$

where $\chi(x)$ is some function of a dimensionless coordinate.

Having at our disposal solutions which describe the distribution of temperature along the radius for the simplest contours, which individually approximate the peripheral and central parts of the disks, with the given boundary conditions we can find an expression for calculating the temperature in a disk of more complex profile. For this purpose, at the point where one contour becomes another it is necessary to combine solutions (15). Designating by subscripts 1 and 2 the values in the expression for the peripheral and central parts of a disk, respectively, for the transition point ($x = \xi$) we get

the condition

$$\left.\begin{aligned} t_1 &= t_2, \\ \frac{dt_1}{dx} &= \frac{dt_2}{dx}. \end{aligned}\right\} \qquad (16)$$

Obviously, for the given values of $t_{об}$ and $\theta_{вх}$ conditions (16) are mutually exclusive. In order to observe equality of the heat flows at the transition point, temperature $\theta_{вх1}$ must be selected so as to assure the required heat transfer on the part of the peripheral section when replacing the poorly approximating contour in the central part. We designate this temperature as $\theta_{вх,эк}$. We proceed analogously when selecting temperature $t_{об2}$ and correspondingly introducing the designation $t_{об,эк}$. Then the expression for calculating heat transfer and temperature distribution along the disk radius assumes the form

$$Q = 2\pi l l_{об1} \lambda (t_{об1} - \theta_{вх,эк}) \frac{\chi_1'(1)}{\chi_1(1)}. \qquad (17)$$

The values in formula (17) are the equivalent temperature of the cooling medium for approximation contour 1

$$\theta_{вх,эк} = \frac{\chi_1(1)\chi_2'(\xi)\theta_{вх} + t_{об}[\chi_1'(\xi)\chi_2(\xi) - \chi_1(\xi)\chi_2'(\xi)]}{\chi_1(1)\chi_2'(\xi) + \chi_1'(\xi)\chi_2(\xi) - \chi_1(\xi)\chi_2'(\xi)}; \qquad (18)$$

$$\left.\begin{aligned} t_1 &= \theta_{вх.эк} + \frac{t_{об} - \theta_{вх.эк}}{\chi_1(1)}\chi_1(x) \text{ when } 1 \leqslant x \leqslant \xi, \\ t_2 &= \theta_{вх} + \frac{t_{об.эк} - \theta_{вх}}{\chi_2(1)}\chi_2(x) \text{ when } \xi \leqslant x \leqslant 1 \end{aligned}\right\} \qquad (19)$$

and the equivalent temperature on the crown for approximation contour 2

$$t_{об.эк} = \theta_{вх} + (t_{об} - \theta_{вх.эк}) \frac{\chi_2(1)\chi_1'(\xi)}{\chi_2'(\xi)\chi_1(1)}. \qquad (20)$$

In a number of cases, when performing actual calculations it is possible to simplify considerably the derived formulas. For example, when approximating the constricted peripheral sections $\chi_1(1) = 1$. Then, for relatively thin disks, with high values of the heat-transfer coefficients, the dimensionless parameters for the central parts are quite large ($n_2 > 10$). In these cases $\theta_{вх,эк}$ and $t_{об,эк}$ tend toward $\theta_{вх}$ and then relationships (17)-(20) degenerate into elemental

formulas (8) and (10). This indicates that for large values of parameter n, basic heat transfer occurs on the peripheral sections of the disk, and the shape of the central portions has no substantial influence on it.

We should note that a calculation expression of the type of (6), which is a particular case of expression (8), was proposed in Stodola's work [3], and at that time was widely used [4]. However, criticism contained in [5] resulted in the fact that the Stodola method was generally relegated to obscurity. This was not quite justified.

Figure 4 shows curves of relative heat transfer from a disk $Q/2\pi r^2\alpha(t_{об} - \theta)$ as a function of parameter n for various values of p. With an increase in n the influence of constant p on heat transfer decreases. Consequently, the Stodola formula and calculation methods based thereon can be used in cases when $n \geq 15$. Such conditions, as a rule, exist for the disks of aviation gas turbines.

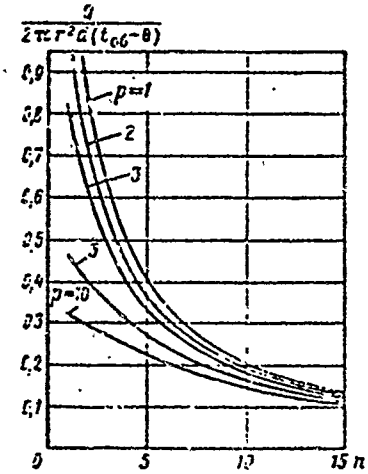

Fig. 4. Change in relative heat transfer from disk crown as a function of parameters n and q.

In conclusion, let us estimate the error when reducing the two-dimensional heat-conduction to a one-dimensional one.

Let us examine temperature distribution in a flat disk under the assumption that the temperature of the cooling medium does not change along the radius. The initial heat-conduction equation for this case

$$\frac{\partial^2 t}{\partial x^2} + \frac{1}{x}\frac{\partial t}{\partial x} + \frac{\partial^2 t}{\partial y^2} = 0, \qquad (21)$$

where $x = rH$, $y = h/H$ are dimensionless coordinates.

Let us find the general solution for the following boundary conditions:

$$\left.\begin{aligned} &1)\quad t=t_{об}\ \text{when}\ x=x_{об},\\ &2)\quad -\frac{\partial t'}{\partial y}=\frac{\alpha''H}{\lambda}(t-\delta)\ \text{when}\ y=1,\\ &3)\quad \frac{\partial t}{\partial y}=\frac{\alpha'H}{\lambda}(t-\delta)\ \text{when}\ y=0. \end{aligned}\right\} \qquad (22)$$

Designating

$$\mathrm{Bi}'=\frac{\alpha'H}{\lambda},\quad \mathrm{Bi}''=\frac{\alpha''H}{\lambda},\quad k=\frac{\mathrm{Bi}''(t_{сб}-\delta'')}{\mathrm{Bi}'(t_{сб}-\delta')},$$

after the solution, presented in [6], we get calculation expressions for determining the temperature field through a flat disk and the value of heat transfer from the crown:

$$t=t_{об}-2(t_{об}-\delta')\mathrm{Bi}'\sum_{m=1}^{\infty}\frac{[M_m\,\mathrm{ch}\,(p_m y)+\mathrm{sh}\,(p_m y)]\,J_0(p_m x)}{(\mathrm{Bi}'M_m-p_m)\mu_m J_1(\mu_m)}; \qquad (23)$$

$$Q=4\pi r_{об}^2\lambda(t_{об}-\delta')\mathrm{Bi}'\sum_{m=1}^{\infty}\frac{M_m\,\mathrm{sh}\,p_m+\mathrm{ch}\,p_m-1}{(\mathrm{Bi}'M_m-p_m)\mu_m}, \qquad (24)$$

where $M_m=-\frac{\mathrm{Bi}''\,\mathrm{sh}\,p_m+p_m\,\mathrm{ch}\,p_m+kp_m}{p_m\,\mathrm{sh}\,p_m+\mathrm{Bi}''\,\mathrm{ch}\,p_m-k\,\mathrm{Bi}'}$; $p_m=\mu_m/x_{об}$ is an expansion parameter; μ_m is the value of the roots of a zero-order Bessel function of a real argument.

In the case of symmetrical cooling conditions (Bi' = Bi" = Bi, k = 1), calculation expression (24) is considerably simplified:

$$Q=8\pi r_{об}^2\lambda(t_{об}-\delta)\mathrm{Bi}\sum_{m=1}^{\infty}\frac{1}{(p_m-M_m\mathrm{Bi})\mu_m}. \qquad (25)$$

Having determined heat flows Q_2 from formula (25) for symmetrical boundary conditions, and having calculated their corresponding heat flows Q_1 from formula (4), we can construct the graph $Q_1/Q_2 = f \times (\mathrm{Bi}, x_{об})$ (Fig. 5). From the graph we see that reduction of the two-dimensional problem to a one-dimensional one leads to an error which becomes substantial at large Bi. This error tends to increase the value of heat transfer from the disk and results in lower temperature values on the crown; when Bi $\leq$ 0.2 the error does not exceed 5% and need not be taken into consideration.

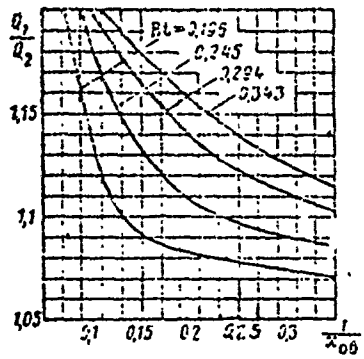

Fig. 5. Change in error when determining heat transfer from the crown of a disk of constant thickness when reducing the two-dimensional heat-conduction problem to a one-dimensional one.

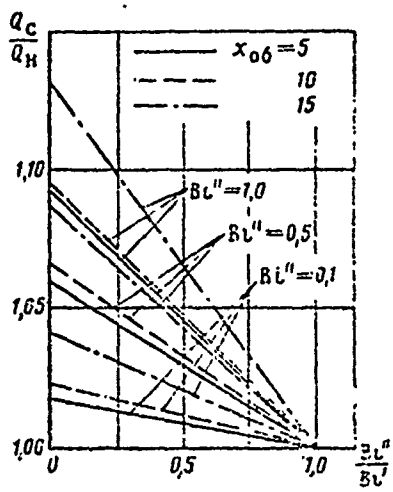

Fig. 6. Influence of nonuniform cooling of the lateral surfaces of a flat disk with fixed average values of Bi on heat transfer from the crown.

In order to bring into accord the heat flows obtained from formulas (4) and (25), it is necessary, when examining the one-dimensional problem, to perform the calculations for a certain effective width $H_{эф} = H/\eta$, where $\eta = Q_1/Q_2$ is a correction factor.

For contours which constrict toward the center, the correction for two-dimensionality will be substantially smaller, since the thermal resistance of such bodies will tend toward its minimum value, determined by the one-dimensional scheme of heat flows [7].

Using expression (24) we can also estimate the influence of asymmetry of the conditions for cooling of the lateral surfaces on heat transfer from a disk. As we know, when solving a one-dimensional heat-conduction problem, to calculate the asymmetry of cooling of the lateral surfaces, by the values t, θ, and α we mean certain average temperatures and average heat-transfer coefficients, which should be defined, as shown in [8], by the formulas

$$t = \frac{\alpha' t' - \alpha'' t''}{\alpha' + \alpha''}; \quad \theta = \frac{\alpha' \theta' + \alpha'' \theta''}{\alpha' + \alpha''}; \quad \alpha = \frac{\alpha' + \alpha''}{2}, \tag{26}$$

where t', t", θ', θ", α', and α" are the temperatures on the surface of the disk, the temperatures of the washing medium, and the heat-transfer coefficients on one side of the disk and the other, respectively.

Such a method is approximate, and therefore the correct result will be obtained only when the temperature on the lateral surfaces,

averaged by the indicated method, does not differ substantially from the average temperature across the section.

Figure 6 shows the results of calculating heat flows by formula (24) in the form of the ratio of Q_c, obtained for the case Bi' = = Bi" = Bi, to the value of Q_w found for Bi' ≠ Bi" with Bi = idem and unchanged temperature of the cooling medium (θ = idem). In accordance with (26), Bi = (Bi' + Bi")/2.

From the graph we see that with a decrease in the ratio Bi"/Bi', i.e., with an increase in the degree of nonuniformity of cooling of the lateral surfaces, heat transfer from the crown decreases, whereupon its maximum deviation from the value corresponding to symmetrical cooling conditions will occur when Bi" = 0 and Bi' = 2Bi. A decrease in heat transfer with asymmetrical cooling depends on the value of Bi and also on the relative disk radius $x_{об}$, and can attain, for real disks, 20-30% of the heat transfer determined from the averaged Bi values. Such asymmetrical conditions can be found in schemes where one of the lateral sides of the disk is shielded from the cooling air. Therefore, when calculating the heat transfer from a disk using dependences of the type of (17) it is necessary, for the indicated cases, to introduce a correction in accordance with the graph in Fig. 6.

Such calculations, carried out for θ' ≠ θ", Bi' = Bi" = Bi, and θ = (θ' + θ")/2 = idem, showed that a change in the value of $(t_{об} - \theta")/(t_{об} - \theta')$ within limits from one to zero leads to a decrease in heat transfer from the disk crown by no more than 1.5% compared with the heat transfer corresponding to symmetrical cooling conditions with $0.1 \leq Bi \leq 10$ and $1 \leq x_{об} \leq 10$. Thus, nonuniformity of cooling, caused by varying temperatures of the washing medium, does not result in noticeable errors.

The simple dependences obtained can be used when calculating the cooling of gas-turbine rotors, with consideration of the variable area of the cylindrical disk section and heating of the coolant.

REFERENCES

1. Шнеп Н. Т., Либин Е. П., Воздушное охлаждение роторов газовых турбин, Изд. Киевского Университета, 1950.

2. Костюк А. Г., Температурное поле турбинного диска, Изд. АН СССР, ОТН, 1954, № 6.

3. Stodola A., Dampf- und Gasturbinen, 1924.

4. Жирицкий Г. С., Газовые турбины, Госэнергоиздат, 1948.

5. Либин Е. М., Об одной ошибке, «Котлотурбостроение», 1952, № 5.

6. Кильченко А. Д., Пластины и оболочки в роторах турбомашин, Изд. АН УССР, 1953.

7. Эккерт Э. Р., Введение в теорию тепло- и массообмена, Госэнергоиздат, 1957.

8. Шереметьев Л. Г., К расчету температур диска газовой турбины при различных условиях теплообмена его сторон, «Котлотурбостроение», 1952, № 2.

EXPERIMENTAL STUDY OF THE TEMPERATURE STATE OF THE ROTOR OF AN AXIAL GAS TURBINE

A. A. Luzhin, V. S. Petrovskiy, M. I. Tsaplin, and V. I. Krichakin

Experimental study of the temperature state of a gas-turbine rotor is of primary importance for estimating its reserve strength, determining the service life of the entire turbine, explaining deficiencies in the rotor cooling system, and discussing prospects for raising the temperature of the gas ahead of the turbine. Direct thermometry allows us to refine a vast number of calculation characteristics used as the basis for designing the turbine. Besides, accumulation of information on the actual temperature fields in real gas-turbine designs allows us to improve the calculation methods for studying the temperature states of the rotors, and develop new theoretical methods for studying boundary conditions in operating turbines.

In this article we give the results of thermometry of the rotor of a small, three-stage, axial gas turbine.

The mean-mass temperature of the gas ahead of the turbine during the tests reached 1100°K; the flow of air for cooling the rotor was no more than 5% of the gas flow through the turbine. Air for cooling the turbine rotor is taken at the compressor outlet and its temperature under rated conditions ≈ 520-530°K.

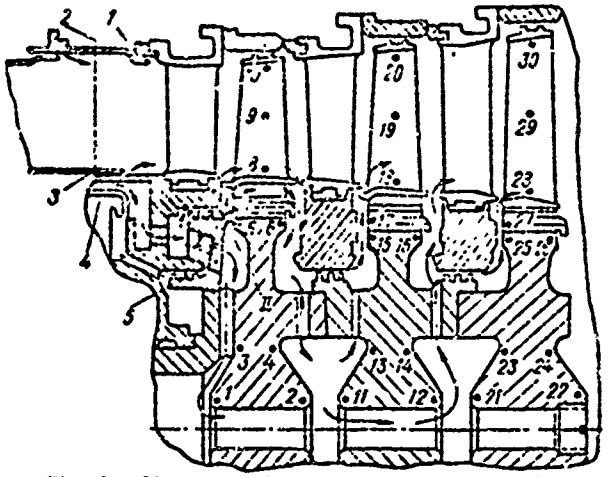

Fig. 1. Diagram of the positioning, on the turbine rotor, of the thermometry points. The Roman numerals designate the cavities which the cooling air enters. 1 – gap between flame tube and transfer ring of the upper shroud of the first nozzle cascade; 2 – point of location of the thermocouple connecting strips for measuring t_1^*; 3 – gap between flame tube and lower shroud of first nozzle cascade; 4 – annular slit through which cooling air passes from the compressor to the rotor; 5 – openings in the deflector on the leading side of the disk of stage I for feeding cooling air to stages II and III.

To reduce the temperature differential along the disks of the first stages, in the lower parts of the rotor blades we created unique heat chokes in the form of cooling channels. The rotor blades of all three turbine stages have upper and lower shrouds. The cooling channels, as can be seen from Fig. 1, are formed by the blade root, the lower blade shrouds, and the outer surface of the disk crown.

Air from the compressor is fed to cool the turbine through an annular gap between the flame tube and the support housing, and goes to cavity I. From here it is directed through labyrinth seals to the rear bearing and to the peripheral part of the stage I disk crown, and also through 6 openings in the deflector to the lateral surface of the disk and then through central openings in the stage I disk to stages II and III of the turbine.

Air enters the cooling channels of stage I from cavity II, passing through the labyrinth seal; only a certain part of the air enters the channels. The rest passes through the annular gap to the turbine blading and creates unique film protection at the bottoms of the blades.

The upper, peripheral, parts of the rotor blades, just as the roots, will be in a zone of reduced-temperature gas flow since the air which cools the stator is mixed with the gas. Thus, the middle sections of the blades undergo the greatest heating.

Since the distribution of gas temperature with height of the

vane cascade determines, to a considerable extent, the temperature field in the turbine rotor blades and disks, the results of rotor thermometry can be correctly explained only if we simultaneously measure the gas temperature at various sections of the rotor blades. This was taken into consideration when setting up the experiment.

The following basics were used to prepare the turbine for thermometry.

The turbine rotor is the most stressed part, and therefore we provided for temperature measurements at all of its most important points, from the standpoint of strength. Basically, these were those points at which we can obtain data on the temperature differential along the disk radius from the periphery to the center, through the disks, and in the blade firtree joints. It was also important to measure the temperature of the blade foil at various sections along its height.

Besides the turbine rotor, when conducting the experiment as a whole we prepared for thermometry the following: the blades of the nozzle cascades, the front and rear turbine shaft supports, the stator shrouds, and a number of other items. Below we will examine questions pertaining only to the thermal state of the rotor.

To obtain the required results from study of cooling effectiveness it was necessary, in addition to measuring the rotor temperature, to determine the temperature of the gas at the turbine inlet (t_3^*), the temperature field of the gas flow along the height of the vane cascades of all three stages, and the air temperature behind the compressor (t_2^*) and at the compressor intake (t_H).

In addition, it is necessary to know the air pressure at the compressor intake and outlet (p_H and p_2) and the gas pressure at the turbine inlet and outlet (p_3^* and p_4).

The positioning of the thermometry points on the rotor also had

to be associated with data from a theoretical preliminary determination of the temperature field in the turbine disks and rotor blades to make possible later comparison of the results of theory and experiment. The final scheme for positioning the thermometry points on the rotor is shown in Fig. 1.

Measurement of t_3^* was carried out in two steps. In addition to the thermocouples on the rotor, 12 thermocouples were placed at the turbine inlet around the periphery, on the average diameter of the blading. To measure the distribution of gas temperature along the vane cascades $[t_г^*(x)]$ we first installed, in the nozzle cascades of all three stages, thermocouples on one nozzle blade of each stage, as shown in Fig. 2. Processing of the results showed that it is impossible to determine $t_г^*(x)$ from one blade per stage, since the gas temperature is nonuniform around the turbine blading. Therefore, to measure $t_г^*(x)$ we performed additional thermometry for which, besides the 12 thermocouples on the average diameter, we placed connecting strips of 5 thermocouples each at six locations around the periphery ahead of the nozzle cascade of stage I; then in the nozzle cascade of each stage we set up 6 blades with thermocouples positioned in shown in Fig. 2. The resulting distribution of $T_г^*(x)$ at the outlet from the flame tube and in the nozzle cascade of each stage, shown below in Figs. 4 and 5, was constructed from points, each of which is the arithmetic mean of the readings of 6 thermocouples placed on the same diameter around the periphery of the blading.

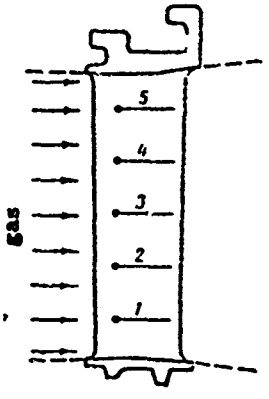

Fig. 2. Diagram of the location of the thermocouples on the nozzle blade (the numbers are read from the root sections of nozzle cascades).

We must mention the following relative to the thermocouples on the nozzle blades. Since the bead of the thermocouple was 1.5 mm above the blade surface, it was in the boundary layer of the gas flow. Measurement of the temperature of the boundary layer, combined with the damping exhibited by the thermocouple bead itself, assured measurement of $T_г^*$, to a certain extent. As additional verification

showed, the error of this method when measuring stagnation temperature, did not exceed the errors arising from other causes (limited accuracy of the thermocouple itself and the recording instrument, due to heat transfer), and was within acceptable limits.

The air temperature at the compressor outlet was measured with six thermocouples. This was a sufficient number, since t_2^* varies only insignificantly around the periphery of the compressor blading.

Four thermocouples were installed at the compressor inlet ahead of the protective cascade to measure t_H. For greater experiment reliability, the turbine rotor contained, as shown in Fig. 1, duplicate thermocouples on the same radii as the main thermocouples but shifted 120° and 180° in a plane perpendicular to the turbine axis.

An indexing system, which facilitated operations during the experiment, was developed for the entire thermocouple system.

To measure the temperature of the gas and the rotor parts we used Chromel-Alumel thermocouples, while to measure t_2^* and t_H we used Chromel-Kopel thermocouples of class 1 accuracy. The diameter of the thermoelectrodes, depending on the measurement site, was 0.2-0.5 mm. On the rotor blades and disks the thermocouple beads were welded to the surface, while the thermoelectrode leads in the heat-resistant insulation were covered with 0.1-mm thick refractory steel foil, spot-welded to the surface of the blades or disks. Figure 3 shows a rotor prepared for thermometry. The foil assures the necessary strength and protection of the thermocouple against the action of the gas, and also guarantees measurement accuracy, since it shields the thermocouple beads from direct action by the washing medium.

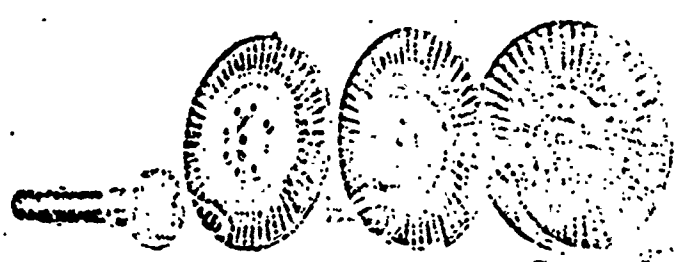

Fig. 3. Turbine rotor disks prepared for thermometry.

The thermoelectrodes from the thermocouples were braided together and fed to a mercury slip ring attached to a bracket on the exhaust pipe. Stage III of the turbine was used to drive the slip ring.

The mercury slip ring is intended to transmit an electrical signal from sensors mounted on the rotating parts to fixed recorders. It has 22 pairs of mercury contacts. Each pair of contacts is an individual section; the moving contact is located on the rotor shaft while the fixed contact is imbedded in the slip-ring stator. All sections of the contacts are insulated from one another by textolite washers.

The thermocouple leads fed to the slip ring are soldered to the contacts on a sliding insulating ring placed on an intermediate shaft. The contacts of the sliding ring, in turn, are connected to the sliding mercury contacts of the slip ring. The intermediate ring was introduced into the design to facilitate resoldering of the thermocouples.

The cold junctions of the rotor thermocouples were located on an insulating (textolite) washer which rotates inside a recess in the bracket which holds the slip ring. A jet of air is directed into the recess to balance the temperature of the cold junctions. The temperature of the junctions varied depending on the injection rate, the temperature of the ambient air, and other factors. The result is recording not of the true value of the temperature at the investigated point but the difference in temperatures of the hot and cold thermocouple junctions. To obtain the true temperature it was necessary, when processing the measurement results, to add the cold-junction temperature to the instrument readings. This temperature was considered equal to that of the injected air, and was measured by a separate thermocouple.

A total of 90 thermoccuples were installed on the rotor. Since the number of contacts allowed for the simultaneous use of no more

than 11 thermocouples, some of them were periodically resoldered in order to compare the measurement results and compile them into a single temperature field such as would be obtained if all thermocouples worked simultaneously.

As the measurement instruments for the turbine rotor we used single-point high-speed potentiometers, accuracy class 0.5, with continuous recording. To measure the cold-junction temperatures t_H, t_2^*, and t_3^* we used multiple-point potentiometers with complete carriage coverage of the scale in 2.5 seconds. The high speed of the carriage of the discrete potentiometers and the great number of points for measuring each of the indicated temperatures made it possible, when processing the measurement results, to clarify the trend of the temperature dependences during transitional regimes as well (start-up, stop).

To measure the distribution of gas temperature along the vane cascade we used multiple-point, discrete-recording potentiometers. The readings for identical thermocouples were recorded less frequently than with thermometry of the rotor but, since we studied only the steady state of the turbine, the number of repetitions was quite satisfactory for obtaining precise results.

The correctness of the instrument readings was systematically monitored using an additional potentiometer coupled in parallel with all the others to measure the rotor temperature. If necessary, the signal of the thermocouple of any potentiometer could be fed to this instrument using a switch.

The switch-on of all instruments was synchronized, using one start button on the operator's control panel.

The steady turbine operating mode under various loads was of particular interest. At the same time it was also important to study the nonsteady temperature states of the rotor.

During start-up, the turbine operates under severe thermal conditions, under which we can observe high temperature differentials on the disks, jumps in the thermal stresses in the joint section of the disks, and other unfavorable phenomena. Study of nonsteady temperature states should answer the question of the number of start-ups which limit reliable turbine service life.

These then are the basic concepts for compiling a graph of turbine operation during thermometry. The entire period from start-up to shutdown of the engine was divided into the following stages.

1. Start-up, idle, warmup, and measurement of all parameters characteristic of turbine operation.

2. A gradual increase of the load on the shaft with a rise in temperature from t_3^* to t_{3max}^* in the intermediate mode. In both the intermediate and maximum modes the measurements were made after a slight delay, for the turbine to achieve the steady temperature state.

3. A gradual decrease in load on the shaft and a corresponding drop in gas temperature ahead of the turbine to idle t_3^* through an intermediate load, with temperatures measured in each regime.

The results of all measurements were obtained in the form of graphs or a group of points on the recorder tapes. Each group of tapes, obtained for one day's testing, was processed individually. All recorder tapes for one day were coordinated relative to the reference point and the check marks which were made periodically, during turbine testing, on the tapes of all instruments by simultaneously shutting them off. On the coordinated tapes we noted the steady portions and the data obtained were compiled into tables. Nonsteady sections were noted only after the first start-up, when the entire engine was still cold and its temperature was equal to that of the ambient medium $\left(t_{H_0}\right)$. The discrete values of t_3^*, t_2^*, and t_H were averaged, and from them we constructed, on the tapes,

the continuous dependences $t_3^*(\tau)$, $t_2^*(\tau)$, and $t_H(\tau)$. The time of the nonsteady regime was reckoned from the moment of start-up using the tape showing the temperature of the cold junction, which thus served as a unique time scale.

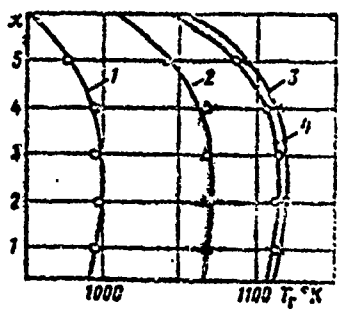

Fig. 4. Dependence $T_г^*(x)$, measured using thermocouples at the exit from the flame tube. Each point is the average of the readings of six thermocouples positioned around the blading. 1 – idle, t_H = +30°C; 2 – intermediate regime, t_H = +30°C; 3 – maximum regime, t_H = +30°C; 4 – maximum regime, t_H = +50°C.

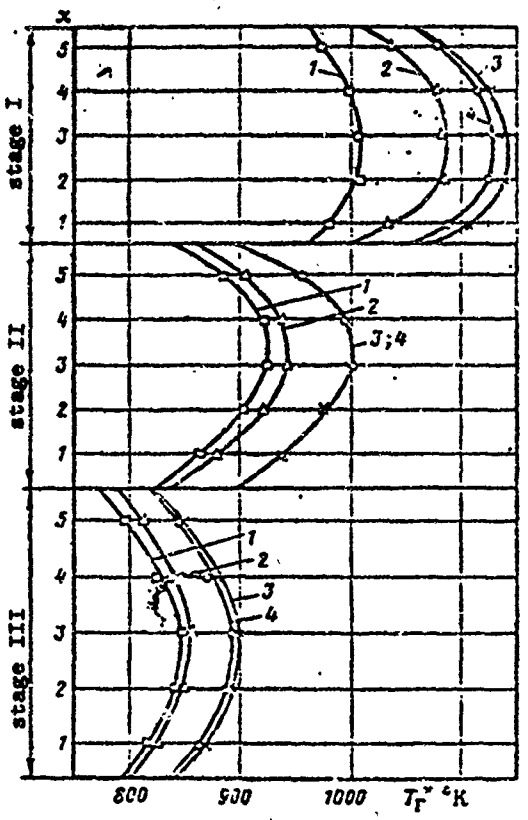

Fig. 5. Dependence $T_г^*(x)$, measured by thermocouples on nozzle blades of stages I, II, and III. Each point is the average of the readings of six thermocouples positioned around the blading. 1-4 – same as Fig. 4.

Figures 4 and 5 give the resulting graphs of the change in gas temperature with height of the turbine blading. Measurements were made in three regimes: idle, with an intermediate load, and with maximum load on the shaft (with maximum mean-mass temperature of the gas) at t_H = +30 and +50°C. Each point on these graphs is the average reading from six thermocouples positioned about the periphery of the blading.

Simultaneous thermometry of the gas flow at four points of the turbine blading made it possible to get a clear picture of the change in $T_г^*(x)$ from the outlet from the flame tube to the nozzle cascade of stage III. Associating the obtained dependences with the turbine design features, it is easy to explain the reason for certain anomalies in the gas-flow temperature field and to explain their effect on turbine characteristics.

The lowering of the temperature in the peripheral and root sections of vane cascades is explained only by the admixture of cooling air. This is indicated by the comparatively slight distortion of the gas temperature field at the flame-tube outlet. A certain reduction in temperature in the peripheral region can be explained here by the flow of air from the region around the stator into the turbine blading through the gap between the flame tube and the inner surface of the transfer ring of the upper shroud of the stage I nozzle cascade (see Fig. 1).

The intensity of flow through the gap increases with an increase in the pressure differential between the air cavity and the inlet to the stage I nozzle cascade. This is observed when there is an increased load on the turbine (an increase in shaft load) and is confirmed by deformation of the temperature field, which is evident in Figs. 4 and 5 for stage I upon transition from idle to maximum take-off. A reduction in temperature of the gas of the peripheral region at the outlet from the flame tube and the stage I nozzle cascade does not appreciably influence turbine performance, since it has an insignificant effect on the mean-mass gas temperature and it corresponds approximately to the calculated temperature.

A slight reduction in gas temperature is also noted in the root section of the first nozzle cascade (see Fig. 5). This can be explained by the leakage of air into the turbine blading at the point where the flame-tube outlet and the inner shroud of the stage I nozzle cascade meet.

Distribution of gas temperature at the inlet to the stage II nozzle cascade is deformed in both the peripheral and the root sections of the cascade. Cooling in the peripheral region is explained mainly by the influence of the air which reaches the blading through the gap along the outer perimeter of the flame-tube outlet, and then by the addition of air which cools the peripheral shroud of the stage I nozzle cascade.

A lowering of the temperature in the root section is explained by the feed, to the blading, of air used to cool the rotor. The trend of curves $T_r^*(x)$ for the nozzle cascades of stages II and III attests to the fact that the basic rotor-cooling air is expended in stage I.

The nature of the dependences $T_r^*(x)$ for all three stages allows us to conclude that the real change in mean-mass T_r^* along the turbine stages corresponds to the calculated change.

An explanation is required for the certain discrepancy in gas temperatures at the flame-tube outlet and at the inlet to the stage I nozzle cascade, although the maximum gas temperature in both cases should have been practically identical or somewhat higher at the flame-tube outlet. But the measurement results show just the opposite: the gas temperature at the inlet to the first nozzle cascade is somewhat higher than at the flame-tube outlet. This can be explained by the nonuniformity of the gas temperature around the turbine blading and by a slight displacement of the thermocouple connecting strips relative to the stage I nozzle cascades.

The results of measurements of rotor temperature in steady regimes are shown in Fig. 6 as functions $t_л(T_3^*)$ and $t_л(T_3^*)$. Here T_3^* is the mean-mass temperature at the inlet to the first nozzle cascade, obtained after processing the results of gas-temperature measurements by 12 thermocouples simultaneously with thermometry of the turbine rotor. Each line in Fig. 6 was constructed from the readings of a specific thermocouple during operation of the turbine in various regimes. Naturally, during the tests T_3^* did not exceed the maximum permitted value. All the lines are extrapolated to the region of high values of T_3^*. We can assume that such extrapolation is permissible for a specific turbine design. In this particular case, with an increase in T_3^* the nature of the function $T_r^*(x)$ for the entire turbine blading will hardly change, since the distribution of the cooling air over the stator and rotor does not, in all probability, depend on T_3^*. Therefore, with an increase in

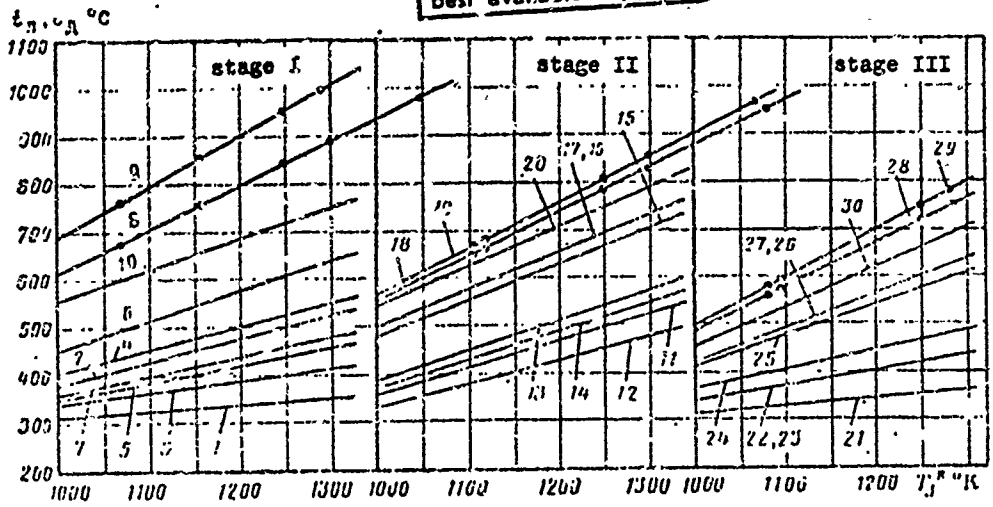

Fig. 6. Dependence of rotor temperature on gas temperature at the turbine inlet T_3^* (the lines correspond to the points of temperature measurement as shown in Fig. 1. The points on lines 8, 9, 18, 19, 28, and 29 designate temperatures for which we calculated the reserve strength of a blade in a given section for rated turbine rpm (see Fig. 10).

in T_3^* the similarity of the temperature fields in the rotor parts will be preserved. The possibility of extrapolation and its sufficient accuracy are also confirmed by the linear nature of the dependences $t_л(T_3^*)$ and $t_д(T_3^*)$.

Extrapolation of $t_л$ and $t_д$ beyond T_3^* = 1150°K allows us to more accurately establish the connection between rotor strength characteristics and the temperature field and find the most likely places which limit the maximum temperature T_3^*.

The linear nature of the graphs of the dependence of blade and disk temperature on gas temperature at the turbine inlet, and their varying slopes, confirm the results of a theoretical study of temperature fields in gas-turbine rotors, presented in [1] and others.

Using the lines in Fig. 6 we can find the radial temperature field in the disk and blades for each stage. This was done for temperatures T_3^* = 1100 and 1200°K (Fig. 7). Comparison of the lines makes it possible to estimate the effect of cooling of each rotor stage. The very high temperature gradient from the middle of the

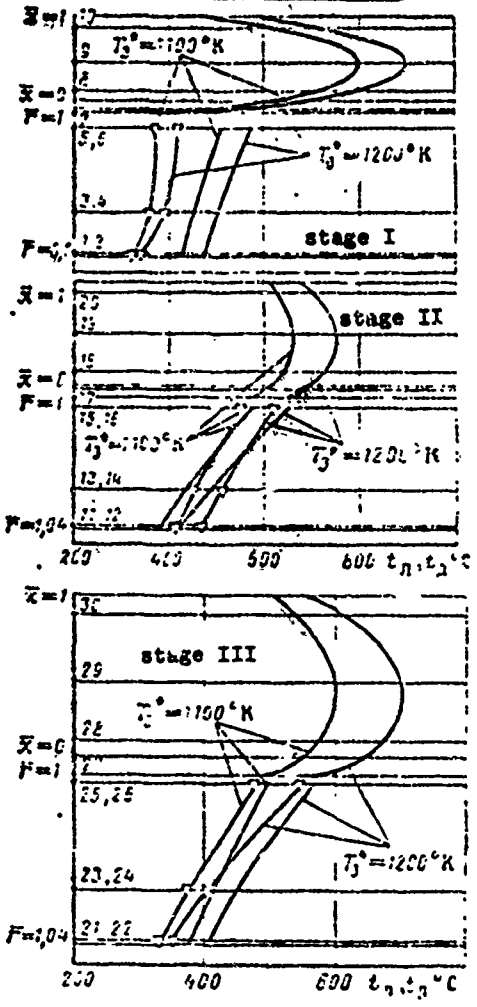

Fig. 7. Radial temperature distribution in a turbine rotor in the stationary mode, from thermometry results. To the left are the measurement points as in Fig. 1.

blade to the base and tip for stage I attests to the intensity of blade cooling in the peripheral and base sections. This result agrees with the distribution of gas temperature along the nozzle vane cascades of stages I and II (see Fig. 5). Such an effect of cooling is not observed for the rotor blades of stages II and III. The more uniform heating of the blades of stage II and the high temperature differentials along the disk indicate that the main portion of air fed to the rotor from the compressor is used to cool stage I and the rear support bearing. This can be considered as expedient, since stage I operates under the severest temperature conditions. Calculations also show that the temperature differentials along the stage II disk under operating conditions are quite acceptable, since the reserve strength in this case does not drop below standard.

Judging from the lines in Fig. 7, from the standpoint of cooling, stages II and III are under practically identical conditions, if we consider that somewhat more heat enters the stage II than the stage III disk from the gas.

The change in temperature along the leading and trailing sides of the disks of all three stages also confirms the weak cooling of stage II. Nevertheless, this cooling does exist, as attested to by the higher temperature of the rear side of the stage III disk. Cooling of the fronts and backs of the stage II disk is symmetrical,

since there is practically no temperature differential here.

Of great interest is the break in the temperature dependences at the junction of the blade and disk; this can be explained by the entrainment of part of the heat by the cooling air in the steady state and, in addition, by the thermal resistance of the blade firtree joints. Naturally, thermal resistance of the joint is characterized by a temperature differential from the stem of the blade to the projections on the disk (Fig. 8), but the combined effect of both factors is more complex. Figure 9 shows the temperature dependences $t_д(r)$ and $t_л(x)$ under nonsteady conditions, determined theoretically for stage I of a turbine. Figure 9a also gives an experimental dependence (curve A). Comparison of Fig. 9a (with cooling of the lower part of the blade) and Fig. 9b (without cooling) shows the great part played by the cooling channels. We also see the influence of the thermal resistance of the joint on the temperature function with transition from the blade to the disk since, despite the lack of cooling (see Fig. 9b), there is still a break in the lines. We can conclude that thermal resistance of a firtree joint with no air passing through its channels leads to a 10-20°C temperature differential on the blade/disk boundary.

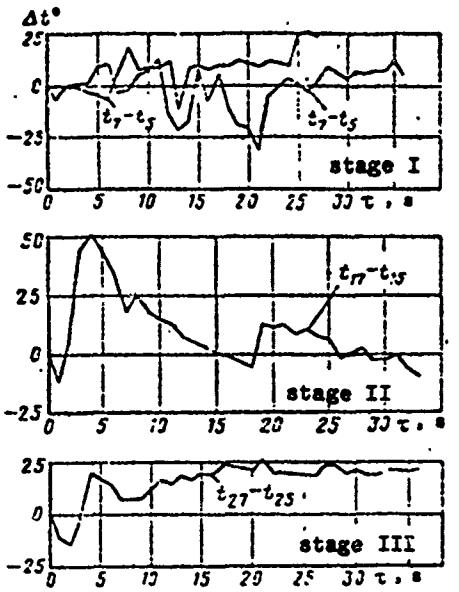

Fig. 8. Dependence of temperature differential in a firtree joint on time when starting-up a turbine.

The strength of the rotor disks is determined, to a considerable extent, by the temperature differential from the center to the periphery of the disk. Table 1 gives temperatures of the centers and peripheries of the disks of all three stages of a turbine rotor under steady conditions and with $T_3^* = 1100°K$, and the corresponding temperature differentials. As is to be expected, the maximum differentials are observed in the stage II disk. When designing a disk

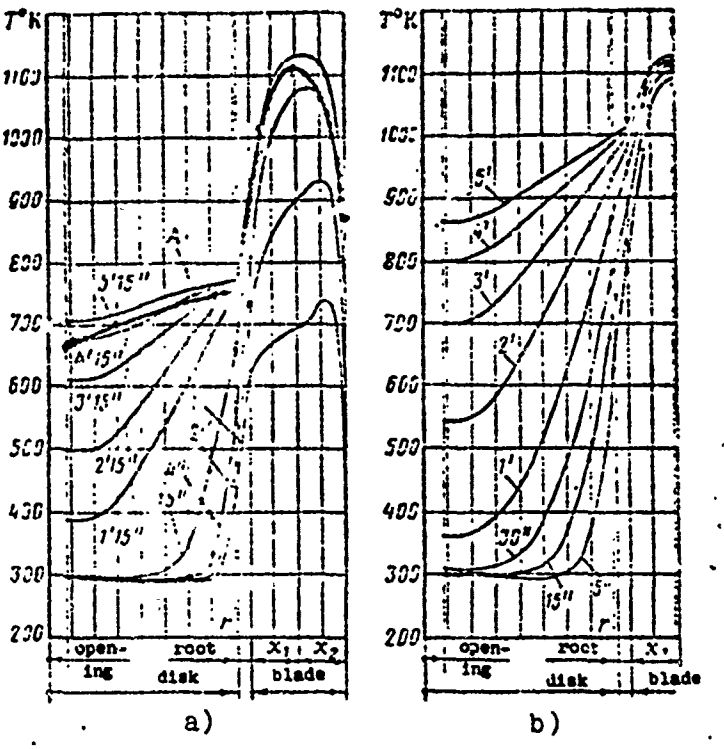

Fig. 9. Radial temperature distribution in a turbine rotor at various moments of time after start-up (shown on the curves in minutes and seconds): a – blowing of cooling air through channels in the lower parts of root-shrouded blades; b – without air blowing.

Table 1.

Stage	Side of disk	Center of disk: Designation (see Fig. 1)	Center of disk: Temperature, °C	Periphery of disk: Designation (see Fig. 1)	Periphery of disk: Temperature, °C	Temperature differential on side surfaces, °C	Temperature differential at alternate points, °C
I	Front	t_1	325	t_5	385	$t_5 - t_1 = 60$	$t_5 - t_2 = -40$
	Back	t_2	425	t_6	512	$t_6 - t_2 = 87$	$t_6 - t_1 = 187$
II	Front	t_{11}	415	t_{15}	555	$t_{15} - t_{11} = 140$	$t_{15} - t_{12} = 175$
	Back	t_{12}	380	t_{16}	570	$t_{16} - t_{12} = 198$	$t_{16} - t_{11} = 163$
III	Front	t_{21}	330	t_{25}	480	$t_{25} - t_{21} = 150$	$t_{25} - t_{21} = 105$
	Back	t_{22}	375	t_{26}	495	$t_{26} - t_{22} = 120$	$t_{26} - t_{21} = 165$

for strength we used temperature differentials higher than those measured. As a result, for a stage II disk operating under more severe temperature conditions, the reserve strength with given $\sigma_{дл}$ was 3.8 for the center of the disk and 3.4 for the periphery.

Table 2.

Position of thermometry points on blade	Stage I			Stage II			Stage III		
	Designation (see Fig. 1)	Temperature °C	Reserve strength, k	Designation (see Fig. 1)	Temperature °C	Reserve strength, k	Designation (see Fig. 1)	Temperature °C	Reserve strength, k
Periphery	$t_{1в}$	622	6.05	$t_{2в}$	628	6.50	$t_{3в}$	536	4.90
Middle	$t_в$	795	3.37	$t_{1в}$	660	4.20	$t_{2в}$	600	2.78
Root	$t_в$	703	3.96	$t_{1в}$	645	3.64	$t_{2в}$	580	2.46

Table 2 gives the blade temperatures for the stationary regime and $T_3^* = 1100°K$. Because of high heating, the middle parts of stage I disks have the least strength. Figure 10 shows dependences of the coefficient of reserve strength on T_3^*, which show that a rise in gas temperature ahead of the turbine is limited to the root section of the stage III rotor blade. This can be explained by the fact that the material of the stage III blades is less heat-resistant than the stage I and II blades. However, the stage III vane cascade is under rather stable temperature conditions, and therefore the reserve strength of the blades, even at maximum gas temperatures, completely assures reliable efficiency of the turbine.

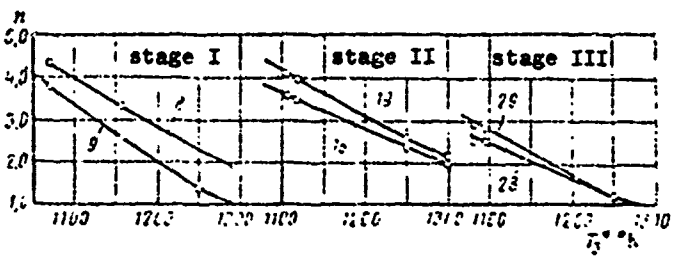

Fig. 10. Dependence of strength reserve on temperature T_3^* for some of the most stressed cross sections of turbine rotor blades. The points indicate the calculation results.

Practice has shown that the most important parts of vane cascades is the midsection of the stage I rotor blades, which undergo the action of the nonuniform temperature field of the gas flow, both

along as well as around the turbine blading. Therefore, here the possibility of short-term heating of the midsection of the blade is very likely and, during turbine operation with maximum values of T_3^*, the reserve strength of stage I blades in the midsection will vary and can assume lower values than in stage III. In addition, we cannot help but consider the possibility of overheating of the thermally-stressed leading and trailing edges of the blade foil.

Thus, we can consider that the rise in gas temperature ahead of the turbine is limited by the reserve strength in the midsection of the stage I rotor blades. The influence of variations in the temperature field around the blading on the temperature and, consequently, on the strength characteristics of the blades requires additional study.

When processing the thermometry results we also examined the nonstationary temperature state in the process of heating of the rotor during start-up. Some of the more typical of the obtained graphs for the temperature dependence are given in Figs. 11-13 for stages I, II, and III (the marking of the measurement points is as in Fig. 3).

The change in temperature of a stage I disk and blades is shown in Fig. 11a. The first start-up (see Fig. 11a) was not stable, and was characterized by sharp variations in t_3^* right up to the moment of transfer from start-up fuel to main fuel at the 13th second. Such a turbine operating regime allowed us to explain that the thermal inertia of the blades is very low: variations in blade temperature follow the variations in the gas temperature. This indicates the significant predominance of the amount of heat from the gas over the amount of heat fed from the working part of the blades to the disk and the correspondingly slight difference between the temperature of the blade midsection and that of the gas.

Above it was noted that the rear of the stage I disk is hotter than the front. The trend of the temperature at points 1, 3, 5, 2,

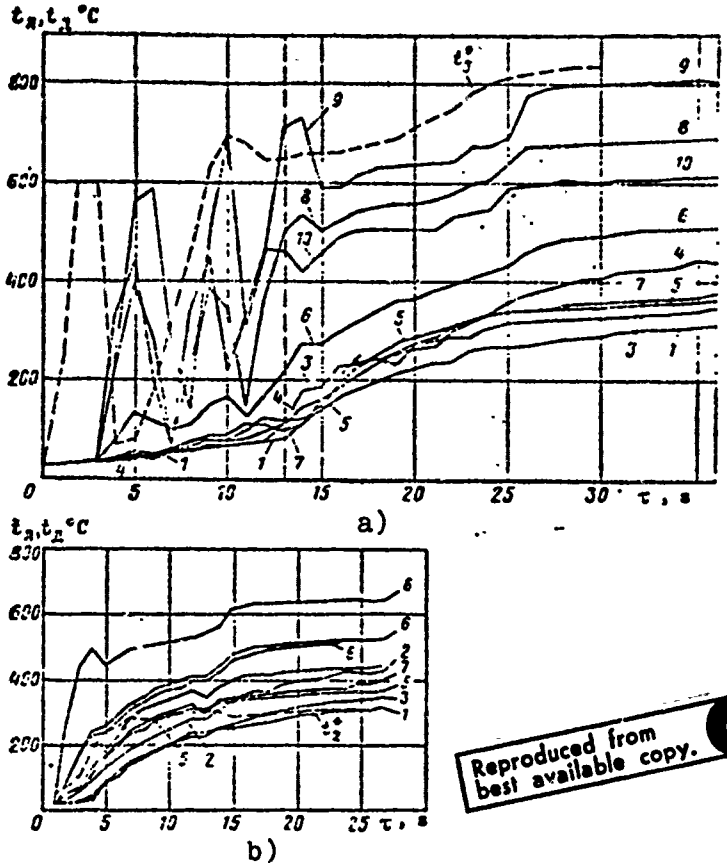

Fig. 11. Change in disk and blade temperature of stage I during start-up: a – unstable regime; b – stable regime.

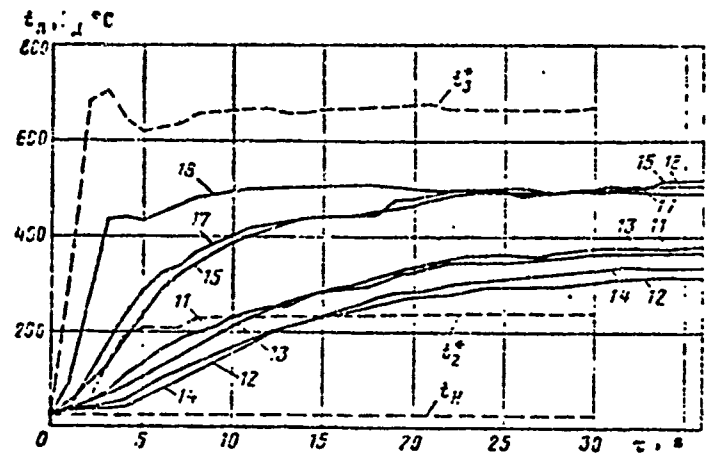

Fig 12. Change in disk and blade temperature of stage II during start-up.

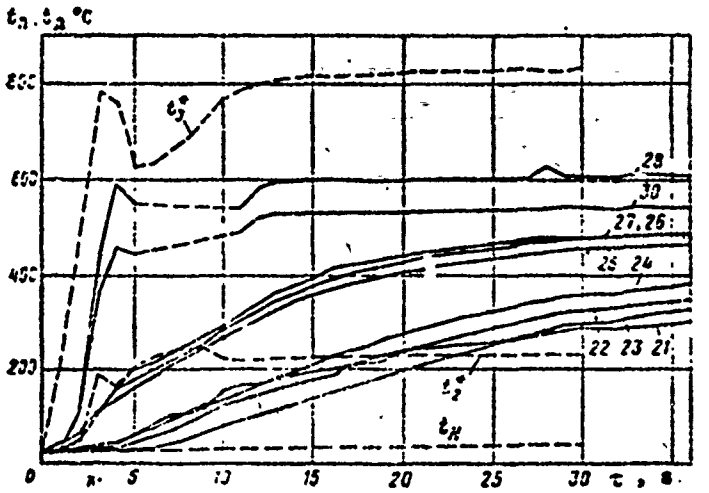

Fig. 13. Change in disk and blade temperature of stage III during start-up.

4, and 6 of the disk in the nonstationary regime makes it possible to trace how, from the very first seconds, there is a discrepancy in the thermocouple readings; the rear of the disk is more strongly heated. This indicates the maintenance of the distribution, in the turbine, of the cooling air by stages, in both steady and transitional regimes.

The maximum rate of heating of the peripheral part of the disk in the first 4 seconds is 60-90°C/s.

Let us mention the feature of function $t_2^*(\tau)$ noted on the graphs for all stages. If the nature of the change of t_3^* with time can be expressed approximately by an exponential function, temperature t_2^* changes, in the first 4-5 second, by a parabolic law, and then the rate of its increase decreases and it asymptotically approaches the rated value. These regularities must be taken into consideration when stating problems of heat conduction for a gas-turbine rotor.

The graphs given in Fig. 11 were used to determine the dependences of the temperature differentials along the disk on the time for all stages (Fig. 14). The graphs show that during start-up the temperature differentials along the radius of the stage I disk are somewhat higher than in the stationary temperature state. If in steady-state regimes $t_5 - t_1$ is 60°, during start-up this difference reaches 95°, while the differential $t_6 - t_2$ reaches 140° instead of 87° in the stationary state. We can observe anomalies in which the

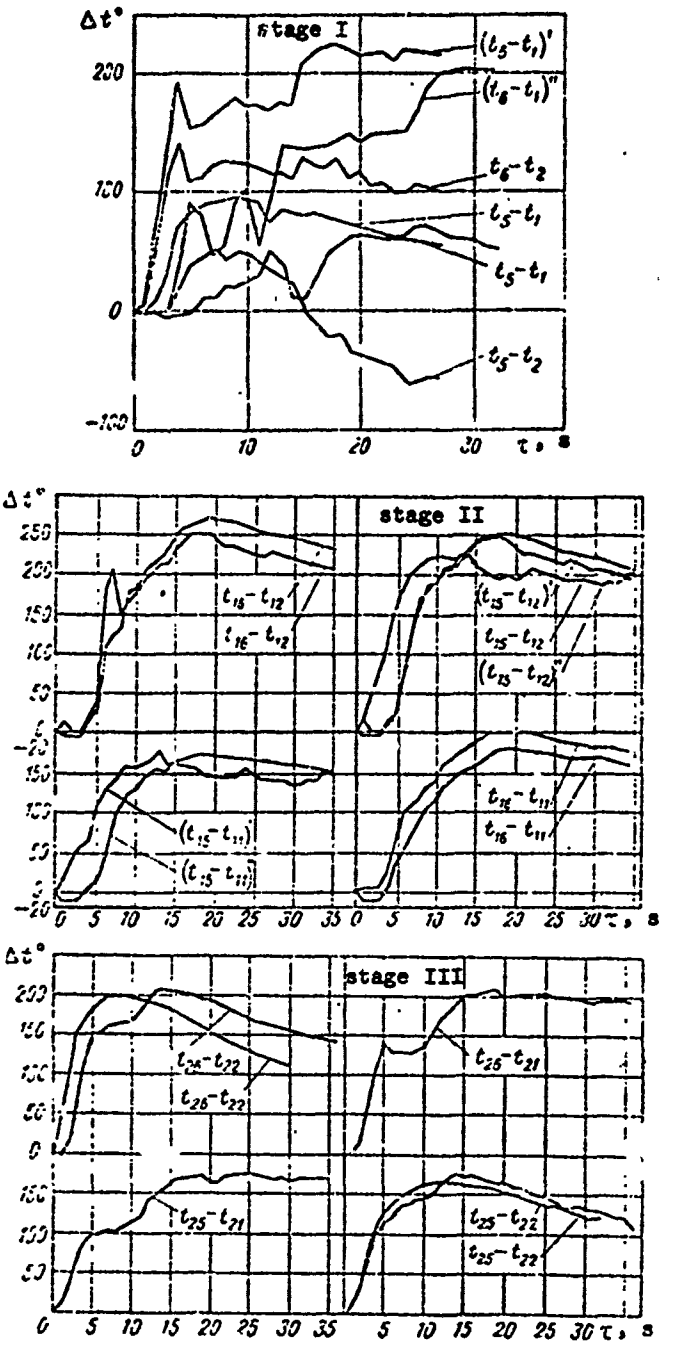

Fig. 14. Change in temperature differential from the periphery of the disk to its center during turbine start-up.

differential increases continually with certain variations (line $t_5 - t_1$), but they cannot be considered typical. The nature of the curve $t_5 - t_2$ indicates that because of the more rapid heating of the disk periphery on the front side (lines 5 in Fig. 11) the differential $t_5 - t_2$ is first greater than zero and only after the 15th second does it become negative, i.e., $t_5 < t_2$.

The trend of dependences $t_6 - t_1$ and $t_5 - t_2$ shows the absence, during start-up, of a maximum temperature differential for alternate points.

The maximum temperature differential for a stage I disk during start-up is lower than that which served as the initial one for the strength calculations with steady heating. Consequently, the transitional temperature state has no influence whatsoever on the efficiency and reliability of a disk. The time-dependence of the temperature of stage II blades and sisks shows the low thermal inertia of the blades (curve 18 in Fig. 12). Thanks to stable start-up we easily see that the rate of heating of the central part of the disk is somewhat less than that of the peripheral part.

Curves 11, 13, 12, and 14 show that in the first seconds after start-up the center of the stage II disk is heated more rapidly than its middle part. To explain this we must simultaneously analyze the temperature dependences for stage I and II disks. Above we noted that air from the compressor is almost completely expended on cooling only the leading edge of the stage I disk. Therefore, we cannot explain the higher heating at points 11 and 12 than at points 13 and 14 (see Fig. 12) in the first seconds after start-up by the fact that the center of the stage II disk is washed by hot air from the compressor during this time, all the more so since in this case, point 1 of the stage I disk (see Fig. 11b) would be heated most rapidly of all in this case. However, its temperature is lower than at point 2, both during start-up as well as during subsequent operation of the turbine.

Such a heating peculiarity can be explained as follows. Cooling air on its way to exhausting into the turbine blading between the first rotor and the second nozzle cascade loses so much head that it cannot counteract the pressure on the part of the gas flow. At the same time, the difference in pressures at the inlet to and outlet from the root section of the second and third nozzle cascades (Fig. 1) leads to suction of the gas into the gap between the first rotor and the second nozzle cascade. The temperature of the gas entering the gap is low, since in the lower part of the first nozzle cascade there is mixed, with the gas flow, cooling air from the gap between the first nozzle cascade and the first rotor. When the gas enters the gap its temperature is reduced still more due to mixing of the air coming from the cooling channels in the lower part of the first rotor cascade. The gas, mixing with the cooling air, penetrates through the radial openings in the skirt of the stage I disk and washes its rear side. This is attested to by the synchronous variation of temperature dependences 2 and 4. A small amount of the gas-air mixture leaks through the labyrinth seal between stages I and II, and also through the radial channels in the skirt of the stage II disk, and enters the blading of the turbine between the second nozsle cascade and the second rotor. The fact that this amount of gas-air mixture is really slight is confirmed by the lower temperature at point 13 than at point 11 during start-up (see Fig. 12).

The gas-air mixture, reaching the central recess between the stage I and II disks, passes to stage III, washing the walls of the opening of the second disk and heating its central part. Along the way it is again mixed with a certain quantity of cooling air from the central opening of the first disk, and its temperature continues to drop. Then from the cavity between the second and third disks the gas-air mixture exits to the blading through the radial channels in the skirt of the stage II disk. Here the rear surface of this disk and the central part of the third disk are washed, which is well illustrated by Fig. 13. The temperature at point 21 first rises rather rapidly but, with influx of heat from the peripheral part, heating on the part of the gas-air mixture plays a lesser role, and

the temperature at points 22, 23, and 24 becomes higher than at point 21.

It is important to note that circulation of the gas-air mixture, in final analysis, cools stages II and III of the turbine rotor. The temperature of the mixture washing the rear surface of the first disk does not exceed 390-400°C, while that washing the rear surface of the second disk and the front surface of the third disk does not exceed 310-320°C. Therefore, the gas-air mixture heats the disks only during the first few seconds after start-up. As the disks become heated from the periphery, the mixture acts as a coolant, assuring, under stationary turbine operating conditions, a stable temperature field for the disks, which is taken into consideration in strength calculations of disks. In the absence of such circulation, heating of the central parts of stage II and III disks would be determined by the temperature of the air coming from the compressor, which would lead to an increased temperature differential along the disk radius and, consequently, to increased thermal stresses.

Heating of the central part of rotor disks also aids in rapid heating of the rotor and passage to the stationary temperature regime.

Judging from the graphs of nonstationary heating (see Fig. 11), the washing medium begins to cool the stage I disk approximately 20 seconds after start-up, and the disks of stages II and III – after 30 seconds.

The rule for the change in temperature differential in the stage II disk from the periphery to the center during start-up is the same as for the stage I disk, but the magnitude of the differentials increases (see Fig. 14). In connection with the fact that the disk is cooled symmetrically, the maximum temperature differential in the first seconds of turbine operation is also observed for alternate points. For strength calculation of the stage II disk we assigned a temperature differential of 300°C, and therefore the maximum

occurring during start-up for $t_{16} - t_{12}$ and $t_{15} - t_{11}$ is not definitive. A negative differential can occur at the very beginning of start-up, as already stated, due to heating of the central part.

The rules for temperature distribution in stage III disks and blades during turbine start-up are the same as for stages I and II (see Fig. 13).

The temperature differentials in a stage III disk are shown in Fig. 14. From the graphs we see that heating of point 21 in the first few seconds after start-up allows us to make the temperature increase monotonic. As a result, function $t_{25} - t_{21}$ became almost monotonic, just as $t_{26} - t_{21}$.

REFERENCE

1. Жирицкий Г. С., Локай В. И., Максутова М. К., Струнки н В. А., Газовые турбины авиационных двигателей, М., Оборонгиз, 1963.

THE NONSTATIONARY HEAT CONDUCTION OF BODIES OF COMPLEX CONFIGURATION

M. N. Galkin and S. P. Kolesnikov

Many parts of airborne vehicles and their engines have sharp edges and projections in the form of dihedral and polyhedral angles. During operation, these parts are subjected to short-term heating or cooling, and from a thermal standpoint can be examined as semi-bounded bodies.

In this work we give our general theoretical solutions to problems on determining the temperature field and the heat-retaining capabilities of semi-bounded bodies having the form of dihedral and polyhedral, acute and obtuse angles. The solutions are approximate and have been obtained for the case of constant temperature on the surface of the bodies.

The essence of the solution of the multidimensional nonstationary problem is first examined in detail using, as our example, a dihedral angle (the two-dimensional problem), and is then extended to polyhedral angles.

The particular solution to the problem for the temperature field of a dihedral right angle (Fig. 1) is the product of the solution for two semi-bounded bodies (A. V. Lykov: *Teoriya teplcprovodnosti*

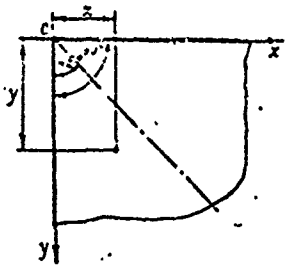

Fig. 1. Determining the temperature field of the dihedral angle $\varphi = 90°$.

(The theory of heat conduction), GITTL, 1952):

$$\vartheta = 1 - \operatorname{erf}\left(\frac{x}{2\sqrt{a\tau}}\right)\operatorname{erf}\left(\frac{y}{2\sqrt{a\tau}}\right),$$

or

$$\vartheta = 1 - \operatorname{erf}\left(\frac{1}{2\sqrt{Fo_x}}\right)\operatorname{erf}\left(\frac{\bar{y}}{2\sqrt{Fo_x}}\right). \qquad (1)$$

where $\vartheta = \frac{t(x, y, \tau) - t_0}{t_c - t_0}$ is the relative temperature of the body at a point with coordinates x and y at time τ; t_c is the constant temperature of the body surface; t_0 is the initial temperature of the body; $a = \lambda/c\rho$ is the coefficient of thermal conductivity of the body material; λ, c, and ρ are the heat conduction, specific heat, and density of the body material; $Fo_x = a\tau/x^2$ is the Fourier criterion; $\bar{y} = y/x$; erf(U) is the Gauss error function, which is equal to zero when U = = 0 and is practically equal to one when $U \geq 2$.

To derive the approximate general solution we used the scheme shown in Fig. 2. The temperature at point x,y of investigated angle φ was determined on the basis of the equivalent right angle, at which the examined point has coordinates Xy. Considering this, equation (1) can be represented in the form

$$\vartheta = 1 - \operatorname{erf}\left(\frac{x \operatorname{tg}\frac{\varphi}{2}}{2\sqrt{a\tau}}\right)\operatorname{erf}\left(\frac{y}{2\sqrt{a\tau}}\right),$$

or

$$\vartheta = 1 - \operatorname{erf}\left(\frac{\operatorname{tg}\frac{\varphi}{2}}{2\sqrt{Fo_x}}\right)\operatorname{erf}\left(\frac{\bar{y}}{2\sqrt{Fo_x}}\right). \qquad (2)$$

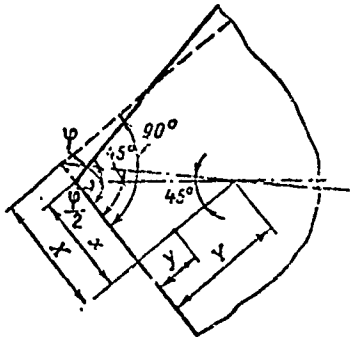

Fig. 2. Determining the temperature field of dihedral angle φ of any magnitude.

Equation (2) allows us to approximately calculate the temperature field of a body with any angle φ, while it gives a precise solution in the two particular cases when angles φ are 180° and 90°. If $\varphi = 180°$, then tan 90° = ∞, erf(∞) = 1 and

$$\vartheta = 1 - \operatorname{erf}\left(\frac{\bar{y}}{2\sqrt{Fo_x}}\right) = 1 - \operatorname{erf}\left(\frac{y}{2\sqrt{a\tau}}\right). \qquad (3)$$

Equation (3) is the known precise solution of the problem a semi-bounded body.

If $\varphi = 90°$, then $\tan 45° = 1$ and equation (2) is simplified, assuming the form of equation (1), which is the precise solution to the problem for a right angle.

When calculating bodies with small angles φ and, in particular, when angle $\varphi \to 0$, i.e., the sides of the body are parallel, an indeterminacy arises in equation (2), since $\tan 0 = 0$, $\operatorname{erf}(0) = 0$, and $\$ = 1$. To expose this indeterminacy in equation (2) we must exclude the coordinate x:

$$\theta = 1 - \operatorname{erf}\left(\frac{Y}{2\sqrt{a\tau}}\right)\operatorname{erf}\left(\frac{y}{2\sqrt{a\tau}}\right), \qquad (4)$$

where Y is half the distance between sides (or half the plate thickness).

To estimate the accuracy of approximate solution (2) we experimentally studied the temperature field of bodies having various thermophysical properties and angles φ from 0° to 180°. The maximum deviation of the calculation data from experimental data occurred on the bisector of angle φ and in the range $\varphi = 50°$-180°, and did not exceed ±5%. The deviations were estimated using the criterion $(t_{пр} - t_0)/(t_д - t_0)$, where $t_{пр} - t_0$ is the excess temperature, calculated from formula (2), and $t_д - t_0$ is that found from experiment ($t_{пр}$ is the approximate temperature, $t_д$ is the real temperature).

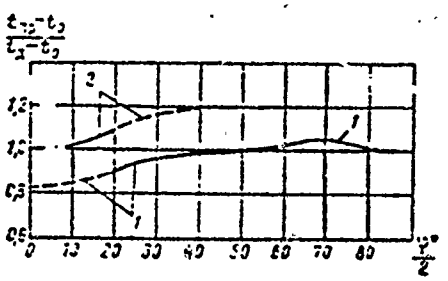

Fig. 3. Dependence of the criterion $(t_{пр} - t_0)/(t_д - t_0)$ on angle φ, characteriting the maximum deviations of the calculated temperature field from the experimental one. Curve 1 is constructed from equation (2), curve 2 – from equation (5).

Figure 3 shows the values of these criteria for angles φ from 0° to 180° (curve 1).

From Fig. 3 it follows that theoretical solution (2) gives an accurate result for angles $\varphi = 180°$ and 90°, an overvalued result for angles $180° > \varphi > 90°$ (the maximum error is obtained at $\varphi = 140°$ and reaches 5%), and an undervalued result for $90° > \varphi \geq 0°$ (maximum error is obtained when $\varphi = 0°$ and reaches 7%).

These deviations occur since, according to the scheme (Fig. 2) used for deriving equation (2), we get an undervalued heat flow along the bisector of the angle when $180° > \varphi > 90°$ and an overvalued flow when $0° \leq \varphi < 90°$.

To increase the accuracy in calculating the temperature field of bodies with small angles φ, it is expedient to seek the theoretical solution on the basis of the scheme shown in Fig. 4, which generally excludes heat transport along the bisector of the angle. In such a case, each cross section x of angle φ at depth Y can, from a thermal standpoint, be examined as half the thickness of a plate, for which the solution (see Lykov's book mentioned above) has the following form:

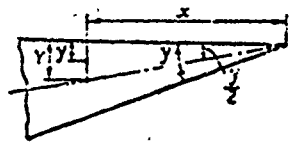

Fig. 4. Deriving the approximate solution to the problem for the temperature field of bodies with small angles ($\varphi < 40°$).

$$\theta = 1 - \sum_{n=1}^{\infty} A_n \cos \mu_n \left(1 - \frac{\bar{y}}{\operatorname{tg} \frac{\varphi}{2}}\right) \exp\left(-\mu_n^2 \frac{Fo_x}{\operatorname{tg}^2 \frac{\varphi}{2}}\right), \qquad (5)$$

where $A_n = \frac{2}{\mu_n}(-1)^{n-1}$ is the initial thermal amplitude $\left(\mu_n = (2n-1)\frac{\pi}{2}\right)$.

In the particular case when $\varphi = 0$, in equation (5) we must exclude coordinate x:

$$\theta = 1 - \sum_{n=1}^{\infty} A_n \cos \mu_n \left(1 - \frac{y}{\gamma}\right) \exp\left(-\mu_n^2 \frac{a\tau}{\gamma^2}\right). \qquad (6)$$

Equation (6) is the precise solution of the problem for an unbounded plate. Curve 2 in Fig. 3 corresponds to the relative excess temperature $\frac{t_{np} - t_0}{t_x - t_0}$ calculated from formula (5). Figure 3 shows that for $\varphi = 0°$-$40°$ we must use approximate solution (5), while for $\varphi = 40°$-$180°$ we use solution (2). Here the maximum temperature-calculation error does not exceed 9% (on the bisector, and only for a body with angle $\varphi = 40°$).

In Fig. 3 we also see that the calculation error using approximate solutions (2) and (5) does not exceed 2% for angles $\varphi = 0°$-$20°$,

φ

φ = 70°-110°, and φ = 160°-180°.

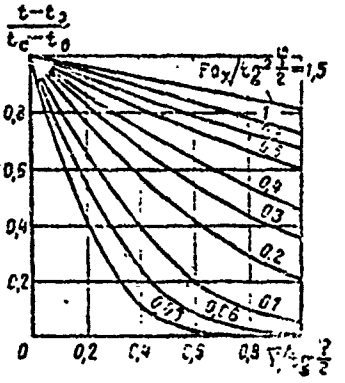

Fig. 5. Curves of the distribution of relative excess temperature in dihedral angles 40° ≤ φ ≤ 180° as a function of the criterion $Fo_x/\tan^2\varphi/2$.

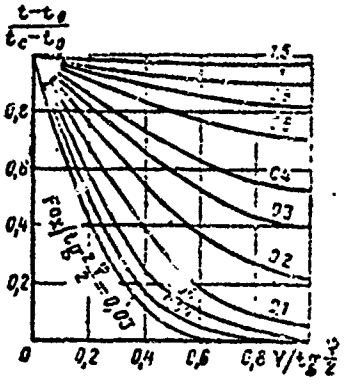

Fig. 6. Curves of the distribution of relative excess temperature in dihedral angles 0° ≤ φ ≤ 40° as a function of the criterion $Fo_x/\tan^2\varphi/2$.

Figures 5 and 6 show curves of the distribution of relative excess temperature in dihedral angles for various values of the criterion $Fo_x/\tan^2\varphi/2$, constructed from solutions (2) and (5), respectively.

The specific heat flow arriving at the body at time τ per unit area of heating surface, located at distance x from the vertex of the angle (Fig. 7), is determined from the Fourier law of heat conduction:

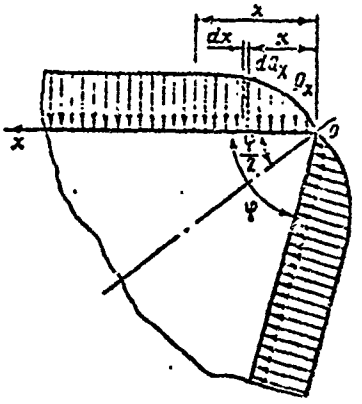

Fig. 7. Diagram of the heat flow on the surface of a dihedral angle.

$$q_\tau = -\lambda\left[\frac{\partial t(x,y,\tau)}{\partial y}\right]_{y=0},$$

where $\left[\frac{\partial t(x,y,\tau)}{\partial y}\right]_{y=0}$ is the temperature gradient on surface ox of the dihedral angle at time τ, determined with consideration of formula (2) or (5) as a function of the value of angle φ.

It should be noted that formulas (2) and (5) give, for all practical purposes, an accurate temperature at the body surface. Therefore, the value of the heat flow found with consideration of formulas

(2) or (5) will be, for all practical purposes, accurate.

Let us find the heat flow when $\varphi = 180°-40°$.

Having determined the gradient $[\partial t(x,y,\tau)/\partial y]_{y=0}$ with consideration of formula (2) for the body surface ($y = 0$), we find

$$q_x = \frac{b}{\sqrt{\pi\tau}}(t_c - t_0)\operatorname{erf}\left(\frac{x\operatorname{tg}\varphi/2}{2\sqrt{a\tau}}\right). \tag{7}$$

where $b = \sqrt{\lambda c\rho}$ is the coefficient of accumulation of heat by the body material.

The quantity of heat passing in time interval τ across a unit of surface located at distance x from the vertex of the angle

$$Q_x = \int_0^\tau q_x\, d\tau. \tag{7'}$$

Substituting q_x from formula (7), after integration we get

$$Q_x = \frac{2b}{\sqrt{\pi}}(t_c - t_0)\sqrt{\tau}\left[\operatorname{erf}\left(\frac{x\operatorname{tg}\varphi/2}{2\sqrt{a\tau}}\right) - \frac{x\operatorname{tg}\varphi/2}{\sqrt{\pi}\,2\sqrt{a\tau}}\operatorname{Ei}\left(-\frac{x^2\operatorname{tg}^2\varphi/2}{4a\tau}\right)\right], \tag{8}$$

or

$$Q_x = \frac{2b}{\sqrt{\pi}}(t_c - t_0)\sqrt{\tau}\left[\operatorname{erf}\left(\frac{\operatorname{tg}\varphi/2}{2\sqrt{\mathrm{Fo}_x}}\right) - \frac{\operatorname{tg}\varphi/2}{2\sqrt{\pi}\sqrt{\mathrm{Fo}_x}}\operatorname{Ei}\left(-\frac{\operatorname{tg}^2\varphi/2}{4\mathrm{Fo}_x}\right)\right]. \tag{9}$$

The quantity of heat entering the body on segment X of unit width in finite time τ

$$Q_X = \int_0^X Q_x\, dx.$$

while after substitution of Q_x from formula (8) and integrating

$$Q_X = \frac{2b}{\sqrt{\pi}}(t_c - t_0)X\sqrt{\tau}\left[\operatorname{erf}\frac{X\operatorname{tg}\varphi/2}{2\sqrt{a\tau}} + \frac{\sqrt{a\tau}}{X\operatorname{tg}\varphi/2\sqrt{\pi}}\left(-e^{-\frac{X^2\operatorname{tg}^2\varphi/2}{4a\tau}} - 1\right) - \frac{X^2\operatorname{tg}^2\varphi/2}{4\sqrt{\pi}\sqrt{a\tau}}\operatorname{Ei}\left(-\frac{X^2\operatorname{tg}^2\varphi/2}{4a\tau}\right)\right], \tag{10}$$

or

$$Q_X = \frac{2b}{\sqrt{\pi}}(t_c - t_0)X\sqrt{\tau}\left[\operatorname{erf}\left(\frac{\operatorname{tg}\varphi/2}{2\sqrt{\mathrm{Fo}_X}}\right) +\right.$$

$$+\frac{\sqrt{Fo_x}}{\operatorname{tg}\varphi/2\sqrt{\pi}}\left(e^{-\frac{\operatorname{tg}^2\varphi/2}{4Fo_x}}-1\right)-\frac{\operatorname{tg}^2\varphi/2}{4\sqrt{\pi}\sqrt{Fo_x}}\operatorname{Ei}\left(-\frac{\operatorname{tg}^2\varphi/2}{4Fo_x}\right)\Bigg]. \qquad (11)$$

where $Fo_X = a\tau/X^2$ is the Fourier criterion.

Let us find the heat flow for angle $\varphi = 40°-0°$.

Having determined the gradient $[\partial t(x,y,\tau)/\partial y]_{y=0}$ with consideration of formula (5) for the body surface ($y = 0$) we get

$$q_x = \lambda(t_c - t_0)\frac{2}{x\operatorname{tg}\varphi/2}\sum_{n=1}^{\infty}\exp\left(-\mu_n^2\frac{a\tau}{x^2\operatorname{tg}^2\varphi/2}\right). \qquad (12)$$

After substituting the value of q_x from formula (12) into formula (7') and integrating, we get

$$Q_c = b(t_c - t_0)\sqrt{\tau}\,\frac{(1-\bar{\vartheta})\operatorname{tg}\varphi/2}{\sqrt{Fo_x}}; \qquad (13)$$

here the average relative excess temperature on the surface of a dihedral angle in section x

$$\bar{\vartheta} = \frac{t_c - \bar{t}(x,\tau)}{t_c - t_0} = \sum_{n=1}^{\infty}\frac{2}{\mu_n^2}\exp\left(-\mu_n^2\frac{Fo_x}{\operatorname{tg}^2\varphi/2}\right). \qquad (14)$$

The quantity of heat entering the body in segment X of unit width in finite time τ

$$Q_X = \int_0^X Q_x dx.$$

Considering formulas (13) and (14), after integration we get

$$Q_X = b(t_c - t_0)X\sqrt{\tau}\,\frac{\left[1-\bar{\vartheta}-\frac{2Fo_X}{\operatorname{tg}^2\varphi/2}\sum_{n=1}^{\infty}\operatorname{Ei}\left(-\mu_n^2\frac{Fo_X}{\operatorname{tg}^2\varphi/2}\right)\right]\operatorname{tg}\varphi/2}{2\sqrt{Fo_X}}. \qquad (15)$$

From equation (8) it follows that when $x \to \infty$, heat flow Q_x reaches its maximum value

$$Q^* = \frac{2b}{\sqrt{\pi}}(t_c - t_0)\sqrt{\tau}. \qquad (16)$$

Equation (16) is the known particular solution to the problem of the heat-retaining capability of a semi-bounded body (see Lykov).

The ratio Q_x/Q^* – the actual amount of heat to the maximum amount – is the parametric criterion K_x which characterizes the influence of the angle (bilateral heat feed) on the heat-retaining capabilities of the body in section x.

From equations (9) and (16) it follows that for angles $40° \leq \varphi < 180°$ the criterion

$$K_x = \operatorname{erf}\left(\frac{\operatorname{tg}\frac{\varphi}{2}}{2\sqrt{\mathrm{Fo}_x}}\right) - \frac{\operatorname{tg}\frac{\varphi}{2}}{2\sqrt{\pi\,\mathrm{Fo}_x}}\,\mathrm{Ei}\left(-\frac{\operatorname{tg}^2\frac{\varphi}{2}}{4\,\mathrm{Fo}_x}\right), \tag{17}$$

while for angles $0 < \varphi \leq 40°$, from equations (13) and (16) we get

$$K_x = \frac{\sqrt{\pi}(1-\bar{x})\operatorname{tg}\frac{\varphi}{2}}{2\sqrt{\mathrm{Fo}_x}}. \tag{18}$$

Figure 8 shows the dependence of criterion K_x on criterion $1/\mathrm{Fo}_x = x^2/a\tau$, calculated from formula (18), for various values of angle $\varphi/2$ within limits from 5° to 20°, while Figs. 9 and 10 show analogous dependences, calculated from formula (17) for angles $\varphi/2 =$ $= 20°-45°$ and $\varphi/2 = 45°-75°$, respectively.

From the graphs we see that the influence of the angle on the heat-retaining properties of a body increases with decreasing criterion $1/\mathrm{Fo}_x$, i.e., as the examined section x approaches the vertex of the angle, while with decreasing angle φ this influence increases.

From equations (17) and (18) we see that if criterion $1/\mathrm{Fo}_x$ vanishes, for any value of angle $\varphi/2$ (except $\varphi/2 = 90°$, when $\tan \varphi/2 = \infty$) the criterion $K_x = 0$. Consequently, heat flow $Q_x =$ $= Q^*K_x$, passing through the vertex of any angle, is equal to zero.

If criterion $1/\mathrm{Fo}_x \to \infty$, in accordance with equations (17) and (18) $K_x \to 1$. In this case the heat flow reaches the value Q^* which characterizes the heat-retaining capability of a semi-bounded body (16).

Theoretical analysis shows that section x_0, behind which the angle is heated practically as a semi-bounded body, can be found from the condition

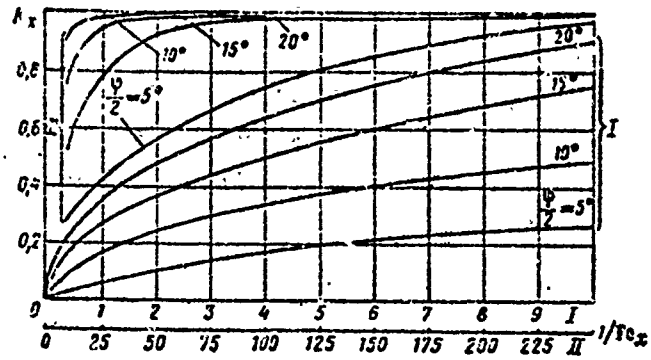

Fig. 8. Dependence of parametric criterion K_x on the criterion $1/Fo_x$ for angles $\varphi/2$ from 5° to 20°.

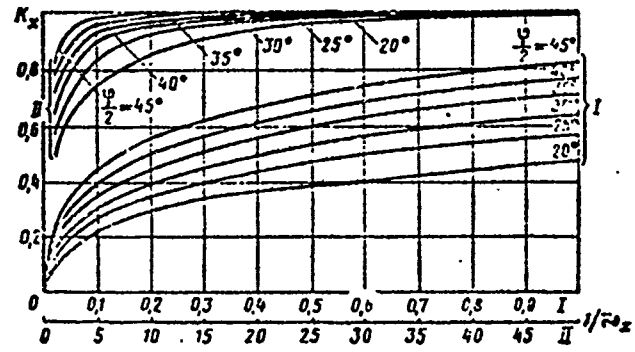

Fig. 9. Same as Fig. 8, $\varphi/2$ = 20°-45°.

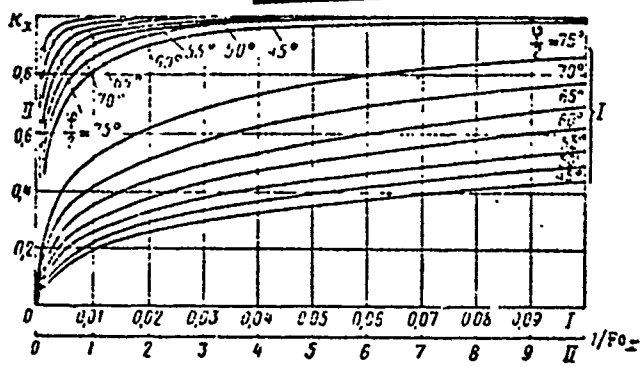

Fig. 10. Same as Fig. 8, $\varphi/2$ = 45°-75°.

$$\frac{\operatorname{tg}\varphi/2}{2\sqrt{a\tau_1}x_0}=2. \qquad (19)$$

Actually, when the argument $z=\frac{\operatorname{tg}\varphi/2}{2\sqrt{Fo_x}}\geqslant 2$, function erf z is practically equal to one, while function $Ei(-z^2)=0$.

In this case, from equation (17) it follows that $K_x = 1$.

An analogous conclusion is also obtained from equation (18). For example, as Lykov showed, when $z \geq 2$ formula (14) for the average temperature can be given in the form

$$\bar{\theta}=1-\frac{1}{\sqrt{\pi}}\frac{2\sqrt{Fo_x}}{\operatorname{tg}\varphi/2}.$$

Considering this, from formula (18) it follows that $K_x = 1$.

Using criterion K_x, formulas (9) and (13) can be written in a general form, convenient for practical calculations:

$$Q_x=\frac{2b}{\sqrt{\pi}}(t_c-t_0)\sqrt{\tau}K_x. \qquad (20)$$

In many practical cases it is important to know the total quantity of heat Q_X absorbed by the surface of a body in a certain section X (see Fig. 7). This heat can be expressed in percents K_X of the heat flow Q_X^* passing in this same section X to a semi-bounded body, in accordance with equation (16):

$$Q_X^*=\frac{2b}{\sqrt{\pi}}(t_c-t_0)X\sqrt{\tau}. \qquad (21)$$

The value $K_X = Q_X/Q_X^*$ is a parametric criterion which characterizes the influence of the angle (bilateral heat feed) on the heat-retaining properties of a body in section X.

From equations (11) and (21) it follows that for angles $40° \leq \varphi < 180°$

$$K_X=\operatorname{erf}\left(\frac{\operatorname{tg}\varphi/2}{2\sqrt{Fo_X}}\right)+\frac{\sqrt{Fo_X}}{\operatorname{tg}\varphi/2\sqrt{\pi}}\left(e^{-\frac{\operatorname{tg}^2\varphi/2}{4Fo_X}}-1\right)-\frac{\operatorname{tg}^2\varphi/2}{4\sqrt{\pi}\sqrt{Fo_X}}\operatorname{Ei}\left(-\frac{\operatorname{tg}^2\varphi/2}{4Fo_X}\right), \qquad (22)$$

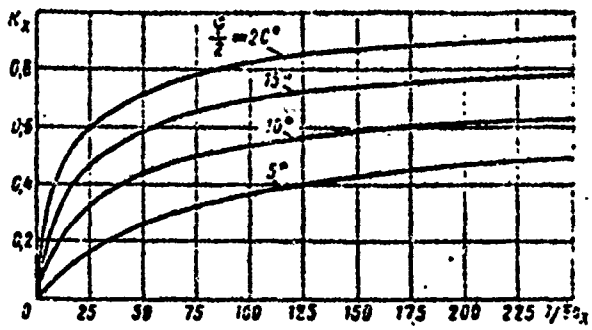

Fig. 11. Dependence of parametric criterion K_x on the criterion $1/Fo_x$ for angles $\varphi/2$ from 5° to 20°.

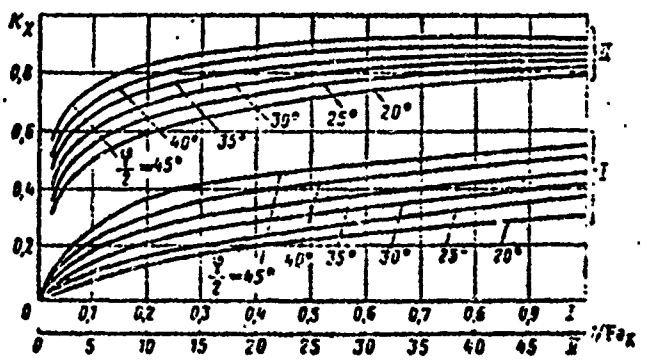

Fig. 12. Same as Fig. 11, $\varphi/2$ = 20°-45°.

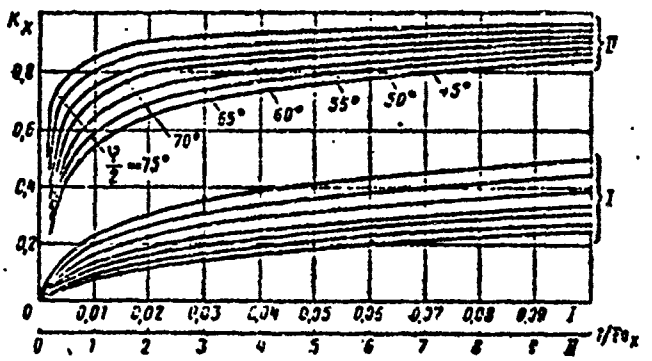

Fig. 13. Same as Fig. 11, $\varphi/2$ = 45°-75°.

while from equations (15) and (21), for angles $0° < \varphi \leq 40°$ we get

$$K_X = \frac{1\sqrt{\pi}}{4} \frac{\left[1 - \frac{\varphi}{\pi} - 2\frac{Fo_X}{tg^2\varphi/2}\sum_{n=1}^{\infty} Ei\left(-\mu_n^2 \frac{Fo_X}{tg^2\varphi/2}\right)\right] tg\varphi/2}{\sqrt{Fo_X}}. \quad (23)$$

Figure 11 shows the dependence of criterion K_X on criterion $1/Fo_X$, calculated from formula (23), for various values of the angle $\varphi/2$ from 5° to 20°.

Figures 12 and 13 give analogous dependences, calculated from formula (22) for angles $\varphi/2 = 20°-45°$ and $\varphi/2 = 45°-75°$, respectively.

Criterion K_X allows us to write formulas (11) and (15) in a form which is general and convenient for practical use:

$$Q_X = \frac{2h}{\sqrt{\pi}}(t_c - t_0)X\sqrt{\tau}K_X. \quad (24)$$

The theoretical dependences obtained were verified experimentally on a device which is shown schematically in Fig. 14. Into a bath of molten pure aluminum, having a temperature of 662 ± 2°, i.e., superheated by 3 ± 2°, we immersed for 60 seconds prisms made of refractory magnesite brick whose coefficient of thermal conductivity $a = 8 \cdot 10^{-3}$ m^2/hr. The working element of the prisms was a dihedral angle which varied within limits $\varphi/2 = 15°-90°$ at 15° intervals. The other faces of the prisms were insulated by sheet asbestos ($a = 0.712 \cdot 10^{-3}$ m^2/hr) 20 mm thick.

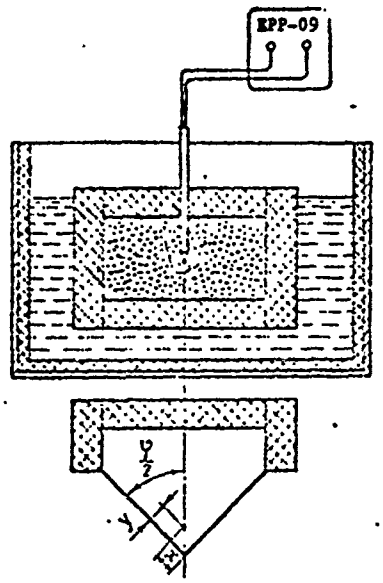

Fig. 14. Diagram of the device for studying the temperature field of dihedral angles.

At the control point of each prism we installed a Chromel-Alumel thermocouple whose readings were recorded by an EPP-09 electronic potentiometer. The thermocouple leads (0.5 mm in diameter) were insulated near the hot junction by a two-channel porcelain tube 3 mm in diameter and a cambric covering.

Based on the location of the control point relative to the vertex of the angle, all the prisms were divided into two groups: the first group had angles $\varphi/2 = 15°$, 30°, and 45°; the second group had angles $\varphi/2 = 45°$, 60°, 75°, and 90°. The control points had the following coordinates: group 1 – $x = 22$ mm, $y = 5.5$ mm ($\bar{y} = 0.25$); group 2 – $x = 6.8$ mm, $y = 6.8$ mm ($\bar{y} = 1$).

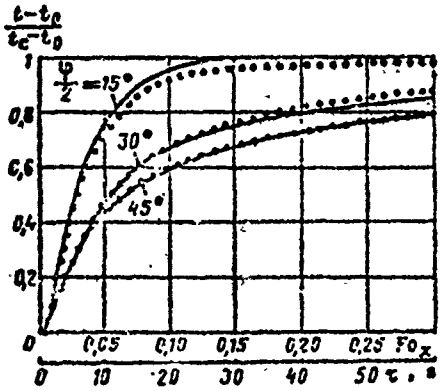

Fig. 15. Experimental and calculation graphs of the change in relative excess temperature at the control point of group 1 prisms.

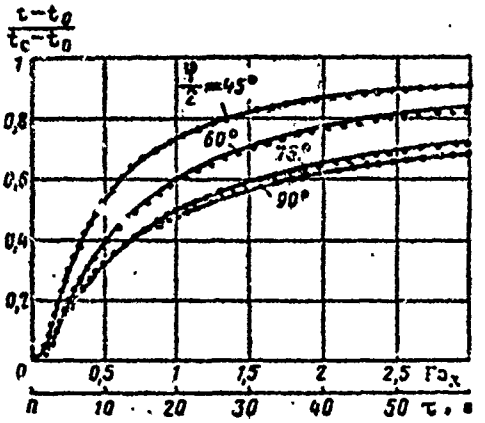

Fig. 16. Same as Fig. 15, group 2 prisms.

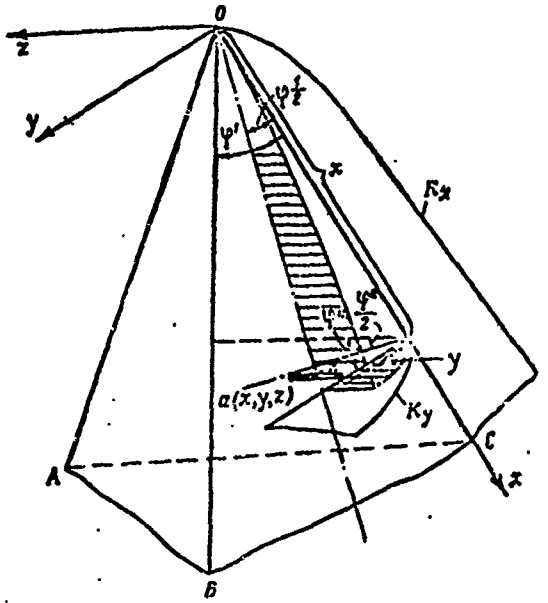

Fig. 17. Diagram of the distribution of heat flow on the surface of a trihedral angle.

Figures 15 and 16 show the experimental points and calculation curves of the change in relative excess temperature at the prism control point as a function of criterion Fo_x and time τ. From the graphs we see that the calculation results are in good agreement with experimental data.

Now let us examine the temperature field and heat flow on the surface of a trihedral angle.

Figure 17 shows the trihedral angle OABC whose temperature field can be approximately described by the following equation, derived from the scheme given above (Fig. 2):

$$\theta = \frac{t(x,y,z,\tau) - t_0}{t_c - t_0} = 1 - \operatorname{erf}\left(\frac{\operatorname{tg}\varphi'/2}{2\sqrt{Fo_x}}\right)\operatorname{erf}\left(\frac{\bar{y}\operatorname{tg}\varphi''/2}{2\sqrt{Fo_x}}\right)\operatorname{erf}\left(\frac{\bar{z}}{2\sqrt{Fo_x}}\right). \quad (25)$$

where $\theta = \frac{t(x,y,z,\tau) - t_0}{t_c - t_0}$ is the relative temperature of the body at point a with coordinates x,y,z at time τ; φ' and φ'' are the plane and dihedral angles of the trihedral angle; $\bar{z} = z/x$.

The heat flow entering the trihedral angle in time τ across a unit area with coordinates xy can be found, approximately, from the following expression:

$$Q_{(x,y)} = \frac{2b}{\sqrt{\pi}}(t_c - t_0)\sqrt{\tau}\cdot K_x \cdot K_y, \quad (26)$$

where K_x and K_y are criteria which characterize the influence of angles φ' and φ'' on the heat-retaining properties of a trihedral angle at point xy. They are functions of, besides angles φ' and φ'', criteria $1/Fo_x$ and $1/Fo_y$, and are determined from the graphs given above in Figs. 8-10.

Thus, the formulas obtained from theoretical studies make it possible to calculate the nonstationary temperature field and the heat-retaining properties of bodies having the form of di- and trihedral angles.

The results of an experimental verification of these formulas confirmed the fact that they are correct, which allows us to recommend them for actual calculations.

HEAT TRANSFER IN A FLUID FLOW WITH CONSIDERATION OF THE INFLUENCE OF DISSIPATION

M. N. Galkin and S. V. Lomazov

When turbine blades are cooled by convection heat transfer, the cooling fluid flows at high velocities through very narrow channels. In this case the distribution of temperature along the flow is influenced by the dissipative heat released as a result of viscous friction.

With laminar flow of a Newtonian fluid, the dissipation of mechanical energy per unit time [1] is defined by the formula

$$\frac{dE}{dt} = -\frac{\eta}{2}\int\left(\frac{\partial v_i}{\partial x_k}+\frac{\partial v_k}{\partial x_i}\right)^2 dV, \qquad (1)$$

where η is the coefficient of dynamic viscosity and $\partial v_1/\partial x_k$ are derivatives of the velocity components with respect to the coordinates.

In the integrand, according to the symbolic notation of tensor algebra, there is summation over the repeating indices in the product from 1 to 3.

The dissipated mechanical energy is converted into heat, and therefore

$$-\frac{dE}{d\tau}=\frac{dQ_{\text{д}}}{d\tau}, \tag{2}$$

where $dQ_{д}/d\tau$ is the heat released per unit time in the examined volume.

Let us examine flow of a fluid along rectangular and round channels. We direct coordinate z along the channel, while coordinates x and y are in its cross-sectional plane. With steady motion in a channel of constant cross section, the velocity will be a function only of coordinates x and y. In particular, in a rectangular channel, with small height/width ratio

$$2h/b\ll 1, \tag{3}$$

where h is one-half the height and b is the width of the channel section, we can consider that the velocity changes only with the height of the section, disregarding the derivative of velocity with respect to coordinate x. In this case [1] the velocity will be a parabolic function of coordinate y:

$$v=\frac{1}{2\eta}\frac{dp}{dz}(h^2-y^2), \tag{4}$$

where dp/dz is the change in pressure per unit flow length.

As fluid moves along a cylindrical tube of radius R, in the case of Poiseuille flow we have the familiar analogous formula

$$v=-\frac{1}{4\eta}\frac{dp}{dz}(R^2-r^2). \tag{5}$$

Let us average the velocity across the channel. For a rectangular section

$$\bar{v}=\frac{1}{2h}\int_{-h}^{h}v\,dy=-\frac{h^2}{3\eta}\frac{dp}{dz}, \tag{6}$$

for a round section

$$\bar{v}=\frac{1}{\pi R^2}\int_{0}^{2\pi}\int_{0}^{R}v\,r\,dr\,d\varphi=-\frac{R^2}{8\eta}\frac{dp}{dz}. \tag{7}$$

Considering (6) and (7), formulas (4) and (5) assume the form

$$v=\frac{3}{2}\bar{v}\frac{(h^2-y^2)}{h^2}, \tag{8}$$

$$v = 2\bar{v}\frac{R^2 - r^2}{R^2}. \qquad (9)$$

Let us determine the quantity of heat released during dissipation of mechanical energy per unit length of the channel. For this let us integrate equation (1) across the section, with consideration of (8) for a rectangular section and (9) for a round one. Let us designate by $dq_д/d\tau$ the quantity of heat released per unit time per unit channel length. Then, for the rectangular section

$$\frac{dq_1}{d\tau} = \frac{\eta}{2}\int_0^b \int_{-h}^{h} \left(\frac{dv}{dy}\right)^2 dx\, dy$$

and, finally,

$$\frac{dq_1}{d\tau} = 3\eta\frac{b}{h}\bar{v}^2. \qquad (10)$$

For the round channel

$$\frac{dq_1}{d\tau} = \frac{\eta}{2}\int\left[\left(\frac{\partial v}{\partial x}\right)^2 + \left(\frac{\partial v}{\partial y}\right)^2\right] ds = \frac{\eta}{2}\int_0^{2\pi}\int_0^R 2\left(\frac{dv}{dr}\right)^2 r\, dr\, d\varphi$$

and, finally,

$$\frac{dq_1}{d\tau} = 8\pi\eta\bar{v}^2. \qquad (11)$$

Formulas (10) and (11) show that the heat-release power per unit channel length is proportional to the square of the average velocity; for a round section it does not depend on the channel radius.

As a fluid moves along narrow channels, under conditions of insignificant relative intensity of heat transfer between the fluid and the channel walls, the temperature differential along the flow section can be disregarded as a small value compared with the temperature head on the surface (Bi << 1). In this case the thermal state of the flow can be characterized by the temperature which depends only on one coordinate, z.

Let us assume that heat transfer between the fluid and the channel walls is characterized by heat-transfer coefficient α. Then the change in heat content of a flow element dz is expressed by the algebraic sum of the heat of dissipation and the exchange heat between the channel and the fluid. The corresponding heat-balance

equation

$$\varrho cSdzdt = dq_2 dz + \alpha F(t_c - t)dzd\tau, \tag{12}$$

where ρ, c are the density and specific heat of the fluid; S and F are the area of the section and the perimeter of the channel; t_c is the characteristic temperature of the medium.

After transformation we get

$$\frac{dt}{d\tau} - \frac{\alpha F}{\varrho cS}(t_c - t) - \frac{dq_2}{d\tau}\frac{1}{\varrho cS} = 0. \tag{13}$$

The differential equation compiled characterizes the change, with time, of the temperature of an isolated flow element. With stationary flow we can turn to an examination of the temperature field of the entire flow by exchange of variables from the relationship

$$d\tau = \frac{dz}{v}. \tag{14}$$

Substituting (14) into (13) and separating the variables, let us integrate the obtained expression:

$$z = \bar{v}\int_{t_0}^{t} \frac{dt}{\frac{\alpha F}{\varrho cS}(t_c - t) + \frac{1}{\varrho cS}\frac{dq_2}{d\tau}}, \tag{15}$$

or, in dimensionless coordinates,

$$\frac{z}{l} = \frac{1}{\tau^*}\int_{t_0}^{t} \frac{dt}{\frac{\alpha F}{\varrho cS}(t_c - t) + \frac{dq_2}{d\tau}\frac{1}{\varrho cS}}, \tag{16}$$

where l is the channel length; $\tau^* = l/\bar{v}$ is the characteristic time for the total volume of fluid in the channel.

Precise integration of equation (15) is possible if we know the dependences of fluid density, specific heat, and viscosity on the temperature.

To explain the influence of the heat of dissipation on the nature of the temperature field of the flow, in first approximation we can assume

$\varrho = \text{const}$, $c = \text{const}$, $\eta = \text{const}$. (17)

These physical values can be replaced by their average values, if the total change in temperature as the fluid moves along the channel is insignificant and is not accompanied by phase transitions. In this case, integration of equation (15) gives

$$z = -\frac{\bar{v}}{\bar{v}} \frac{\varrho c S}{\alpha F} \ln \frac{\alpha F (t_c - t) + \frac{dq_1}{d\tau}}{\alpha F (t_c - t_1) + \frac{dq_1}{d\tau}}, \quad (18)$$

or, after involution,

$$\frac{\alpha F (t_c - t) + \frac{dq_1}{d\tau}}{\alpha F (t_c - t_1) + \frac{dq_1}{d\tau}} = \exp\left(-\frac{z}{\bar{v}} \frac{\alpha F}{\varrho c S}\right). \quad (19)$$

Let us expand the right side in a series, restricted to the linear approximation:

$$\frac{\alpha F (t_c - t) + \frac{dq_1}{d\tau}}{\alpha F (t_c - t_1) + \frac{dq_1}{d\tau}} = 1 - \frac{z}{\bar{v}} \frac{\alpha F}{\varrho c S}.$$

After transformations we get

$$t = t_0 + \frac{z}{\bar{v}} \frac{1}{\varrho c S} \left[\alpha F (t_c - t_1) + \frac{dq_1}{d\tau}\right]. \quad (20)$$

Equation (20) solves the problem in the approximation used. For a rectangular channel, considering (10),

$$t = t_0 + \frac{z}{2bh\varrho c} \left[\frac{2a(2h + b)}{\bar{v}} (t_c - t_1) + 3 \frac{\eta \bar{v} h}{h}\right]. \quad (21)$$

For a round channel, using (11), we get

$$t = t_0 + \frac{z}{\pi R^2 \varrho c} \left[\frac{2\pi a R}{\bar{v}} (t_c - t_1) + 8\pi\eta\bar{v}\right]. \quad (22)$$

From equations (21) and (22) we can determine the conditions under which dissipation becomes substantial. Obviously, in this case the terms in brackets should be of the same order. For a rectangular section this condition (with b >> h) will be

$$\frac{2ah}{\bar{v}} (t_0 - t_1) \simeq \frac{3\eta\bar{v}h}{h},$$

from which

$$\bar{v} \simeq \sqrt{\frac{2}{3}\frac{ah}{\eta}(t_c - t_j)}. \qquad (23)$$

Analogously, for a round section

$$\bar{v} \simeq \sqrt{\frac{1}{4}\frac{cR}{\eta}(t_c - t_j)}. \qquad (24)$$

Besides conditions (23) and (24), which determine the order of the flow velocities $\bar{v}$ for which the dissipative processes become substantial under the given conditions, we must take into account the limit of applicability of formulas (21) and (22), associated with retention of flow laminarity, i.e.,

$$Re \leqslant Re_c. \qquad (25)$$

Condition (25) determines the upper boundary of velocity $\bar{v}$, up to which the obtained dependences remain valid.

If the flow velocities exceed the critical values, corresponding to condition (25), dependences (21) and (22) become invalid, since the heat of dissipation $dq_д/d\tau$ will no longer be defined by formulas (10) and (11), which are quadratic functions of the average velocity. In a turbulent regime we determine the heat of dissipation from the conditions of conservation of energy, considering that the work of external forces is completely converted into heat:

$$dq_д = dpS, \qquad (25')$$

where dp and $dq_д$ are the drop in pressure and, correspondingly, the average release of dissipative heat in channel section dz.

From known hydraulics formulas, the drop in pressure is determined from the relationship

$$dp = \lambda\rho\frac{dz}{4R_г}\bar{v}^2, \qquad (26)$$

where $R_г = S/F$ is the hydraulic radius; $\lambda = f(Re)$ is the friction resistance coefficient.

Substituting (26) into (25') and dividing both sides of the equation by $d\tau$, we get

$$\frac{dq_2}{d\tau} = \lambda \rho F \bar{v}^3. \qquad (27)$$

The expression obtained for the dissipative function is substituted into equation (20):

$$t = t_0 + \frac{zF}{\rho c S}\left[\frac{\alpha(t_c - t_0)}{\bar{v}} + \lambda \rho \bar{v}^2\right]. \qquad (28)$$

Equation (28) defines the temperature field of the flow under conditions of turbulent flow. Here, consideration of the dissipative heat is necessary with flow velocities defined by the relationship

$$\frac{\alpha(t_c - t_0)}{\bar{v}} \simeq \lambda \rho \bar{v}^2, \qquad (29)$$

or

$$\bar{v} = \sqrt[3]{\frac{\alpha}{\lambda \rho}(t_c - t_0)}. \qquad (30)$$

The conclusions arrived at are valid if the physical parameters (ρ, c, η) are constant, which occurs under flow conditions close to adiabatic ($\alpha \approx 0$) and with low temperature heads on the contact surface between the fluid and the channel walls ($t_c - t_0 \approx 0$). Let us determine, under these conditions, the influence of fluid viscosity on the nature of heat transfer with laminar flow. Examining a round channel section, let us transform somewhat equation (22), expressing velocity $\bar{v}$ in terms of viscosity η [see formula (7)] and the pressure gradient dp/dz:

$$t - t_0 = -\frac{z}{\rho c}\left[\frac{16 Re \eta}{\frac{dp}{dz}}(t_c - t_0) + \frac{dp}{dz}\right]. \qquad (31)$$

From equation (31) it follows that a change in flow temperature under adiabatic conditions (with $\alpha = 0$) does not depend on the viscosity of the flowing fluid:

$$(t - t_0)_{\alpha = 0} = -\frac{z}{\rho c}\frac{dp}{dz} = -\frac{\tau}{\rho c}\frac{\Delta p}{l}. \qquad (32)$$

Equation (32) could have been obtained directly from the law of conservation of energy for a moving fluid with constant viscosity in the absence of heat transfer with the ambient medium.

If there is heat transfer between the fluid and the channel walls, as follows from equation (31) the viscosity increases its role in the total energy balance, and an increase in η with constant moving flow forces ($dp/dz = \Delta p/l = \text{const}$) leads to a relative reduction in the role of the dissipative processes.

We should once more stress that these conclusions pertain to small α and small initial differences in temperatures $t_c - t_0$. Under conditions of intense heat transfer, equation (20) is invalid, while with large initial differences in temperatures between the fluid and the channel walls equation (19) is also invalid, since the temperature changes of density, specific heat, and viscosity of the fluid begin to play an essential role. For drop fluids, of the indicated physical parameters it is the viscosity which changes particularly greatly. Consideration of the temperature dependence of viscosity leads to considerable complications in integrating equation (15), while the average velocity can no longer be calculated by formulas (6) and (7), which result from solution of the hydrodynamics equations for fluids with constant viscosity. Since the flow temperature is a function of coordinate z, the viscosity must be treated as a function of this same argument. The pressure gradient along the flow will also be variable. Therefore, equations (6) and (7) must be examined as differential equations, while the average velocity is determined by integrating them along the channel. For a rectangular channel, from equation (6) we get

$$dp = -(3\eta/h^2)\,\bar{v}\,dz,$$

from which

$$\bar{v} = -\frac{h^2 \Delta p}{3\int_0^l \eta\,dz}. \tag{33}$$

For a round section

$$\bar{v} = -\frac{R^2 \Delta p}{8\int_0^l \eta\,dz}. \tag{34}$$

For a rectangular section the rate of release of the heat of dissipation, defined by equations (10) and (11) with consideration of

(33) and (34), will be

$$\frac{dq_1}{d\tau}=\eta\frac{bh^3}{3}\left(\frac{\Delta p}{\int_0^l \eta\,dz}\right)^2. \tag{35}$$

For a round section

$$\frac{dq_1}{d\tau}=\eta\frac{\pi R^4}{8}\left(\frac{\Delta p}{\int_0^l \eta\,dz}\right)^2. \tag{36}$$

Equation (13), which describes the temperature field of a fluid flow, with consideration of (14), (35), and (36) assumes the form

$$dz=\frac{\rho c\,dt}{\frac{\bar{c}}{S}ak\frac{\delta}{\Delta p}(t_c-t)\int_0^l \eta\,dz+\frac{\eta}{\int_0^l \eta\,dz}\Delta p}. \tag{37}$$

For a rectangular section the coefficient

$$k=3/h^2, \tag{38}$$

for a round section

$$k=8/R^2. \tag{39}$$

If the temperature dependence of viscosity $\eta(t)$ is known, the integral $\int_0^l \eta dz$ can be calculated. For this we must know the temperature field of the flow z(t). Then, replacing the variables under the definite integral, we get

$$\int_0^l \eta\,dz=\int_{t_0}^{t_l}\eta(t)\frac{dz}{dt}dt, \tag{40}$$

where t_l is the temperature of the flow at the channel outlet.

Substitution of (40) into (37) results in a nonlinear integro-differential equation for determining the dependence z(t). To obtain an approximate solution to equation (37) let us assume that the density and specific heat of the fluid are constant and equal to their average values in the examined temperature range. For drop fluids ρ and c change considerably less than viscosity η with a

change in temperature, and therefore such an assumption is justified. Further, using the theorem of the mean, let us represent integral (40) in the form

$$\int_0^l \eta\, dz = \eta^* l, \tag{41}$$

where η^* is an intermediate value for viscosity in the interval $[\eta_0, \eta_l]$; η_0 and η_l are the viscosities of the fluid at the channel inlet and outlet, respectively.

Let us rewrite equation (37) considering (41):

$$dz = \frac{cc\,dt}{\frac{F}{S} a k \eta^* \frac{1}{\Delta p}(t_c - t) + \frac{\eta}{\eta^*}\frac{\Delta p}{l}}. \tag{42}$$

Dimensionless viscosity η/η^* is a temperature function, equal to one within the temperature range $[t_0, t_l]$. In linear approximation

$$\frac{\eta}{\eta^*} = \varkappa\left(\frac{t}{t^*} - 1\right) + 1; \tag{43}$$

coefficient $\varkappa$ is selected such that at point $t = t^*$ linear function (43) has a general derivative with function η/η^* (see the figure):

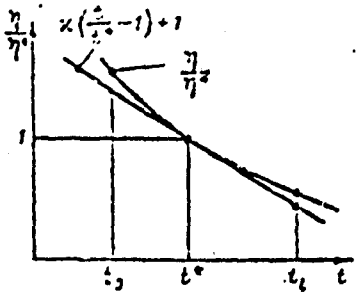

$$\varkappa = \frac{t^*}{\eta^*}\frac{d\eta_{t=t^*}}{dt}. \tag{44}$$

Substituting expression (43) into (42) we get

$$dz = \frac{cc\,dt}{\frac{F}{S} a k \eta^* \frac{1}{\Delta p}(t_c - t) + \frac{\Delta p}{l}\left[\varkappa\left(\frac{t}{t^*} - 1\right) + 1\right]}. \tag{45}$$

Integrating the obtained equation, we arrive at the following expression for the flow temperature field:

$$\frac{\frac{F}{S} a k \eta^* \frac{1}{\Delta p}(t_c - t) + \Delta p\left[(1-\varkappa) - \varkappa\frac{t}{t^*}\right]}{\frac{F}{S} a k \eta^* \frac{1}{\Delta p}(t_c - t_0) + \Delta p\left[(1-\varkappa) - \varkappa\frac{t_0}{t^*}\right]} = \exp\left(-z\frac{\frac{E}{S} a k \eta^* \frac{1}{\Delta p} - \frac{\Delta p}{l}\frac{\varkappa}{t^*}}{cc}\right). \tag{46}$$

When $z = l$ expression (46) is the equation for determining the temperature of the fluid at the channel outlet (t_l). However, solution of this equation is possible if we know the values of η^* and

$\varkappa$. These parameters can be determined by the method of successive approximations. In first approximation we can set $\eta_1^* = \eta_0$ and $\varkappa_1 = -1$. After this, from equation (46) we determine t_{l1} and dz/dt; then, using equations (40) and (41), knowing the temperature dependence of viscosity $\eta(t)$, we find the second approximation for η_2^*:

$$\eta_2^* = \frac{1}{l} \int_{t_0}^{t_{l1}} \eta(t) \frac{dz}{dt} dt. \tag{47}$$

Solving the equation $\eta = \eta(t)$ for l (or graphically), let us determine the temperature t_2^* corresponding to viscosity η_2^*. Substituting this temperature into equation (43), we find the second approximation for coefficient $\varkappa$:

$$\varkappa_2 = -\frac{t_0^*}{\eta_0^*} \frac{d\eta_t}{dt} \bigg|_{t_0^*}. \tag{48}$$

The values of η_2^* and $\varkappa_2$ are substituted into equation (46) and when $z = l$ we find the second approximation for the flow temperature at the channel outlet t_{l2}. To determine the third approximation, the entire calculation process is repeated.

The method described allows us to construct the temperature field of a flow of fluid as it moves in narrow channels, with consideration of the temperature dependence of viscosity and the dissipation energy.

REFERENCES

1. Ландау Л. Д., Лившиц Е. М., Механика сплошных сред, Гостехиздат, 1954.
2. Френкель Н. З., Гидравлика, Госэнергоиздат, 1956.